Vectored antibody delivery: impact on and synergy with the host's immune defense in chronic viral infection

Inauguraldissertation

zur

Erlangung der Würde eines Doktors der Philosophie

vorgelegt der

Philosophisch-Naturwissenschaftlichen Fakultät

der Universität Basel

von

Yusuf Ismail Ertuna

aus Adana, Turkey

Basel, 2021

Genehmigt von der Philosophisch-Naturwissenschaftlichen Fakultät

auf Antrag von

Prof. Christoph Hess, Prof. Daniel Pinschewer, Prof. Hanspeter Pircher

Basel, den 19.11. 2019

Prof. Dr. Martin Spiess

Table of Contents

List of Figures

List of Tables

Abbreviations

7AAD	7-aminoactinomycin D
AAP	Assembly-activating protein
AAV	Adeno-associated virus
Ab	Antibody
ABTS	2,2′-Azino-bis (3-ethylbenzothiazoline-6-sulfonic acid) diammonium salt
AID	Activation-induced cytidine deaminase
AIDS	Acute immunodeficiency syndrome
AM	Atypical memory
ANOVA	Analysis of variance
APC	Antibody-presenting cell
ART	Antiretroviral therapy
ASC	Antibody-secreting cell
AUC	Area under the curve
AV	Adenovirus
BAFF	B-cell activation factor
BCL6	B-cell lymphoma 6 protein
BCR	B cell receptor
BHK-21	Baby Hamster Kidney 21 cells
BLIMP1	B lymphocyte-induced maturation protein-1
BLT	Bone-marrow-liver-thymus
BM	Bone marrow
bnAb	broadly neutralizing Antibody
CAR	Chimeric antigen receptor
CCL	Chemokine ligand
CCR2	C-C chemokine receptor type 2
CD	Cluster of differentiation
CD40L	CD40 ligand
cDNA	complementary DNA
CFSE	Carboxyfluorescein succinimidyl ester
Cl13	Clone-13
CSR	Class switch recombination
CTL	Cytotoxic T lymphocyte
ctrl	control
CTV	Cell trace violet
CXCL13	Chemokine (C-X-C motif) ligand 13
CXCR5	C-X-C chemokine receptor type 5
DAB	3,3′-Diaminobenzidine
DAPI	4',6-diamidino-2-phénylindole
DC	Dendritic cell
DNA	Deoxyribonucleic acid

DNase	Deoxyribonuclease
dsDNA	double-stranded deoxyribonucleic acid
EBV	Epstein-Barr virus
EDTA	Ethylenediaminetetraacetic acid
ELISA	Enzyme-linked immunosorbent assay
EMA	European Medicines Agency
FACS	Fluorescence-activated cell sorting
FasL	Fas ligand
Fc	Fragment crystallizable
FCRL4	Fc receptor-like protein 4
FDA	Food and drug administration
FDC	Follicular dendritic cell
FITC	Fluorescein isothiocyanate
FIX	Factor IX
GC	Germinal center
GFP	Green fluorescent protein
GP	Glycoprotein
GTMP	Gene therapy medicinal product
Gy	Gray
HBV	Hepatitis B virus
HCMV	Human cytomegalovirus
HCV	Hepatits C virus
HEK-293	Human embryonic kidney 293 cells
HEL	Hen-egg lyzozyme
HIV	Human immunodeficiency virus
HLA	Human leukocyte antigen
HRP	Horseradish peroxsidase
HSC	Haematopoietic stemm cell
HSV	Herpes simplex virus
i.m.	intramuscular
i.p.	intraperitonial
i.v.	intravenous
ICAM-1	Intracellular adhesion molecule 1
ICOS	Inducible co-stimulator
ICOSL	Inducible co-stimulator ligand
ICS	Intracellular staining
IE	Immediate early
IFN	Interferon
IFNAR	IFN-alpha/beta receptor
Ig	Immunoglobulin
IL	Interleukin
iLN	inguinal Lymph node
InfMo	Inflammatory monocyte

iNOS	inducible Nitric oxide synthase
IRES	Internal ribosome entry site
IRF	Interferon regulatory factor
ISG	Interferon-stimulated gene
ITR	Inverted terminal repeats
Jak	Janus kinase
KL25H	KL25 heavy chain
KL25HL	KL25 heavy and light chains
KL25L	KL25 light chain
LAG-3	Lymphocyte-activation gene 3
LC	Light chain
LCMV	Lymphocytic choriomeningitis virus
LFA	Lymphocyte function-asociated antigen
LLPC	Long-lived plasma cell
LN	Lymph node
LPLD	Lipoprotein lipase deficiency
LPS	*Lipopolysaccharide*
LV	Lentivirus
Ly6C	Lymphocyte antigen 6 complex, locus C
Ly6G	Lymphocyte antigen 6 complex, locus G
mAb	monoclonal Antibody
MACS	Magnetic-activated cell sorting
MBC	Memory B cell
MCP1	Monocyte chemoattractant protein 1
MDCK	Madin-Darby Canine Kidney
memB	memory B cell
MFI	Mean fluorescence intensity
MHC	Major histocompatibility complex
mio	million
miRNA	micro Ribonucleic acid
MOI	Multiplicty of infeciton
mRNA	messenger Ribonucleic acid
Mx	Myxovirus resistance protein
MZ	Marginal zone
nAb	neutralizing Antibody
Nef	Negative regulatory factor
NK	Natural killer cell
NP	Nucleoprotein
OAS	2’-5’-oligoadenylate synthase
PAX5	Paired box protein 5
PB	Plasmablast
PC	Plasma cell
PCR	Polymerase chain reaction

PD-1	Programmed cell death 1
pDC	plasmacytoid Dendritic cell
PDGFR	Platelet-derived growth factor
PFA	Paraformaldehyde
PFU	Plaque forming unit
PNA	Peanut agglutinin
PRNT	Plaque reduction neutralization test
rAAV	recombinant Adeno-associated viral vector
RAG	Recombination activation gene
RANTES	Regulated on activation, normal T cell expressed and secreted
rCl13	recombinant Cl13-WE/GP
rCl13	recombinant Clone 13
RM	Resting memory
RNA	Ribonucleic acid
RNaseL	Ribonuclease L
ROI	Region of interest
RT	Room temperature
rVSV	recombinant VSV-WE/GP
SCID	Severe-combined immunodeficieiency
SEM	Standard error of the mean
SHIV	Simian-Human immunodeficiency virus
SHM	Somatic hypermutation
siRNA	small-interfering Ribonucleic acid
SIV	Simian immunodeficiency virus
SPF	Specific pathogen free
SRBC	Sheep red blood cell
STAT	Signal transducer and activator of transcription
TCF-1	T-cell factor 1
TD	T-dependent
TF	Transcription factor
Tfh	T follicular helper cell
tg	transgenic
Th1	T helper 1
TI	T-independent
TLM	Tissue-like memory
TLR	Toll-like receptor
TNF	Tumor necrosis factor
UV	Ultraviolet
VIT	Vectored-immunotherapy
VL	Light chain variable
VSV	Vesicular stomatitis virus
VSVG	VSV glycoprotein

VV	Vaccinia virus
WHO	World Health Organization
WT	Wild type
wt	wild type
XBP1	X-box binding protein 1

I. General Introduction

I.1 Passive Antibody Therapy

I.1.1 Brief History of Passive Antibody Therapy and Monoclonal Antibodies

The ability of the specific antibody-based therapies to protect against bacterial toxins was discovered by Behring and Kitasato in 1890s (Behring, 1890). This discovery naturally pioneered the rapid development of the antibody-based (animal serum) therapies for the treatment of several infectious diseases including measles (Janeway, 1945) and polio (ALEXANDER, 1943; Alexander and Heidelberger, 1940; Casadevall and Scharff, 1995; Hammon et al., 1952). These therapies were also known by the term "serum therapy", but effective administration of such big quantities of animal serum resulted in varying degree of side effects (from hypersensitivity syndrome to serum sickness). During 1930s, antibody purification methods were developed and this technology expectedly reduced the amount of toxicity of the serum therapy. Yet, around 1935-1940, the use of antibody-based serum therapy significantly declined due to the introduction of sulphonamides and other antimicrobial chemotherapies.

The area of antibody therapy was drastically revolutionized with the discovery of the *in vitro* production of monoclonal antibodies (mAbs) by immortalized B cell cultures, now known as hybridomas (Köhler and Milstein, 1975). This technology paved the way for the possibility of the production of large quantities of antibodies with a predefined specificity. Following this technology, and with the advancements in molecular cloning and recombinant DNA technology, many different approaches of human mAb production were established (Green et al., 1994; Lonberg et al., 1994; McCafferty et al., 1990; Steinitz et al., 1977; Wrammert et al., 2008).

Another revolutionary technique was developed to allow the amplification of the heavy and light chain genes from a single human B cell, followed by the cloning of these respective genes into the expression vectors (Wardemann et al., 2003). These advancements made it possible to use these monoclonal antibodies in the field of infectious diseases. Vaccine-induced immunity or the pathogenesis of the disease can be better investigated by using such antibodies. When the new sequencing technologies were taken into account, investigating the neutralization sensitivity or the isolation of the antibodies with the particular functional properties had become more applicable.

I.1.2 Passive Antibody Administration Against Infectious Diseases

In the context of viral infections, passive antibody administration of neutralizing antibodies (nAb) to control or protect against the infection has been studied for various virus models. In HIV field, combination of high-throughput neutralization assays, and single-B cell receptor sequencing (using HIV-envelope specific probes) techniques made it possible to identify extremely potent new generation broadly neutralizing antibodies (bNAbs) that were 100-fold more potent than the earlier generations (Scheid et al., 2009; Walker et al., 2009; Wu et al., 2010). bNAbs are antibodies that have the ability to neutralize a broad range of strains of a highly antigenically variable pathogen (Corti and Lanzavecchia, 2013).

Antibodies mediate their functions via targeting a specific epitope with their variable domains. Effector functions are mediated by the constant domains by engaging with the Fc receptors of the host. Currently, over 70 monoclonal antibodies are used in the clinic with the aim of treating a wide spectrum of diseases (Kaplon and Reichert, 2019). Chronic viral infections and cancer share some common features that eventually makes the treatment complicated, including high degrees of genetic adaptation to the therapeutic interventions, rare occurrence of spontaneous immune control and the necessity of the combinatorial drug therapy. Considering the

significant impact of immunotherapy in the treatment of several cancer types, the applicability of such similar ideas to the treatment of chronic viral infections is a necessary concept, which needs to be investigated. One signature example of such chronic viral infections is human immunodeficiency virus (HIV) infections. mAbs were shown to be protective against HIV-1 in chimpanzees already three decades ago (Emini et al., 1992). In Rhesus macaques, first generation anti-HIV mAbs or pooled-sera from HIV-infected individuals were shown to be protective even at low doses against high-dose mucosal challenge (Parren et al., 2001). Such protective capacity was shown to be directly related to the potency of the given mAb. For instance, considering two most clinically advanced anti-HIV-1 bNAbs; 3BNC117 and VRC01 (binding to the same target site on the viral glycoprotein Env "CD4 binding site" (CD4bs)), 3BNC117 confers protection for over a median of 13 weeks, whereas VRC01 (less potent than 3BNC117) protects only for 8 weeks in macaques challenged with simian-human immunodeficiency virus (SHIV), a virus that combines the elements from simian immunodeficiency virus (SIV) with the HIV-1 Env (Gautam et al., 2016; Li et al., 1992; Shibata et al., 1991).

Therapeutic effects of passive administration of mAbs against HIV-1 were studied both in mice and macaques. In humanized mice, initial tests were done nearly two decades ago with the first generation mAbs, but these studies shown little or no effect on viremia, neither with individual administration, nor with the combination therapy. Second generation bNAbs were much more potent (Klein et al., 2012; Klein et al., 2013; Poignard et al., 1999). Viral loads were reduced significantly in humanized mice challenged with HIV-1 and were later treated with bNAbs (Klein et al., 2012). The combination therapy with bNAbs were more effective compared to the monotherapy in preventing the occurrence of the viral escape variants. Combination therapies were targeting non-overlapping sites on Env, and viremia was completely suppressed, and suppression was maintained over 60 days. Moreover, the rebounding virus was still

susceptible to the bNAbs as shown in humanized mice (Diskin et al., 2013; Freund et al., 2017; Klein et al., 2014). Similar studies were conducted on macaques. No escape mutations were observed in SHIV infected macaques receiving the combination therapy, whereas the viral escape occurrence was detected in monotherapies depending on the SHIV strain used or the mAb chosen (Barouch et al., 2013; Shingai et al., 2013). In terms of remission efficacy in the preclinical models, 50% of the humanized mice infected with HIV-1 shown remission after the combination treatment with bNAbs and checkpoint-blockade inhibitors (Halper-Stromberg et al., 2014). In macaques, from 13 macaques that were challenged with SHIV and were treated 3 days later with the combination therapy, 6 macaques were shown to be undetectable after 1 year. Yet, another study has shown that clearance was dependent on the initial viral loads; lower loads associated with viral clearance. These therapies were given as a combination of antiretroviral therapy (ART) and TLR-7 agonist (Borducchi et al., 2018; Nishimura et al., 2017).

I.1.2.1 Effects of Passive Antibody Therapy on Endogenous Immune System

Passive antibody therapies are giving quite encouraging results to understand the alternative strategies to control infectious diseases. In addition to their effectivity, it will be very precious to delineate the impact of antibody therapies on the endogenous immune compartments. The synergy of the therapy with the endogenous immune system would be another advantage of such therapies. There is only limited research investigating the impact of antibody therapies on endogenous immune compartments. One such study focuses on the effects of an aforementioned promising bNAb (3BNC117A) on HIV-infected individuals (Schoofs et al., 2016). The host endogenous antibody responses were shown to be improved for neutralizing activity against heterologous tier-2 viruses. Passively administered antibody was also shown to accelerate the clearance of the infected $CD4^+$ T cells via an FcγR-mediated mechanism in

HIV-1 infection model *in vivo*, in mice (Lu et al., 2016). Antibodies can be transferred from a pregnant mother to its offspring perinatally. In order to mimic the transfer of nAbs from HIV-infected mothers to the fetus perinatally, new born macaques were passively administered with nAb against SHIV. These macaques have shown rapid increase in the endogenous nAb levels, as well as a more robust reduction in viremia (Ng et al., 2010). These studies try to address antibody responses upon passive antibody infusion, but the effects on endogenous antibody responses against the escape variants or virus specific B cell compartments remain to be elucidated.

I.1.2.2 Passive Antibody Therapy in Clinical Trials

The first clinical trial for treating HIV-infected individuals was conducted in 1992, by using pooled polyclonal antibodies, and little or no antiviral effect was observed (Vittecoq et al., 1992). In 1998, the first monoclonal antibody trial was conducted in viremic individuals, again with little or no effect on viral loads (Cavacini et al., 1998). Combination therapies with first generation antibodies, in addition, did not show any significant effect on the infection control (Armbruster et al., 2004).

The introduction of second generation bNAbs has shown that a single infusion of 3BNC117 led to a drop in the viral loads in 10 out of 11 viremic individuals, and viral suppression was maintained about 28 days post administration (Caskey et al., 2015). Similar results were observed with an alternative bNAb (10-1074) (Caskey et al., 2017). In line with the observations with the preclinical studies, combination therapy with these two bNAbs was far more effective than the monotherapy in the viremic individuals (Bar-On et al., 2018). Yet, again, the suppression of the viral loads was dependent on the initial baseline viral loads. The participants with the high viral loads could not completely suppress viremia.

I.2 Somatic Gene Therapy

Gene therapy is defined by Food and Drug Administration (FDA) as "products that mediate their effects by transcription and/or translation of transgenic genetic material and/or integrating into the host genome and that are administered as nucleic acids, viruses or genetically engineered microorganisms" and European Medicines Agency (EMA) classifies them as gene therapy medicinal product (GTMP) and defines as "biological medicinal product that contains an active substance which contains or consists of a recombinant nucleic acid in or administered to humans to regulate, replace, add or delete genetic sequences or its therapeutic, prophylactic or diagnostic effect relates directly to recombinant nucleic acid it contains, or to the product of genetic expression of this sequence" (Hanna et al., 2017) . To date, there are over 2,500 clinical studies that were initiated that harbor gene therapy. Applicability of such therapies encompasses a wide spectrum of conditions including infectious diseases, monogenic disorders, cancer and neurodegenerative diseases (Ginn et al., 2018). Gene therapy can include delivery of various genetic materials including deoxyribonucleic acid (DNA), messenger ribonucleic acid (mRNA), microRNA (miRNA), small interfering RNA (siRNA), and antisense oligonucleotides to specific cell types, tissues or organs (Chen et al., 2018).

Gene therapies conventionally can be subcategorized depending on the disease (genetic disease or acquired disorder), use of the gene delivery vehicle (integrating or non-integrating), the type of administration (*in vivo*, *in situ* or *ex vivo*), and the target cell (somatic cell or germ-line cell). In somatic gene therapy, cells, except for sperm and egg cells, are targeted. Such therapy confines the genetic changes to the individual and is a safer approach in the sense that these genetical changes are not passed on to the offspring. Delivery approaches for somatic gene therapy can be categorized as *ex vivo*, *in situ*, and *in vivo*. In *ex vivo* gene therapy, target cells are isolated from a patient`s tissue or blood, and are subjected to gene therapy, and re-administered back to the patient. A successful demonstration of such a therapy is chimeric

antigen receptor T-cell therapy (Kymriah – Novartis) which is FDA approved. In this therapy, T cells are isolated from the patients and genetically engineered to recognize CD19 presented on B cell lymphomas, and cells are reintroduced into the patients afterwards (Ruella and Kenderian, 2017). In situ delivery, on the other hand, involves the direct administration of the genetic material into the specific cell or to the tissue. The therapies being worked on with this technique include ischemia, cancer and cystic fibrosis (Deev et al., 2018; Guan et al., 2017; Manunta et al., 2017). In vivo gene therapy, however, is one of the most promising therapy types, and it can contain viral and non-viral vectors to deliver the therapeutic products. Viral vector delivery in gene therapy has become a reliable and effective therapy method with accumulating research.

I.2.1 Viral Vectors in Gene Therapy

Viral vectors used in gene therapy have a broad spectrum containing temporary expression or long-term permanent expression gene delivery vehicles. Viruses used in gene therapy include DNA and RNA viruses with single-stranded (ssRNA or ssDNA) or double-stranded (dsDNA) genomes. The most commonly used viral vectors are adenoviral vectors and adeno-associated virus vectors. Yet, gene therapy with lentiviral vectors, retroviral vectors and herpex simplex virus (HSV) vectors is also relatively commonly used.

I.2.1.1 Retroviral and Lentiviral Vectors in Gene Therapy

Retroviruses are enveloped single-stranded RNA viruses (Solly et al., 2003). One of the major concerns for the usage of the retrovirus delivery is the random integration ability of the virus, as previously shown in severe-combined immunodeficiency (SCID) patients (Hacein-Bey-Abina et al., 2008). Yet, recently, targeted integration vectors were developed, and with the use of helper cell lines, random integration issue was circumvented (Hu and Pathak, 2000).

One of the biggest advantages of this system is that it can accommodate up to 8 kilobases (kb) of gene inserts. Another challenge with the usage of retroviruses was their inability to infect non-dividing cells, however, this was circumvented with the lentiviruses which is a genus within the retrovirus family. Lentiviruses are able to infect both dividing and non-dividing cells (Kay et al., 2001). There are numerous clinical trials ongoing that make use of lentiviruses as gene therapy, and most of these studies are *ex vivo* gene therapies. Gene therapy of $CD34^+$ hematopoietic stem cells (HSCs) was applied for the treatment of several genetic diseases (β-thalassemia (Cavazzana-Calvo et al., 2010), X-linked adrenoleukodystrophy (Cartier et al., 2009) and Wiskott-Aldrich Syndrome (Aiuti et al., 2013)). No adverse effects were observed following the therapy. Yet, one of the most exciting applications of such therapies is the famous chimeric antigen receptor T (CAR-T) cell therapy. More than 60% of the patients with B-cell acute lymphoblastic leukemia have shown complete response rates after CAR-T cell therapy (Maude et al., 2014; Turtle et al., 2016).

I.2.1.2 Adenoviral Vectors in Gene Therapy

Adenoviral (AV) vectors are commonly used gene therapy vehicles. Adenoviruses were firstly isolated from human adenoid tissue-derived cultures, and they belong to a family of non-enveloped dsDNA virus family called Adenoviridae (Rowe et al., 1953). AV vectors are very rarely known to be causing any serious illnesses in healthy individuals, but in immunocompromised individuals it may cause some illnesses including sore throat, common cold, diarrhea, and bronchitis. AV vectors naturally possess a linear dsDNA consisting of 26 to 45 kb genome, yet the genome of AV vectors has been manipulated to render it a safer gene therapy approach (Nemerow et al., 2012). In the third generation (gutless) vectors most of the viral genes are missing, the only genes remaining comprise inverted terminal repeats (ITRs) and Ψ packaging sequences (Sakhuja et al., 2003). Gutless AV vectors were shown to express

the transgenes in animal models for over 2 years (Alba et al., 2005; Vetrini and Ng, 2010). And since they allow the episomal or stable insertion of the genes, they are safer compared to other genome integrating viral vector therapies. AV vector-mediated gene therapy is currently being used in numerous clinical trials with a focus on vaccination and oncolytic gene therapy. A recent report on Phase I-III clinical trials using the AV vector-based Onyx-015 which replicates selectively in tumor cells shows significant antitumor activity (Kirn, 2001; Zhang et al., 2018). In HIV field, AV vectors that encode site-specific endonucleases were used to edit the CCR5 gene in HSCs in clinical trials for AIDS (Saydaminova et al., 2015). Although promising, several serious concerns are present for AV vector therapy. Despite the promising and recently developed chimeric AV vector production technologies, anti-vector immunity is a major concern. This can lead to reduced transduction efficiency and in severe cases may even lead to inflammatory shock, therefore, personalized design of the vectors depending on the predisposed individual is necessary.

I.2.1.3 Adeno-associated Virus Vectors in Gene Therapy

Adeno-associated viruses (AAV) were first isolated as the contaminants of simian adenovirus preparations, and furthermore were isolated in the samples from humans, non-human primates, avian, bovine, and bats (Atchison et al., 1965; Hoggan et al., 1966). AAV possesses a 4.7kb ssDNA genome that is packed with a non-enveloped viral particle. The genome comprises the promoters (p15, p19 and p40) as well as rep and cap genes, and 145 bp inverted terminal repeats. ITRs contain palindromic sequences that allow the synthesis of the complementary DNA (cDNA) by serving as the replication origin and also the packaging signal (Laughlin et al., 1979). Alternative splicing allows the expression of different rep genes (Rep78, Rep68, Rep52, Rep40), cap genes and a non-structural assembly activating protein (AAP), which later helps the assembly of the capsid proteins (Sonntag et al., 2010). Transgene of interest can be

cloned in between the ITR sequences, and the produced AAV particles containing the genome with the transgene of interest are administered as a therapy (For the production of recombinant AAV (rAAV) particles see section I.4). A major advantage of AAV vector therapies is that the transgene expression can be maintained for long-time periods. In a clinical trial, a patient that was administered with rAAV-Factor IX (FIX) blood coagulation factor, and the transgene activity was detected for over 10 years (Buchlis et al., 2012). Currently, there are more than 200 clinical trials ongoing with AAV gene therapy. Many of these therapies are focused on genetic disorders. Three AAV-based products (Luxturna™, Gendicine® and Glybera®) are approved and in the market. Glybera® was the first approved AAV-therapy by EMA to treat lipoprotein lipase deficiency (LPLD), yet it was withdrawn from the market due to not high patient demand and expensive therapy costs. Luxturna™, an FDA approved drug, was successfully shown to treat retinal dystrophy with the expression of the RPE65 gene (MacLaren et al., 2014).

I.3 Recombinant Adeno-associated Viral Vector Delivery of Antibodies

AAV was detected in various vertebrate species including non-human primates and humans, and to date it was not associated with any known diseases. The structure and the sequence of the capsid of rAAVs are identical to the wild type AAVs. rAAV genomes lack all protein-coding genes and especially, since they are devoid of the rep genes, their genome integration rates are greatly reduced. The protein-coding genes that are naturally located between the ITRs are replaced, instead, with transgenes of interests, and the only sequences remaining from the original virus are the ITRs. Such gutless vectors give rAAVs the advantage of causing low immunogenicity and cytotoxicity. Nine serotypes of AAVs are endemic to humans (AAV1-9) (Boutin et al., 2010). Host factors play an important role with the interaction with rAAVs after administration. Serotype of the rAAV capsid determines the interaction with serum proteins

and specific cellular receptors that are ultimately determining the target cell type (Denard et al., 2018). Upon interaction with the specific cell surface receptors, rAAV particles are internalized by receptor-mediated endocytosis via clathrin-coated vesicles (Nonnenmacher and Weber, 2011). rAAVs undergo structural changes upon exposure to the specific pH of the endosomes, which are carried via the cytoskeletal network, until rAAV achieves endosomal escape (Sonntag et al., 2006; Xiao and Samulski, 2012). Following endosomal escape rAAV is transferred through the nuclear pore complex to the nucleus where it uncoats the viral capsid (Nicolson and Samulski, 2014). Once in the nucleus, ssDNA needs to be converted into dsDNA with second strand synthesis, via the self-priming ITRs at the 3' end (Ferrari et al., 1996; Fisher et al., 1996; Zhong et al., 2008). After double strand synthesis, dsDNA circularizes via ITR recombination, mediated by inter and intra-molecular interactions (Duan et al., 1998; Duan et al., 1999). This circularization enables AAV dsDNA to remain as episomal concatemers, which eventually leads to the stable expression of the episomal DNA in the post-mitotic cells.

Manufacturing of rAAV particles relies on multiple different techniques, but a very common methodology of manufacturing is the triple transfection of HEK293 cells. In this method, HEK293 cells constitutively expressing adenovirus E1a and E1b genes are transfected with multiple plasmids (Matsushita et al., 1998; Xiao et al., 1998). *Rep* and *cap* genes, that are necessary for the production of rAAV particles, are supplied in *trans* in a plasmid. Second plasmid is a cis-plasmid that encodes the transgene of interest, in between ITRs. The third plasmid is a helper plasmid, that encodes for E2A (essential for replication), E4 (for mRNA processing) and VA RNA (involved in translation) (Matsushita et al., 1998; Xiao et al., 1998). Of note, HEK293 cells are adapted to grow in suspension cultures in order to scale up the yield (Grieger et al., 2016). Thanks to the techniques developed for the production of rAAV vectors

expressing a transgene of interest, the applicability of these vectors to various disease models is possible.

I.3.1 Murine Models

Long-term sustainable gene expression can be achieved by rAAV vector mediated antibody gene therapy with just one intramuscular injection. In such case, encapsidated rAAV particles target the muscle cells, and the protein of interest is produced in these cells. Secretion peptide signals enable the protein to be secreted from the cell to the systemic blood circulation. Of interest, this section will focus on rAAV vector mediated antibody delivery against chronic infections.

First demonstration of sustained antibody levels has shown that RAG-1 mice, receiving the gene therapy with rAAV2 carrying the b12 gene (CD4 binding bNAb) under the expression of two separate promoters for heavy and light chains, shown 4-9 µg/ml antibody in the serum after 12 weeks. Functional analysis of these sera was shown to be neutralizing for HIV-1 as demonstrated *in vitro* (Lewis et al., 2002).

Another study using full-length bNAbs that are identical to human has demonstrated that rAAV vector delivery of such antibodies reach therapeutic levels *in vivo* and can be protective against intravenous challenge with HIV-1 (Balazs et al., 2012). In this study, authors used rAAV8 as capsid, since it targets non-dividing, post-mitotic muscle cells. Moreover, AAV8 has a lower seroprevalence in the human population compared to AAV1 and AAV2 (Gao et al., 2002). Another advantage of AAV8 is its nature to not induce capsid specific CD8 T cells unlike AAV2 does. This effect possibly comes from the lack of heparin binding, and therefore, poor uptake by dendritic T cells, which might lead to immune tolerance against AAV8 capsid (Mays et al., 2014; Vandenberghe et al., 2006). A follow-up study from the same group has investigated the protective capacity of vector immunotherapy (VIT) against low-dose repetitive

mucosal challenge in a bone marrow-liver-thymus (BLT) humanized mouse model. The results from these studies consolidate the protective capacity of rAAV delivered bNAbs against viral infection (Balazs et al., 2014).

rAAV delivered nAb efficacy was investigated in HCV infection as well. rAAV expressed nAbs against HCV was efficiently expressed in highly immunocompromised non-obese diabetic (NOD) RAG1$^{-/-}$ IL2Rγc^{null} (NRG) mice when given intramuscularly (i.m.) (de Jong et al., 2014). *In vivo* produced antibody was successfully neutralizing in *in vitro* neutralization assays against a broad spectrum of intergenotypic HCV chimeric viruses. Furthermore, rAAV mediated nAb expression efficiently inhibited the HCV entry, as well as, was protective against a low-dose i.v. challenge in human liver chimeric mice.

VIT for immunoprophylaxis was studied and shown to be protective against infections in various infection models in the mice including influenza and Ebola (Balazs et al., 2013; van Lieshout et al., 2018).

Therapeutic applications of rAAV vector delivered antibodies also show promising results. In a humanized mouse model, mice were infected with HIV-1 and since antiretroviral therapy (ART) was shown to be interfering with the transduction potential of rAAV, viremia was suppressed initially with ART (Horwitz et al., 2013). Gradually, ART was withdrawn and passive antibody infusion with bNAbs was given, and later bNAb infusion was replaced with rAAV administration, and 6 out of 7 mice have shown functional cure from the infection.

I.3.2 Macaque Models

Immunoprophylaxis experiments for rAAV delivered antibody was also studied in rhesus macaques. A 2009 study has utilized the rAAV delivery of immunoadhesin molecules based on anti-SIV Fabs isolated from the infected macaques (Johnson et al., 2009). These immunoadhesin constructs coded for heavy and light chain variable regions that were

connected with a linker to make a single variable chain that is connected to a rhesus IgG2 Fc fragment. Challenge of these macaques a month later with SIVmac316 demonstrated that six out of nine macaques were protected from the infection. Three animals did not show protection owing to the presence of anti-antibody immune responses.

Other studies attempted to use full-length rhesus IgG1 antibodies and administer with rAAV1 to macaques, but they failed to induce protection. As found later, the animals developed anti-antibody responses against the variable regions of the given antibodies (Fuchs et al., 2015). Simianized versions of various nAb antibodies given more promising results in terms of protection in various follow-up studies (Gardner et al., 2015; Saunders et al., 2015).

I.3.3 Clinical Trials with rAAV Delivered Antibody Therapy

In terms of delivering neutralizing antibodies against infectious diseases, there are currently two clinical trials for HIV, one completed (NCT01937455) and one recruiting (NCT03374202). First study, NCT01937455, aims to check the safety and productive efficiency of rAAV1 mediated PG9 expression when given in escalating doses in healthy adult male participants (Priddy et al., 2019). These patients were pre-tested for the absence of anti-AAV1 capsid antibodies. There was no detectable PG9 antibody in the serum by ELISA at any time point in any of the dose groups. All participants shown anti-AAV1 antibodies after administration. However, PG9 was detected in the serum from four out of sixteen individuals by HIV-1 neutralization assay, and by RT-PCR from the muscle biopsies. In the higher dose group, ten participants showed anti-drug antibodies. This study shows that use of rAAV up to 1.2×10^{14} vector genomes intramuscularly is safe in healthy adults.

The second study, uses rAAV8 delivery of VRC07 in HIV-1 positive individuals, that are under ART therapy and have suppressed viremia at least for the last three months. This is a Phase I

dose escalation study to check the expression levels and safety of such a therapy. This study is still recruiting and the results are not available yet.

I.4 Adaptive Immune Control in Chronic Viral Infections: T Cell Responses, B Cell Responses and ASCs

Viral infections can be divided into two categories in terms of the duration of the infection they cause. Acute infections are short-term infections, where the viremia is controlled rapidly in a short period of time. Chronic infections, on the other hand, as the name suggests result in prolonged viremia, and in some instances such as HBV, HCV and HIV infections, end up in life-long persistence of the virus.

For some specific viral infections, such as lymphocytic choriomeningitis virus (LCMV, a prototypic mouse virus) infection depending on the virus strain, the route of the infection or the major histocompatibility complex (MHC) haplotype, the infection may lead to acute or chronic infection (Moskophidis et al., 1995; Zinkernagel et al., 1985). The virus strain, for instance, is a determinant of persistence for LCMV infection in C57BL/6 mice. LCMV-Armstrong or low-dose infection with LCMV-WE strain result in acute infections, and virus is controlled in about 1-2 weeks. LCMV-Clone 13 or LCMV-Docile infections following administration as high dose, contrarily, cause protracted viremia, and are cleared from the organs only after several months (Ahmed et al., 1984; Moskophidis et al., 1993). Acute LCMV clearance is mainly mediated by cytotoxic T lymphocyte activity (CTL), but during chronic LCMV infection several adaptive immune responses are pivotal for the control of the infection including CD8 T cells, CD4 T cells, B cells, and antibody secreting cells (ASCs) (Wherry et al., 2003).

I.4.1 T Cell Responses During Chronic Viral Infection

Acute LCMV infection can exclusively be controlled by CTLs. Upon encounter with the antigenic stimuli, CTLs undergo activation, followed by clonal expansion and differentiation into effector T cells, which in return acquire the ability to secrete inflammatory cytokines such as IFN-γ, TNFα and IL-2. CTLs also exert direct-killing functions via the activity of perforin and granzyme B. The expansion phase is later replaced by the contraction phase where majority of the cells undergo apoptosis, and remaining cells differentiate into memory T cells, which upon rechallenge can re-expand and mediate their immune functions. Chronic infection, however, although starting with activation which is followed by clonal expansion, leads the T cells to be driven into a state infamously termed as "T cell exhaustion". Such exhausted profile of T cells was initially described in LCMV model (Gallimore et al., 1998; Moskophidis et al., 1993; Zajac et al., 1998). Hallmarks of exhausted T cells include loss of inflammatory cytokine secretion, reduction in proliferative capacity, alteration of transcriptional and epigenetic signatures, and overexpression of inhibitory markers (such as PD-1, CD160, 2B4, Tim-3, Lag-3) (Barber et al., 2006; Day et al., 2006; Pauken et al., 2016; Scott-Browne et al., 2016; Sen et al., 2016; Wherry et al., 2007). One of the main drivers of exhaustion was shown to be the constant exposure to persisting excess antigen load (Mueller and Ahmed, 2009b; Ou et al., 2001). Eventually, these cells during a chronic infection undergo clonal deletion (Moskophidis et al., 1993).

As mentioned previously, resolution of the chronic viral infections relies on both CTLs and CD4 T cells, and later on antibody responses. CD4 T cells are known to provide the helper functions to both CD8 T cells and B cells. CD4 T cells, in addition play a role in the formation of ASCs (or plasma cells (PCs)) as a result of their interactions with the B cells. In the context of chronic viral infections, CD4 T cells have a pivotal role, and the initial transitional absence of CD4 T cells prior to infection results in the failure to control the infection (Matloubian et

al., 1994). Virus specific CTLs get deleted in the absence of the help being provided by CD4 T cells (Battegay et al., 1994; Matloubian et al., 1994). Moreover, the activity of CD4 T cells to interact with B cells is also necessary, since antibody responses are involved in the clearance of the chronic infection several months after the infection (Ciurea et al., 2001). CD4 T cells also suffer from exhaustion, similar to CTLs, during a chronic infection (Brooks et al., 2006). This concept was validated when acute and chronic infections were compared. CD4 T cells get activated and primed similarly efficiently in acute and chronic infections during early stages, yet they become functionally altered and exhausted possibly as a result of the persisting antigenic exposure (Brooks et al., 2005).

I.4.2 B cell and ASC Responses During Chronic Viral Infection

Humoral immune responses in immunity lay its roots to the early work of Ehrlich and Flemming. Migration of B cells to the B cell follicles is guided by the chemokine (C-X-C motif) ligand 13 (CXCL13), produced by follicular dendritic cells (FDCs) or other follicle-associated stromal cells, which interact with C-X-C chemokine receptor type 5 (CXCR5) expressed by naïve B cells. Contact of an antigen (soluble or presented by antigen presenting cells (APCs)) with an antigen-specific B cell initiates the humoral immune responses. After encounter with antigen, B cells get activated through signaling via their B cell receptors (BCR). Naïve B cells initially express surface IgM and IgD. Importantly, for the B cells to carry on to the next step, proliferation has to occur to give rise to clonal expansion. When interacting with low valency antigens, B cells may need helper T cell-derived signals to further proliferate in T-dependent responses. However, also two different T-independent responses are known. In type-I T-independent responses, this necessary help from T-cells might be circumvented upon strong signals received by coreceptors like toll-like receptors. In type-II T-independent responses, a multivalent antigen might trigger a strong BCR engagement, which also leads to

the activation without a need for T-cell help. BAFF and APRIL are involved in augmentation of such responses (Balázs et al., 2002). In T-dependent responses, antigen-experienced B cells must interact with cognate antigen-specific T cells, and this process mostly takes place at the T-B border (Garside et al., 1998) (MacLennan et al., 1997; Okada et al., 2005). Interaction of ICAM1 and ICAM2 on B cells with LFA1 on T-helpers cells, in addition to MHC-peptide interactions, T-B interactions are stabilized and maintained (Zaretsky et al., 2017). Later on, these T-B interactions result in the formation of the germinal centers (GCs). For the maintenance of GC reactions, engagement of several surface molecules (ICOS-ICOS-ligand (ICOSL) and CD40 (B cells)-CD40-ligand (CD40L, T cells)) play pivotal roles (Liu et al., 2014; Mesin et al., 2016). T follicular helper (Tfh) cells expressing such surface molecules impact B cells by secreting two key cytokines: interleukin-4 (IL-4) and interleukin-21 (IL-21) (Shulman et al., 2014). These cytokines regulate class-switch recombination (CSR), differentiation into ASCs, and B cell proliferation. In GCs, B cell proliferation is followed by somatic hypermutation (SHM) and CSR. These processes give the B cells the possibility to accumulate mutations in their variable chains of the immunoglobulin gene. After numerous rounds of mutations, B cells circulate between the light zone and the dark zone, where basically they go through rounds of interactions with T cells and are selected upon their BCR affinity (Allen et al., 2007; Victora et al., 2012). As a result of these reactions, GC B cells can be destined for three outcomes, i) they can recirculate into GC reactions, ii) differentiate into either memory B cells (MBCs) or iii) PCs. PCs can either home to red pulp in the spleen, or to medullary cords in the lymph nodes, or to the specific niches in the bone marrow where they are named as long-lived PCs (LLPCs). These cells have several common features including the upregulation of the surface marker CD138. PCs tremendously decrease and halt their proliferation activity, and finally they downregulate their surface Ig, and instead secrete soluble Ig. MBCs, on the other hand, keep the expression of the surface Ig, and they get involved in

the robust responses in case of a secondary infection. There are several studies about the origins of MBCs debating whether they are differentiated from high-affinity or low-affinity B cells. Yet, reaching a clear conclusion about the actual origins of MBCs remains elusive (Shinnakasu et al., 2016; Suan et al., 2017; Weisel et al., 2016).

As mentioned earlier, CD8+ T cells take a tremendous part in the clearance of LCMV infection. During chronic LCMV infection, nAbs arise only at later time points, about 30-40 days later. Yet, as shown by B cell deficient mice, B cells are pivotal in the clearance of the chronic LCMV infection (Bründler et al., 1996; Christensen et al., 2003; Thomsen et al., 1996). There are limitations to that model as deficiency of B cells causes disturbances in the splenic microarchitecture (Nolte et al., 2004). Moreover, Type-I interferon responses are deficient in mice lacking B cells (Louten et al., 2006). The use of B cell sufficient mice that lack the ability to mount antigen specific antibodies shown that early nonneutralizing IgM antibodies impede the persistence of the virus (Bergthaler et al., 2009). LCMV nucleoprotein (NP) specific nonneutralizing antibodies also accelerates the clearance of the virus (Straub et al., 2013). Nonneutralizing antibodies, when given prior to chronic LCMV challenge, effectively contribute to the control of the infection (Richter and Oxenius, 2013).

I.5 Lymphocytic Choriomeningitis Virus Model

LCMV belongs to *Arenaviridae* family, which phylogenetically is divided into two groups of viruses, namely, Old World viruses and New World viruses. All Areanaviruses are known to be zoonotic, and the majority of them uses rodents (such as Machupo, Lassa, Junin, Guanarito) as host, whereas Tacaribe virus uses bats as their primary host (Emonet et al., 2006). The main host of LCMV is *Mus musculus*. In the nature, infection normally occurs congenitally and passes as a perinatal infection from mother to the offspring of the mice. The offspring is life-long carrier mice. Humans can be infected by LCMV with exposure to infected urine, feces, or

the bedding of the experimental animals, as well as via needle stick injury, or other laboratory accidents. The symptoms associated with the infection in humans encompass from mild-symptoms (mostly resembling flu-like symptoms) to aseptic meningitis.

Arenaviruses are enveloped, bi-segmented negative stranded RNA viruses. Their genomes comprise a small (S) and a large (L) segment. Each of these segments are separated by intergenomic regions (IGRs) that are flanked by the genes of the two proteins which are encoded in an ambisense orientation (Salvato et al., 1989; Salvato et al., 1988). The nucleoprotein (NP) and glycoprotein (GP) genes are located on the S segment (Salvato and Shimomaye, 1989). The glycoprotein is initially translated into a precursor protein (GP-C). This precursor protein, afterwards, undergoes posttranslational modifications to give rise to GP1 and GP2 proteins which eventually form the spikes on the viral envelope. The L segment, on the other hand, encodes for the viral polymerase and the Z matrix protein (Perez et al., 2003).

LCMV, for decades, has been an invaluable model to study the host-pathogen interactions and to investigate the interaction of the viral infections with endogenous immune compartments. As aforementioned in section 1.4, the dose and the strain of LCMV have an important role in the persistence of the virus. High dose infections with two strains, namely, LCMV-Clone 13 and LCMV-Docile result in chronic infection of the mice. LCMV-Clone 13 is a variant of Armstrong strain (Ahmed et al., 1984). LCMV-Docile was isolated from carrier mice infected with LCMV-UBC (Pfau et al., 1982), which is originally is a derivative of LCMV-WE (Hotchin and Weigand, 1961). By using reverse genetics tools, LCMV can be rescued in vitro by transfection of cell lines with the plasmids containing the LCMV RNA genes and trans-acting elements for the intracellular expression (Flatz et al., 2006; Sánchez and de la Torre, 2006). In this technique, LCMV RNA genes are expressed by a polymerase-I driven vector, and the expression of LCMV trans-acting elements such as NP and L is driven by polymerase-

II driven vector. With such a strategy, infectious LCMV can be produced. This enables the possibility to introduce desired mutations to the viral genes, or replace viral genes such as glycoprotein with reporter genes. One frequently used example of such a system is recombinant LCMV Clone 13 expressing the WE-GP (rCL13) (Flatz et al., 2006; Penaloza-MacMaster et al., 2015b).

1. Vectored antibody delivery augments and synergizes with the host's immune defense in chronic viral infection

Yusuf I. Ertuna[1], Benedict Fallet[1], Anna F. Marx[1], Mirela Dimitrova[1], Daniel D. Pinschewer[1]

Affiliations

1 Department of Biomedicine – Haus Petersplatz, Division of Experimental Virology, University of Basel, 4009 Basel, Switzerland.

Corresponding author:

Daniel D. Pinschewer,

Department of Biomedicine – Haus Petersplatz, Division of Experimental Virology,

University of Basel,

4009 Basel, Switzerland.

Daniel.Pinschewer@unibas.ch

1.1 Abstract

Gene therapy-based antibody delivery (vectored immunotherapy, VIT) represents an innovative approach to fight chronic viral diseases but its synergy with and impact on the host's endogenous immune defense remain ill-defined.

Here we developed an adeno-associated viral (AAV) vector to establish persistent high titers of a lymphocytic choriomeningitis virus- (LCMV-) neutralizing monoclonal antibody in chronically infected mice. Chronic viremia subsided in AAV-treated wildtype animals but not in mice lacking either CD8+ T cells or endogenous antiviral antibody responses. Persistence in the latter was due to the emergence of VIT-escape variants, which were effectively controlled by the endogenous antibody response of wildtype hosts. Vectored antibody delivery resulted in lowered expression of PD-1 and LAG3 on antiviral CD8+ T cells, increased endogenous antiviral antibody responses as well as elevated numbers of antiviral germinal center B cells and antibody-secreting cells in spleen.

Our observations document that the therapeutic efficacy of vectored antibody therapy in chronic viral infection relies on its synergy with the host's CD8+ T cell and antibody responses, both of which are functionally improved by vectored antibody delivery and contribute essentially to prevent viral mutational escape. VIT should be considered both an antiviral and an immunostimulatory approach to persistent viral infection.

1.2 Introduction

The discovery of antibody based-therapies for the protection against bacterial toxins paved the way to advanced passive immunization therapies (Behring, 1890). Eventually, however, it was the advent of monoclonal antibody (mAb) technology, which has revolutionized the field (Köhler and Milstein, 1975). With the advancements in recombinant DNA technology and molecular cloning, various methods have been established, which allow for the production of monoclonal antibodies with a defined specificity (Lonberg et al., 1994; McCafferty et al., 1990; Steinitz et al., 1977; Wrammert et al., 2008). Meanwhile, passive mAb therapies have shown efficacy in preclinical models of viral infection as well as in clinical settings (Barouch et al., 2013; Caskey et al., 2015; Caskey et al., 2017; de Jong et al., 2014; Freund et al., 2017; Klein et al., 2012). The limited half-life of antibodies can, however, require repeated re-administrations, depending on the disease indication. Antibodies with engineered Fc regions and increased affinity of binding to the neonatal Fc receptor (FcRn) represent an improvement in this regard but bear inherent risks of long-term immunogenicity (Ko et al., 2014). Costs of goods and logistics of re-administration therefore pose a significant challenge for long-term use, notably when it comes to the prevention or control of chronic infection at a global scale.

Somatic gene therapy for the delivery of antibodies to treat chronic diseases is currently under investigation. Viral vectors or RNA delivering expression cassettes for antibody heavy and light chain genes were shown to be effective *in vitro* and *in vivo* (Hur et al., 2012; Joseph et al., 2010; Kormann et al., 2011; Luo et al., 2009). Recombinant adeno-associated viral (rAAV) vectors are most commonly used owing to their replication-defective nature, low immunogenicity and long-term episomal persistence in the form of concatemers, which largely dispels concerns related to genotoxic risks. Accordingly, rAAVs have yielded

therapeutic mAb levels in the serum of mice (Lewis et al., 2002) (Fang et al., 2005), macaques (Johnson et al., 2009) and in humans (Priddy et al., 2019), an approach also referred to as vectored immunotherapy (VIT). Several studies have demonstrated the efficacy of VIT as an immunoprophylaxis in murine models of HIV, hepatitis C virus (HCV), influenza and Ebola virus challenge (de Jong et al., 2014) (Balazs et al., 2012; Balazs et al., 2014) (Balazs et al., 2013; van Lieshout et al., 2018). In a simian-human immunodeficiency virus (SHIV) infection model of macaques, rAAV-delivered antibodies reached protective levels and controlled the infection, although in some animals anti-mAb antibody responses limited the therapeutic efficacy (Fuchs et al., 2015; Saunders et al., 2015). rAAV delivery of a broadly neutralizing antibody (bnAb) against HIV also was effective at suppressing the virus after antiviral therapy was discontinued in xenografted mice, thus in a therapeutic model (Horwitz et al., 2013). In both of these models, however, the use of an exclusively human pathogen required the use of a xenografted and thus immunodeficient host organism.

It therefore was impossible for these studies to investigate whether and how VIT synergized with and/or impacted the host's endogenous immune responses. A study on the effects of passive antibody therapy in HIV-infected individuals has evidenced an augmentation of host endogenous neutralizing antibody (nAb) responses (Schoofs et al., 2016). Similarly, the administration of sub-protective levels of HIV-nAbs to perinatally SHIV-infected rhesus macaques accelerated the animals' nAb response and improved virus control (Ng et al., 2010).

Prolonged exposure to persisting antigen causes $CD8^+$ T cells to undergo "exhaustion" (Mueller and Ahmed, 2009b), corresponding to a distinct functional and phenotypic differentiation profile as originally described in chronic lymphocytic choriomeningitis virus (LCMV) infection of mice (Gallimore et al., 1998; Moskophidis et al., 1993; Zajac et al., 1998).

Expression of various inhibitory receptors such as PD-1 and LAG3, reduced cytokine secretion upon peptide restimulation and an impaired proliferative capacity are the result of an altered transcriptional profile and epigenetic changes, which occur as CD8+ T cells undergo exhaustion (Barber et al., 2006; Day et al., 2006; Pauken et al., 2016; Scott-Browne et al., 2016; Sen et al., 2016; Wherry et al., 2007). Unlike antiretroviral therapy, which profoundly affects T cell functionality in HIV-infected patients (Streeck et al., 2008) a potential impact of passive antibody therapy and notably of VIT on $CD8^+$ T cell exhaustion remains elusive.

The spontaneous control of protracted or chronic LCMV infection reflects the concerted action of $CD8^+$ T cells and antiviral antibody responses (Bergthaler et al., 2009), both of which are dependent on CD4 T cell help. While LCMV-nAbs responses commonly arise only weeks after viral clearance, owing to the viral glycan shield (Sommerstein et al., 2015a) non-neutralizing IgM and IgG antibodies directed against the outer globular domain of the envelope glycoprotein (GP-1) have been shown to correlate with viral control (Bergthaler et al., 2009). Also non-neutralizing antibodies against the virion-internal NP of LCMV have demonstrated antiviral efficacy by yet incompletely defined mechanisms (Richter and Oxenius, 2013; Straub et al., 2013).

In this study we have used rAAV technology to deliver the LCMV GP-1-specific nAb KL25 to mice with chronic LCMV infection. Our observations reveal that VIT synergizes with both, CD8+ T cell and endogenous antiviral antibody responses, to clear the infection and prevent mutational escape. Further we found that VIT antagonized CD8+ T cell exhaustion and enhanced in antiviral B cell and ASC responses. Our observations establish VIT as an attractive new modality of antiviral therapy with immunostimulatory effects reaching well beyond viral load control, thereby re-establishing endogenous immune control of chronic viral infection.

1.3 Materials and Methods

1.3.1 Mice and animal experimentation

C57BL/6 wild-type, T11µMT (Klein et al., 1997), $K^bD^{b-/-}$ (Pérarnau et al., 1999) and MD4 mice (Goodnow et al., 1988) were bred at the Laboratory Animal Services Center (LASC) of the University of Zurich. Occasionally, C57BL/6J mice were also purchased from Charles River Laboratories. For experiments, animals were housed at the University of Basel Haus Petersplatz animal facility. Animals were always housed under specific-pathogen-free (SPF) conditions. All experiments were conducted at the University of Basel, according to the regulations of Swiss law for animal protection and with authorization by the Cantonal veterinary office.

1.3.2 Viruses, focus forming assays and plaque reduction neutralization tests

The generation of the reverse-genetically engineered LCMV strain Clone 13 virus expressing the LCMV-WE glycoprotein (rCl13) has been described previously (Penaloza-MacMaster et al., 2015b). rCl13 stocks were produced on baby hamster kidney (BHK-21) cells. The LCMV strain Docile (Pfau et al., 1982) was propagated on Madin-Darby canine kidney (MDCK) cells. Infection was performed at a multiplicity of infection (MOI) of 0.01 and supernatant was collected 48 hours later. Viral titers were assessed by focus forming assays (Battegay et al., 1991b). Mice were infected with a dose of 2-3x10^6 plaque forming units (PFU) intravenously (i.v.) into the tail vein.

Focus forming assay was performed to assess the titer of LCMV in blood or in cell culture supernatants (virus stocks). 50 µl of blood was collected into 950 µl of BSS-heparin (Na-heparin, 1 IE/ml final, Braun, Germany) solution and was stored at -80°C prior to titration. Cell culture supernatant was frozen as collected. Undiluted and serial 10-fold dilutions of the virus

or blood were prepared, and 200 µl of each dilution was transferred to a 24-well. Blood or virus stocks were diluted in Minimum Essential Medium Eagle (MEM, Sigma-Merck, Germany) supplemented with 2% fetal calf serum (FCS). 3T3 cells were trypsinized and 200 µl of cell suspension at a density of $6x10^5$ cells per milliliter (ml) were seeded onto the virus-containing specimens in the 24-well plates. Following 2-4 hours of incubation at 37 °C, 200µl of overlay (2 % Methylcellulose in ddH2O, mixed 1:1 with 2x Dulbecco's Minimum Essential Medium Eagle (DMEM)) was added to each well. 48 hours later, the medium was flicked off from the plates and the cells were fixed with 4% paraformaldehyde (PFA) solution for 30 minutes at room temperature (RT). Permeabilization of the cells was performed using BSS with 1% Triton X-100 (Merck, Germany) at RT for 20 minutes. Blocking was performed using PBS with 5% FCS for 30 minutes. Anti-LCMV NP antibody staining was performed with a rat-anti-LCMV-NP monoclonal antibody (VL-4) in PBS supplemented with 2.5% FCS (RT for 60 minutes). After a washing steps, the plates were incubated with HRP-labelled goat-anti-rat IgG antibody in PBS, supplemented with 2.5% FCS at RT for 60 minutes. HRP-substrate solution (PBS containing 2.5% FCS, 3,3'- diamino benzidine (0.5 g/l, DAB, Sigma-Merck, Germany), ammonium nickel sulphate in PBS (0.5 g/l), and 0.015 % H2O2 was added on the plates after washing.
LCMV neutralizing antibody titers were assessed by plaque reduction neutralization assays as described previously (Battegay et al., 1991a).

1.3.3 Production of recombinant AAV constructs and particles, and AAV administration

The transgene for KL25 encoded for the VDJ of the heavy chain followed by the heavy chain constant domain, then followed by a furin recognition site (R-K-R-R), a spacer (S-G-S-G), a foot-and-mouth-disease virus 2A peptide (F2A) and the light chain cDNA, for monocystronic expression of antibody heavy and light chains from a single open reading frame. Due to

payload limitations in AAV vectors, introns of antibody heavy and light chains were excluded from cloning into the recombinant AAV vector. The AAV backbone plasmids was obtained from the PENN Vector Core (Perelman School of Medicine, University of Pennsylvania, PA, USA). The KL25 transgene (synthesized by GenScript® (NJ, USA)) ORF was released from its backbone plasmid with using (New England Biolabs (NEB), MA, USA) and KpnI (NEB) restriction enzymes, and was ligated into the corresponding restriction sites in the multiple cloning site of two AAV backbone plasmids (pENN.AAV.CB7.CI and pENN.AAV.CMV.PI.WRPE, both provided by PENN Vector Core). Recombinant AAV (rAAV) particles with a capsid of AAV8 serotype were generated and the genome copy (GC) titer was assessed by a droplet digital (dd) PCR-based method at the PENN Vector Core (Lock et al., 2013). rAAV particles were administered intramuscularly (i.m.) into the thigh of mice at doses of either $1x10^{10}$ or $10x10^{11}$ GC.

1.3.4 Flow cytometry

Single cells suspensions were obtained by pushing the spleen through a metal mesh using a syringe plunger. Blood was collected in 5 ml staining buffer (PBS containing 2% FCS, 5mM ethylenediaminetetraacetic acid (EDTA) and 0.05% sodium azide, adjusted to mouse osmolarity). CD8+ T cells in spleen cell suspensions and in blood were stained with antibodies against CD8α (53-6.7), CD45R/B220 (RA3-6B2), CD244.2 (2B4, m2B4 (B6) 458.1), CD279 (PD1, 29F.1A12), TCF1 (C63D9) from BioLegend (CA, USA) or against CD223 (LAG-3, C9B7W) from eBioscience (CA, USA). Fluorophore-conjugated donkey anti-rabbit IgG (Poly4064) from BioLegend was used as a secondary antibody. For identification and phenotyping of B cells, antibodies against CD45R/B220 (RA3-6B2), CD138 (281-2), IgD (11-26c.2a), GL7 (GL7), CD38 (90) were purchased from BioLegend and anti-IgM (II/41) was purchased from eBioscience.

Antibodies against CD44 (IM7), CD45R/B220 (RA3-6B2), CD8α (Ly-2/53-6.7) were purchased from Becton Dickinson (BD) Biosciences (NJ, USA), F4/80 (BM8), CD4 (RM4-5), CD279 (PD1, 29F.1A12) and ICOS (C398.4A), CXCR5 (CD185, L138D7) were purchased from BioLegend and these antibodies were used to detect and phenotype CD4 T cells. For all stains, mouse osmolarity-adjusted medium was used (Williams et al., 1972). The Zombie UV^{TM} Fixable viability kit (BioLegend) was used to exclude dead cells as described in the manufacturer`s protocol. CD8+ T cells specific for the LCMV epitope GP33-41 were identified by MHC Class I tetramers (generously provided by the NIH tetramer core, Emory University Vaccine Center, GA, USA) using staining protocol as previously described (Gallimore et al., 1998). For the detection of NP-specific B cells, cells were stained with bacterially expressed fluorochrome-conjugated recombinant LCMV nucleoprotein (rNP) (Sommerstein et al., 2015a) as previously described (Fallet et al., 2016; Schweier et al., 2019). CD4+ T cells specific for the LCMV epitope GP_{66-77} were detected using MHC Class II tetramers (generously provided by the NIH tetramer core). For MHC Class II tetramer staining, splenocytes were prepared as described above. Cells were stained with Zombie UV^{TM} Fixable viability kit (BioLegend) at RT for 15 minutes in the dark with mouse osmolarity adjusted PBS. Cells were washed once with the staining buffer. After the wash, cells were incubated with fluorochrome-labelled GP_{66-77} for 1 hour at 37°C in a 5% CO_2 incubator. Then, cells were washed once with the staining buffer. Cells were, then, incubated with fluorochrome-labelled CXCR5 antibody at RT for 1 hour. Cells were washed once with the staining buffer. Cells were incubated with rest of the staining antibodies (CD44, CD8, F4/80, CD4, PD1and ICOS) at 4°C for 15 minutes. Cells were washed once more and fixed with 2% PFA (Merck, Millipore, Germany). As MHC class II tetramer staining background control, all samples were pooled and incubated with human an MHC Class II tetramer loaded with the $CLIP_{87-101}$ epitope (hCLIP, PVSKMRMATPLLMQA, NIH tetramer core) instead of the

aforementioned tetramer, the rest of the protocol was performed analogously. All the stainings were performed in staining buffer unless mentioned otherwise.

For intracellular cytokine staining (ICS) spleen single cell suspensions were incubated with CD107a (LAMP-1, 1D4B, Biolegend), and restimulated with GP_{64-79} peptide (GPDIYKGVYQFKSVEF, 95% purity, immunograde) (1 µg/ml) or GP_{33-41} peptide (KAVYNFATC) (1 µg/ml) for 5 hours at 37°C in a 5% CO_2 incubator. Brefeldin A (5 µg/ml) was added to the cells 1 hour after the addition of peptide followed by additional 4 hours of incubation. After the 5-hour stimulation period, the cells were fixed with 2% PFA for 5 min. Fixation was followed by permeabilization (permeabilization buffer (staining buffer containing 0.05% saponin (Sigma-Merck, Germany). The antibodies used for ICS were specific for IFN-γ (XMG1.2), TNF-α (MP6-XT22) were purchased from BioLegend, in conjunction surface staining with the antibodies against CD8α (53-6.7), CD45R/B220 (RA3-6B2) and CD4 (RM4-5), all of which were purchased from BioLegend. For flow cytometry measurements, a BD LSRFortessa™ (BD Biosciences) was used.

1.3.5 *In vivo* antibody depletion

Mouse anti mouse-CD8α/Lyt-2 (YTS 169.4) (Absolute Antibody, MA, USA) or rat anti-mouse-CD8α (YTS 169.4) (BioXcell, NH, USA) was administered at a dose of 200µg/ml intraperitoneally (i.p.) to mice on days -3, -1 and day 0, and biweekly thereafter until analysis on day 80. Mouse IgG2a anti-fluorescein antibody (4-4-20e) (Absolute Antibody) was administered as isotype control for mouse anti mouse-CD8α/Lyt-2 (YTS 169.4). Mouse-IgG2b (LTF-2) (BioXCell) was administed as isotype control for rat anti-mouse-CD8α (YTS 169.4). CD4-depletion antibody (YTS 191) (BioXCell) at a dose of 200 µg was administered i.p. 3 days and 1 day prior to infection.

1.3.6 ELISAs and ELISpot assays

LCMV glycoprotein (GP)-specific antibodies were measured by enzyme-linked immunosorbent assay (ELISA). A recombinant fusion protein consisting of the outer globular GP1 domain of the LCMV-WE glycoprotein fused to the human IgG constant domain (GP1-Fc) was used (Eschli et al., 2007b). The analogous construct for the Docile GP1 sequence was generated by cDNA synthesis (GenScript): The Docile GP1 sequence in the resulting expression plasmid was also mutated in a site-directed manner to express the $GP1^{N119S}$ and $GP1^{N119Y}$ variants for use in ELISA assays. IgG1 and IgG2c isotype-specific ELISAs were conducted to differentiate AAV-delivered and endogenous antibody responses, respectively. To perform isotype specific ELISAs, 96-well high binding plates were coated with anti-human IgG Fc specific antibody (JacksonImmunoResearch Europe Ltd, UK) in coating buffer (15 mM Na_2CO_3 35mM $NaHCO_3$ dissolved in ddH_20, pH: 9.6) and incubated overnight at 4°C. The following day, the coating solution was flicked off and the plate was incubated with blocking buffer (5% milk powder PBS-Tween-20 (5%) (PBS-T) (Merk, Germany) at RT for 2 hours. Then, the blocking buffer was flicked off and the respective glycoproteins ($GP1^{N119S}$-Fc or $GP1^{N119Y}$-Fc) were diluted in the blocking buffer and were added to the plates, followed by incubation at RT for 1 hour. Plates were washed 3X with PBS-T. Then, serum from mice was diluted and placed in the wells accordingly and incubated at RT for 1 hour. Plates were washed 3X with PBS-T. HRP-conjugated Anti-IgG2c (Bethyl Laboratories, TX, USA) or HRP-conjugated anti-IgG1 (Zymed (now ThermoFischer) Laboratories, MA, USA) antibodies were diluted in blocking buffer and were distributed into the respective plates. The plates were washed 3X with PBS-T and once with PBS. Then the color reaction solution (2.8 ml Solution A (0.1M Citric acid anhydrous (Fluka) dissolved in ddH_20), 2.2 Solution B (0.2M $Na_2HPO_4.7H_20$ (Sigma, Germany) dissolved in ddH_20), 5ml ddH_20, 10µl H_20_2, 10mg ABTS (2,2'-Azino-bis(3-ethylbenzothiazoline-

6-sulfonic acid) diammonium salt, 2,2'-azino-di-[3-ethylbenzthiazoline sulfonate (6)])), Sigma-Merck, Germany) was added to the wells and 15 minutes later absorbance was measured on an ELISA reader (Safire II™, Tecan Group Ltd, Switzerland). Naïve serum was used to determine technical backgrounds.

Enzyme-linked immunospot (ELISpot) assays were used to quantify the NP-specific antibody secreting cells (ASCs) in the bone marrow and in spleens of mice as described (Schweier et al., 2019). Briefly, single cell suspensions of bone marrow (BM) and splenocytes were prepared. Erythrocytes were lysed and 96-well Multiscreen assay plates (Millipore, Merck) were activated with 35% EtOH. Plates were coated with rNP (3µg/ml) by overnight incubation. Plates were blocked with medium and 2 hours later the cells were plated with 10^6 cells/well followed by 3-fold dilutions. Horseradish peroxidase labeled rabbit-anti mouse Fcγ-specific antibody was used as detection antibody. As substrate, 3-Amino-9-ethylcarbazole (AEC) substrate kit was used (BD Biosciences). Spots were counted by an ImmunoSpot ® reader (CTL Europe GmbH, Germany).

1.3.7 Viral RNA isolation, cDNA synthesis and sequencing

For viral RNA isolation and sequencing, the serum of infected mice was used to infect BHK-21 cells. Virus-containing supernatant was harvested 48 hours later, and viral RNA was extracted using the QIAamp Viral RNA Mini Kit (QIAGEN) in accordance with the manufacturer`s protocol. cDNA synthesis and PCR amplification of the complete LCMV-Docile GP coding region was done using the OneStep RT-PCR kit (QIAGEN) according to the manufacturer`s protocol. An additional round of PCR amplification was performed using the Phusion High-Fidelity DNA Polymerase (New England Biolabs). The amplicons were run on a 1.5% agarose gel, were excised and then were purified using the QIAquick Gel Extraction Kit (QIAGEN) for

subsequent Sanger sequencing (Microsynth AG, Switzerland). (Primers for amplification and sequencing were LCMV GP forward primer: 5'- GCTGGCTTGTCACTAATGGCTC-3', LCMV GP reverse primer: (5'- TCAGCGTCTTTTCCAGATAG-3').

1.3.8 Data and statistical analysis

In order to compare a single parameter between two experimental groups, we have performed unpaired two-tailed Student`s t test. To compare a single parameter between multiple groups, one-way analysis of variance (ANOVA) was performed. To compare antibody responses between groups over time we determined the area under the curve (AUC) of the reverse antibody titer as displayed in the figures. The resulting values of the two groups were compared by Student's t test. Statistical tests were performed using Prism 8 for MacOS (version 8.1.1 (224)). ELISA titer calculation values were log-converted in order to reach a near-normal distribution for statistical analysis. Cell population frequencies obtained in flow cytometry were not log-converted for statistical analysis. *P* values <0.05 were considered statistically significant (*), *P* values <0.01 highly significant (**). FlowJo software (FlowJo LLC, version 10.5.3) was used for the analysis of the flow cytometry data.

1.4 Results

Prophylactic delivery of vectored immunotherapy confers protection against viral challenge

To optimize in vivo KL25 antibody delivery by AAV vectors, we compared a CMV promoter-driven (AAV-CMV-KL25) and a chicken beta-actin (CB7) promoter-driven expression cassette (AAV-CB7-KL25), both with an upstream enhancer element and a downstream intron sequence (Fig. 1.1A).

In order to check the levels and durability of KL25 antibody production *in vivo*, mice were given either AAV-CMV-KL25 or AAV-CB7-KL25 at doses of either 10^{10} or 10^{11} genome copies i.m. (Fig. 1.1B). KL25 levels in serum were determined by measuring LCMV glycoprotein-1 (GP-1) specific immunoglobulin titers over time. Irrespective of the construct, peak KL25 levels were reached by around day 13, which is compatible with a rapid onset and steady production of antibody, the levels of which reaching a plateau after approximately twice the half-life (~7 days (Vieira and Rajewsky, 1988)) of mouse IgG. At both vector doses tested, the CB7 promoter system yielded higher antibody titers than the CMV cassette (Fig. 1.1C). As expected, the in vivo synthesized KL25 antibody was neutralizing as determined by plaque reduction neutralization tests (PRNT, Fig.1D). The AAV-treated mice were followed for 250 days demonstrating that KL25 levels in the serum remained at high levels, at least when relying on CB7 driven expression (Fig. 1.1C-D).

On day 250 after prophylactic administration of rAAV-CB7-KL25, we challenged the corresponding mice and untreated controls (Fig. 1.1B) with a recombinant LCMV strain Clone 13 expressing the glycoprotein (GP) of the LCMV-WE strain (rCl13). This virus can establish chronic infection and is neutralized by KL25 (Penaloza-MacMaster et al., 2015b; Sommerstein et al., 2015a). Accordingly, viremia was high on day 5 after challenge of control mice but was

significantly suppressed by AAV-KL25 prophylaxis given 250 days earlier (Fig. 1.1D). Hence, rAAV delivered KL25 afforded long-term protection against chronic LCMV challenge.

Therapeutic delivery of vectored-immunotherapy clears established virus infection

Amongst the main goals of this study was to understand the efficacy of VIT in established chronic infection. Therefore, mice were infected with rCl13, and 4 days later VIT was administered, the control group was given PBS (Fig. 1.1F). Virus loads were suppressed and viremia was cleared in VIT-treated animals around 2 weeks post-treatment. In the untreated group the mice remained viremic (Fig. 1.1G). In the untreated group, GP-1 binding antibodies were detectable, but lower than in VIT-treated groups, at least until day 31 after infection (Fig. 1.1H). Neutralizing antibodies were only detectable in the VIT treatment group, identifying VIT as their source (Fig. 1.1I). Interestingly, neutralizing antibody titers were lower in rCl13-infected mice receiving AAV-KL25 than in controls without infection, raising the possibility that in the infected VIT-group AAV-produced nAbs might be "consumed" by viral antigen, perhaps in the form of immune complexes. Irrespective thereof, these set of experiments demonstrated the functionality of VIT as a means to prevent the establishment of chronic LCMV infection.

VIT-mediated clearance and control of escape mutants in the chronic phase of infection relies on the host's cellular and humoral immune defense

rCl13 persists in blood of adult wild-type (WT) mice for only about 20-30 days. To investigate the impact of VIT on established chronic infection (day 20 after infection, Fig. 1.2A), when T cell responses commonly show signs of profound exhaustion, we therefore exploited another strain of LCMV (LCMV Docile), which has been shown to establish viremia for 60-90 days (Moskophidis et al., 1995). Further, we set out to test for a potential contribution of the host's

endogenous antibody and CD8 T cells to VIT-mediated virus control. For this we tested MHC class I knockout mice (K^bD^b -/-), which lack $CD8^+$ T cells while retaining normal Vβ diversity in other T cell compartments (Pérarnau et al., 1999). Additionally, T11μMT mice were used, which express a transgenic IgM heavy chain directed against the glycoprotein of vesicular stomatitis virus (VSV) on a Cμ-deficient background (Klein et al., 1997). Hence, these animals are unable to mount significant LCMV-specific antibody responses despite unimpaired antiviral CD4 T cell responses (Bergthaler et al., 2009). Prior to VIT treatment on day 20, viral loads in blood of WT, T11μMT and $K^bD^{b-/-}$ mice were comparable (Fig. 1.2B). By day 44, VIT had completely suppressed viremia in WT mice, and viral loads remained at or below detection limits throughout day 57 while untreated WT controls remained highly viremic (Fig. 1.2B). On day 44, VIT also suppressed viral loads in $K^bD^{b\ -/-}$ and T11μMT mice to below the levels of the respective untreated control animals. Thereafter, however, viral loads rebounded, such that VIT failed to exert a clear effect on viremia at later time points. MD4 mice carrying rearranged heavy and light chains specific for Hen-egg lysozyme (HEL (Goodnow et al., 1988)) were used as a second independent model of B cell receptor repertoire restriction, confirming that VIT was ineffective in the absence of endogenous LCMV-specific antibody responses (Fig. 1.S1A). Analogous findings were also made in CD4 T cell-depleted mice, which were examined for an involvement of helper T cells in VIT-mediated clearance (Fig. 1. S1B). Accordingly, WT mice were the only experimental group to efficiently clear LCMV upon VIT, as also independently confirmed by viral load measurements in brain, kidney, liver and lung (Fig. 1.S2). In light of these findings we measured LCMV GP-1 specific antibody responses in WT, KbDb and T11μMT mice without VIT to assess the animals' capacity to mount antiviral antibody responses. The responses in T11μMT mice were around or below detection limits, as expected. To our surprise, however, also $K^bD^{b-/-}$ exhibited clearly impaired humoral responses (Fig. 1.2C). In $K^bD^{b-/-}$ and T11μMT mice given VIT treatment GP-1 specific antibody titers were

high, as expected. The corresponding titers in WT mice were somewhat above those in $K^bD^{b-/-}$ and T11μMT mice, which was most likely due to differential viral loads and "consumption" (Fig. 1.2C, compare Fig. 1.1G).

Rebound viremia in VIT-treated $K^bD^{b-/-}$ and T11μMT mice raised the possibility of viral mutational escape from KL25 selection pressure. Thus, we sequenced the glycoprotein of the viruses persisting in the blood of VIT-treated or untreated $K^bD^{b-/-}$ and T11μMT mice, as well as the viruses of untreated WT mice. In addition, we determined the glycoprotein sequence of virus circulating in the blood of VIT-treated WT mice immediately prior to clearance ("pre-extinction" virus). We found that in untreated mice, irrespective of their genotype, the consensus sequence of the persisting virus remained identical to the inoculum, i.e. no escape mutations were detectable (Fig. 1.2D-E). In contrast, the viruses persisting in VIT-treated T11μMT, MD4 and CD4 T cell-depleted WT mice exhibited a prototypic KL25 escape mutation (N119S) (Fig. 1.2D-E, Fig. 1.S1C). Escape mutations at position 119 of the glycoprotein were also consistently found in VIT-treated $K^bD^{b-/-}$ mice, albeit of a different type (N119Y) and often in conjunction with a K423R mutation in GP2. The latter mutation is of unknown biological significance.

The AAV-delivered KL25 is of the IgG1 isotype, whereas the host endogenous antibody response to LCMV consists of 90% IgG2a/c (Coutelier et al., 1987). To determine whether the antibody response of WT mice covered KL25 escape mutants we hence determined IgG2c antibodies binding to either Docile wt GP-1 or to the N119S- and N119Y- mutants thereof. On day 50 after infection, the sera of WT mice had significantly higher Docile-GP-1^{WT}-specific antibody titers than those of $K^bD^{b-/-}$ or T11μMT mice (Fig. 1.2F). While $K^bD^{b-/-}$ seroreactivity was clearly detectable, GP-1-specific antibodies of T11μMT were below detection limits, as expected. While WT mice consistently mounted substantial Docile-$GP1^{N119S}$ binding antibody responses (Fig. 1.2G), $K^bD^{b-/-}$ mice had very low to undetectable titers, and T11μMT sera were

devoid of such responses (Fig. 1.2G). When assessing Docile-GP1^{N119Y} specific antibody responses a similar pattern was noted (Fig. 1.2H), These sets of experiments suggested that successful clearance of chronic LCMV infection by VIT depended on CD8 T cells and host endogenous antibody responses.

CD8 T cell depletion interferes with effective VIT-mediated suppression of viral loads

In light of defective antibody responses in KbDb -/- (compare Fig. 1.2F-H) we sought a second independent experimental model to assess the contribution of CD8 T cell responses to VIT-mediated virus control. We depleted CD8 T cells throughout the course of chronic infection (Fig. 1.3A) by means of either the widely used rat-anti-mouse CD8 depletion antibody (RαCD8) or by the corresponding murinized version (mouse-anti-mouse CD8, MαCD8). MαCD8 but not RαCD8 effectively depleted CD8 T cells throughout day 24 after infection (Fig. 1.3B). Even in MαCD8-treated mice, however, CD8 T cells gradually re-emerged at later time points prompting us to analyze viremia on day 29. VIT significantly reduced viral loads in the blood of isotype control antibody-treated animals (Fig. 1.3C). Conversely, VIT was virtually ineffective in CD8-depleted mice, which remained highly viremic. Importantly, endogenous antibody responses against GP-1^{WT} as determined on day 29 were unaffected by CD8 depletion (Fig. 1.3D). This finding was in line with the observations in KbDb-/- mice, lending independent support to the concept that CD8 T cells synergise with VIT in antiviral control. We also analyzed B cell responses at the end of time point of the experiment. Neither CD8-depletion nor VIT altered the size of the splenic B cell compartment on day 80 after infection (Fig. 1.3E). Strikingly, however, MαCD8- as well as RαCD8-treated mice exhibited a substantially reduced germinal center B cell compartment (Fig. 1.3F), irrespective of VIT. These late effects of CD8 T cell depletion on GC B cells were reminiscent of the unexpected humoral immune defects in in KbDb-/- mice and warrant further investigation in future studies.

VIT augments endogenous virus-specific antibody responses, specific B cell frequencies and antibody-secreting cells

The failure of VIT-mediated virus-control in B cell repertoire-restricted T11μMT mice (compare Fig. 1.2B) led us to investigate a potential impact of VIT on the host's endogenous humoral immune response. We found that VIT-treated mice mounted higher titers of Docile-GP1^{WT} specific IgG2c than untreated controls (Fig. 1.4A). An analogous trend was also noted for NP-specific IgG2c titers, although failing to reach statistical significance (Fig. 1.4B). In contrast, antibody responses against Docile-GP1^{N119S} and Docile-GP1^{N119Y} were comparable in VIT-treated and untreated groups (Fig. 1.4C-D).

Higher LCMV-specific antibody levels raised the possibility that virus-specific B cell responses and antibody secreting cells (ASCs) were augmented by VIT. VIT did not affect the size of the B cell compartment overall (Fig. 1.4E, Fig. 1.S3). Neither did VIT affect splenic frequencies of isotype-switched (IgM^{neg}IgD^{neg}) B cells or plasma cells / plasmablasts (Fig. 1.4E-G, Fig. 1.S3). In stark contrast, NP-specific B cells were substantially enriched in VIT treated WT mice (Fig.4H-I). Also, the number of NP-specific germinal center B cells (GC B cells, GL7^{+} CD38^{-}) were significantly augmented upon VIT treatment (Fig. 1.4J). Next, we performed ELISpot assays to enumerate NP-specific antibody secreting cells (ASCs). VIT clearly augmented virus-specific ASC numbers in spleen but not in bone marrow (Fig. 1.4K).

We also investigated antiviral B cell responses in K^{b}D$^{b\ -/-}$ mice. Unlike in WT mice, NP-specific class-switched B cell numbers in K^{b}D$^{b\ -/-}$ mice were in the technical background range, independently of VIT (Fig. 1.4H-I). These observations were in line with impaired antibody responses in K^{b}D$^{b\ -/-}$ mice (compare Fig. 1.2F-H). T11μMT mice served as technical controls in these experiments and were negative.

Taken together, these data indicated that virus-specific B cell and ASC responses were augmented upon VIT. The mechanisms underlying this effect remain to be investigated.

VIT partially reverts CD8 T cell exhaustion

Viral persistence results in T cell exhaustion (Gallimore et al., 1998; Moskophidis et al., 1993; Wherry et al., 2003; Zajac et al., 1998). We therefore assessed whether VIT interfered with exhaustion. The overall size of the splenic $CD8^+$ T cell compartment was unaffected by VIT (Fig. 1.5A-B, Fig. 1.S4), and also the frequency of $CD8^+$ T cells (CTLs) specific for the immunodominant GP33 epitope remained unaltered (Fig. 1.5B, Fig. 1.S4). NP396-specific CD8 T cell responses were very low, as expected (Zajac et al., 1998). Chronic LCMV infection has recently been shown to promote the formation of a subset of CD8+ T cells expressing the master transcription factor T-cell factor 1 (Tcf-1). Here we found that VIT diminished the proportion of Tcf-1 expressing CTLs (Fig. 1.5C). Conversely, intracellular staining for the cytokines IFN-γ and TNFα and surface detection of the lytic granule marker CD107a upon GP33 peptide stimulation did not reveal any clear differences between VIT-treated mice and untreated controls (Fig. 1.5D). Importantly, however, VIT consistently reduced expression levels of the inhibitory receptors programmed cell death protein 1 (PD-1) and lymphocyte-activation gene 3 (LAG3), whereas 2B4 levels remained altered (Fig. 1.5E-F). Altogether, reduced PD-1 and LAG3 levels in conjunction with a lower proportion of Tcf-1-expressing antiviral CD8+ T cells demonstrated that VIT counteracted CTL exhaustion, presumably by lowering viral loads (Mueller and Ahmed, 2009b).

Virus specific CD4 T cell and Tfh compartments shrink upon VIT-mediated suppression of viral loads

An assessment of the CD4+ T cell compartment did not reveal any VIT-related changes in cellularity (Fig. 1.6A, Fig. 1.S5). Interestingly, however, the total number of CD4+ T cells responding to the immunodominant GP66 epitope was somewhat lower in VIT-treated as compared to untreated controls (Fig. 1.6B). Also, the number of GP66-specific CD4+ T follicular helper cells (PD-1^+ $CXCR5^+$; Tfh) was reduced as compared to untreated control mice (Fig. 1.6C). In contrast, intracellular cytokine staining following GP66-peptide stimulation did not reveal any VIT-related differences in CD4 T cells producing either IFN-γ or TNFα (Fig. 1.6D). Of note, such Th1-differentiated CD4 T cells were substantially (~10-fold) less abundant than the corresponding Tfh population of the same specificity (compare Figs. 1.5C and 1.5D), which is known to be driven and augmented by persisting viral antigen (Brooks et al., 2006; Crawford et al., 2014; Oxenius et al., 2001). Reduced overall numbers of (mostly Tfh-differentiated) antiviral CD4+ T cells in VIT-treated animals may thus be a direct consequence of viral load control.

1.5 Discussion

The present study delineates how vectored antibody delivery synergizes with and impacts on the host's endogenous immune defense. Importantly, we found that passive antibody not only has the potential to clear persistent infection (de Jong et al., 2014) but can also restore the host's own antiviral CD8+ T cell and antibody control of arising escape variants. This observation is particularly encouraging for infections with highly mutable viruses such as HIV, where passive antibody coverage of all possible genetic variants is difficult to achieve.

Functional restoration of antiviral CD8+ T cells upon antiviral therapy has previously been documented in human and simian immunodeficiency virus infection (Ndhlovu et al., 2019), and passive antibody administration was shown to augment endogenous nAb responses (Schoofs et al., 2016). Our study goes significantly beyond these earlier observations by documenting that the host's endogenous immune defense contributes essentially to systemic virus control upon passive immunization. Furthermore, our work establishes a cellular correlate of enhanced endogenous antibody responses upon passive antibody therapy: Higher numbers of virus-specific B cells overall and inside germinal centers in particular, as well as elevated numbers of antiviral antibody-secreting cell numbers in spleen. The underlying molecular events remain to be investigated. Plausible mechanisms comprise i) reduction of viral antigenic loads, ii) Enhanced antigen presentation to B cells by means of Fc receptor-mediated display of antibody-complexed antigens on follicular dendritic cells and iii) modulation of CD4+ T follicular helper cell (Tfh) function. Of note though, VIT diminished rather than augmented antiviral Tfh numbers, which is in line with chronic infection being a potent driver of Tfh differentiation and population expansion (Harker et al., 2011; Xin et al., 2018). The negative impact of VIT on Tfh population size was, however, modest and still compatible with the overall beneficially effect of VIT on antiviral B cell responses. Furthermore, a potential beneficial effect of VIT on Tfh functionality remains to be investigated. The VIT effect on

inhibitory receptors by antiviral CD8 T cells is likely related to reduced antigen loads (Mueller and Ahmed, 2009b). A complete loss of PD-1 and/or LAG3 expression was not to be expected, since it represents a differentiation program that persists even when CD8 T cells from chronically infected mice are adoptively transferred into completely antigen-free hosts (Utzschneider et al., 2013). We have not detected a clear impact of VIT on CD8+ T cell functionality or numbers though. The synergistic antiviral effect of VIT and CD8+ T cell responses therefore likely relied on these "exhausted" cells' antiviral efficacy, which is at least partially retained throughout the course of chronic infection (Johnson et al., 2015).

We acknowledge that augmented antiviral antibody titers in VIT-treated mice could be the result of "consumption" by high antigen levels and therefore a relative lack of detection rather than of production in untreated controls. The augmentation of antiviral B cells as determined by flow cytometry and, most notably, of antiviral antibody-secreting cells in ELISpot assays should not, however, be confounded by antigenic loads. The augmentation of splenic ASC responses in VIT-treated animals indicates, therefore, that VIT effects on humoral immune defense extends well beyond simple antibody "unmasking".

Our observations of impaired antiviral antibody responses to chronic LCMV infection in MHC class I-deficient $K^bD^{b-/-}$ mice were unexpected. Unimpaired antibody responses to virally vectored immunization (Pinschewer laboratory, unpublished data) suggest this humoral immune defect of $K^bD^{b-/-}$ mice is context-dependent, i.e. specifically related to chronic infection. In line with this interpretation, defective germinal center responses of CD8+ T cell-depleted WT mice at late stages of chronic LCMV infection argue in favor of a specific role of CD8+ T cells in supporting humoral immunity in the chronic infection context. The recent discovery of CXCR5-expressing antiviral CD8+ T cells inside germinal centers of chronically infected mice may represent a cellular correlate of CD8+ T cells "helping" B cells (He et al., 2016; Im et al., 2016; Leong et al., 2016; Utzschneider et al., 2016), yet such a potential link

requires further investigation. Unfortunately, long-term antibody depletion of CD8+ T cells failed in chronically LCMV-infected mice, even when murinized depletion antibody was used to avoid anti-antibody responses. Inefficient depletion beyond the first ~30 days of infection was supposedly due to defective FcγR-dependent phagocytosis (Wieland et al., 2015; Yamada et al., 2015).

Finally, we acknowledge that LCMV infection of mice can only recreate some but clearly not all relevant immunological features of chronic viral diseases of human such as HIV, HCV or HBV infection. The gradual loss of CD4 T cells with progression of HIV infection, for example, is likely to curtail the synergy of VIT with endogenous immune defense. Similarly, the excessive abundance of HBs in the serum of congenital HBV carriers may trigger mechanisms of humoral immune subversion, which are not recreated in LCMV infection (Burton et al., 2018; Salimzadeh et al., 2018)

In summary, the present work in immunocompetent animals with established chronic infection highlights previously underestimated immunological aspects of vectored antibody delivery on host endogenous immune defense and resulting virus control. Our observations should help to better position and leverage VIT as an innovative new tool in combating persistent viral diseases by revealing previously underappreciated reciprocal interactions between antiviral antibodies, germinal center B cell responses and CD8+ T cells in the context of chronic viral infection.

1.6 Figures

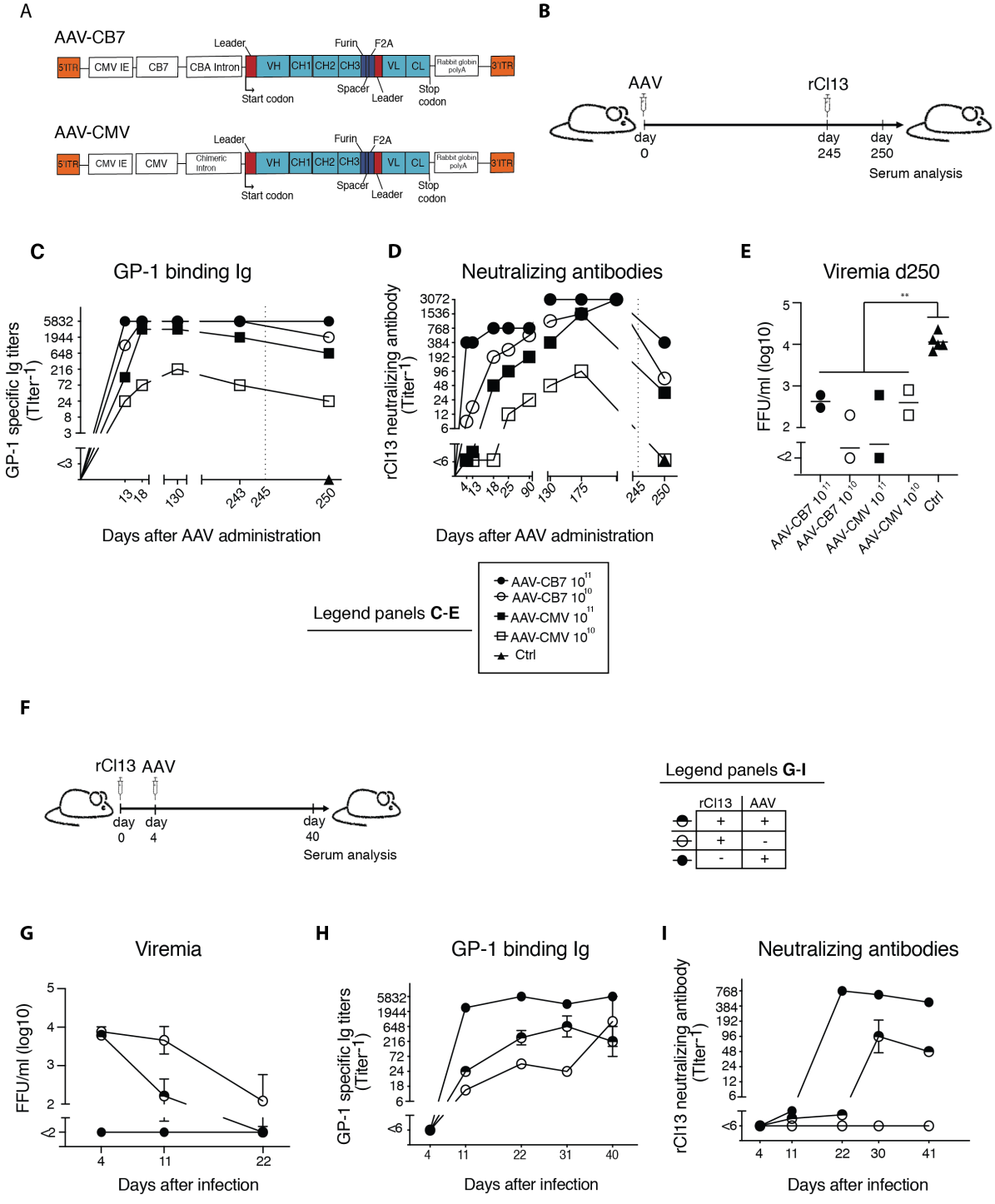

Figure 1.1: AAV-KL25 is effective as immunoprophylaxis against chronic LCMV challenge and can intercept chronic infection shortly after onset.

(A) Schematic of the rAAV-KL25 genomes. (B) Schematic of the experimental protocol for (C-E). WT mice were administered the indicated doses of rAAV-CB7-KL25 or rAAV-CMV-KL25 i.m. on day 0. On day 245, these animals and previously untreated controls were challenged with rCl13. We measured serum KL25 titers by ELISA against LCMV GP-1 (C)

and by plaque reduction neutralization tests (PRNT, D). (E) 5 days post challenge viremia was assessed. (F) Schematic of the experimental protocol for (G-I). We measured the viral titers in blood (G), LCMV GP-1-specific serum Ig titers by ELISA (H) rCl13-neutralizing antibodies by plaque reduction neutralization test (I). Symbols and bars represent the mean ± SEM (C,D,G-I) or individual mice (E). Number of biological replicates (n) = 2 to 5 (C-E), n = 4 (G-I). Number of independent experiments (N) = 1 (C-E), N = 2 (G-I). Unpaired two-tailed Student's t test. $^{**}P < 0.01$. ns, not significant.

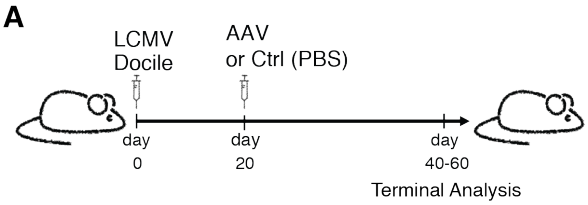

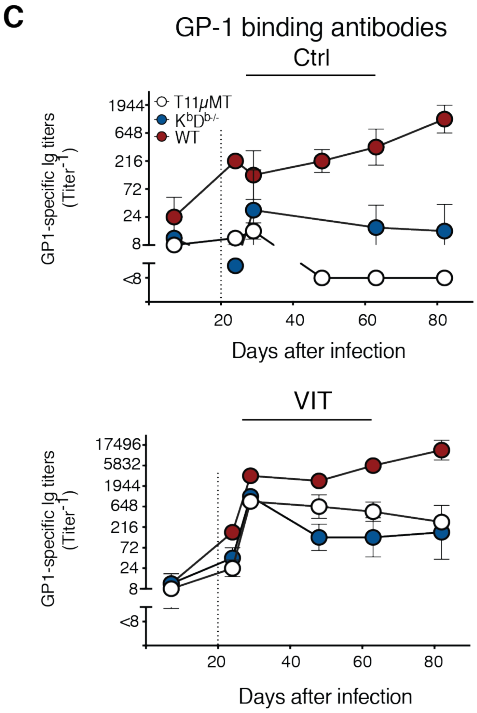

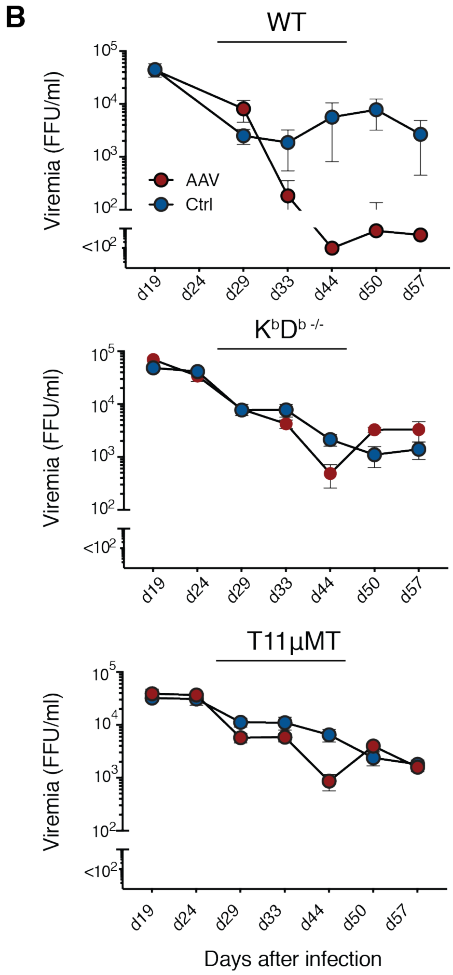

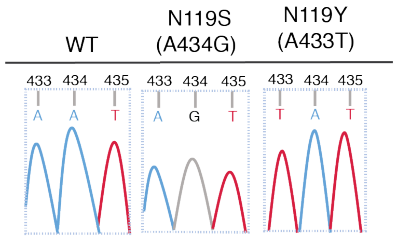

E

Mouse genotype	Occurrence of N119 KL25 escape mutation (# mice with viral mutation / # mice tested) AAV	No treatment
Wildtype	6/11	0/18
CD8 T cell deficient ($K^bD^{b-/-}$)	3/3	0/4
T11μMT	8/8	0/8

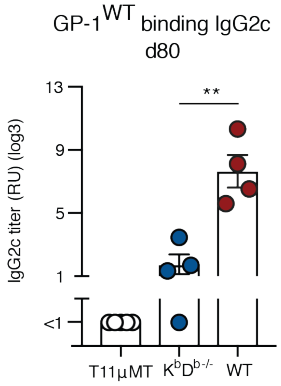

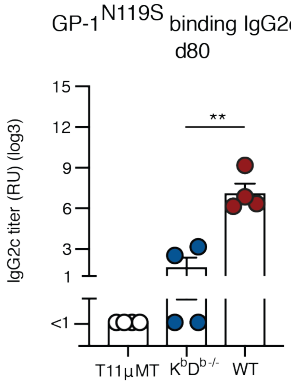

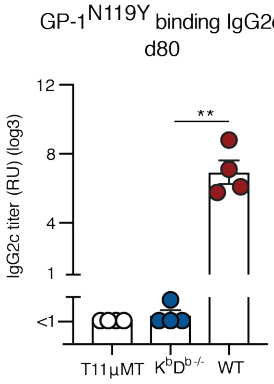

Figure 1.2: Clearance in VIT-administered mice relies on endogenous CD8 T cell and antibody responses.

(A) Schematic of the experimental protocol. We infected WT, $K^bD^{b-/-}$ and T11μMT mice with LCMV Docile and 20 days later the mice were given either VIT (AAV) (10^{11} GC) or PBS (Ctrl) i.m. (B) Viremia was assessed on the indicated time points. (C) LCMV GP-1 specific antibody titers were measured by ELISA. (D) Representative chromatograms of wild-type LCMV Docile and the two commonly found viral escape mutations. (E) Table reporting the occurrence of the two commonly found viral escape mutations. We measured LCMV GP-1^{WT} binding IgG2c (F), LCMV GP-1^{N119S} binding IgG2c (G) and LCMV GP-1^{N119Y} binding IgG2c (H) by ELISA. Symbols in (B-C) and bars in (F-H) represent the mean ± SEM, symbols in (F-H) show individual mice. Number of biological replicates (*n*) = 3 to 5 per experiment (B,C,F-H). Number of independent experiments (*N*) = 2 (A-C and F-H and for E (T11μMT groups), (*N*) = 1 (E, for sequencing of $K^bD^{b-/-}$ groups) and, (*N*) = 3 (E, WT-AAV groups), (*N*) = 4 (E, WT No treatment group). Data sets were analyzed with unpaired two-tailed Student's t test (F-H). $^{**}P < 0.01$. n.s., not significant.

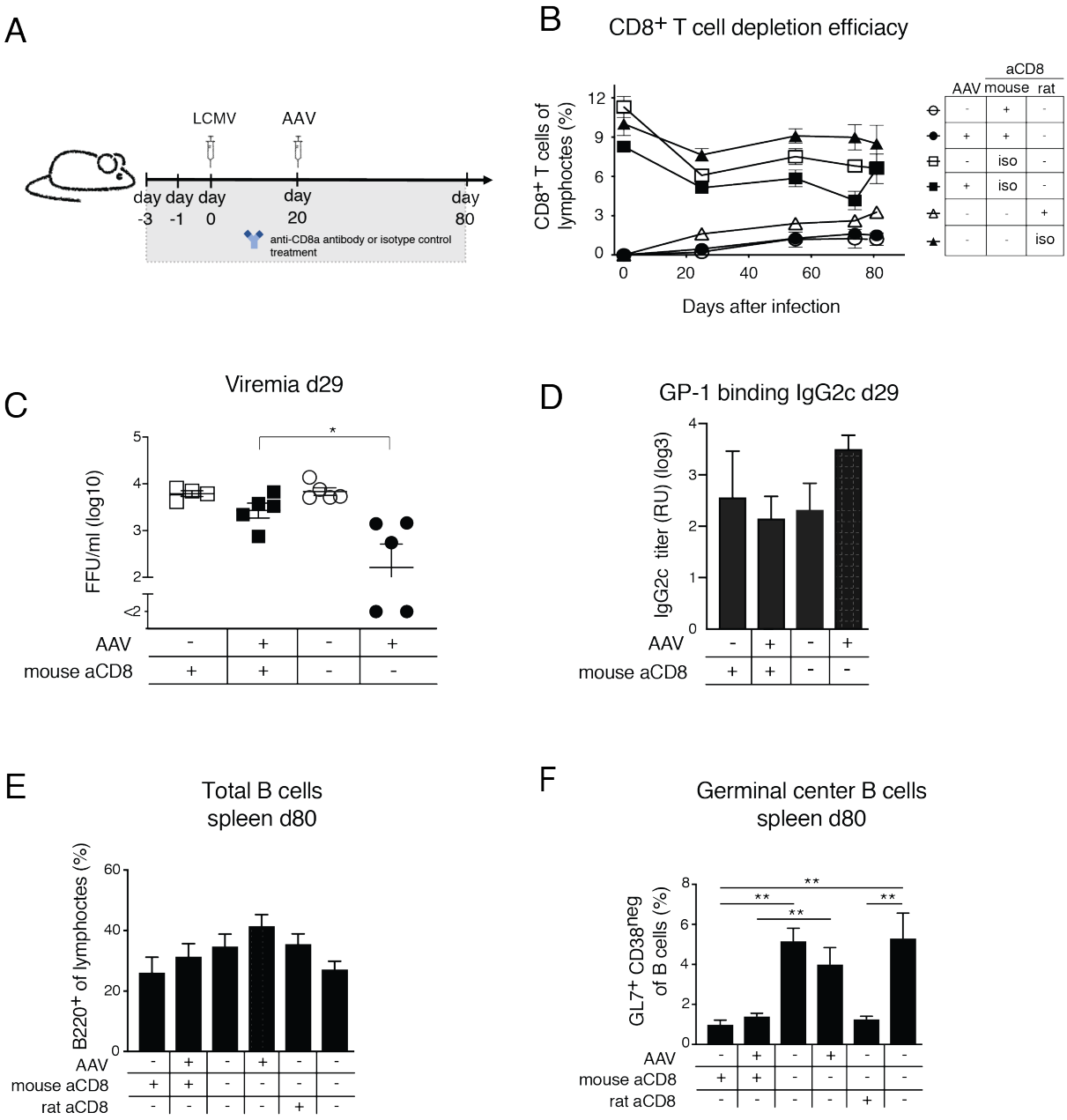

Figure 1.3: VIT is ineffective in CD8 T cell-depleted mice despite unimpaired endogenous antibody responses.

(A) Schematic of the experimental protocol. Mice were either given CD8a depletion antibody (day -3, -1 and 0 of infection and twice weekly thereafter) or isotype control antibody. On day 20 VIT or diluent was administered, and the mice were followed for 80 days. (B) Longitudinal analysis of CD8 depletion efficiency. (C) Viral titers in blood on day 29. (D) We measured LCMV GP-1 binding IgG2c by ELISA on day 29. (E) Frequency of $B220^{+}$ $CD138^{neg}$ B cells within the lymphocyte population on day 80 in the spleen. (F) Frequency of $B220^{+}$ $CD138^{neg}$ $GL7^{+}$ $CD38^{neg}$ germinal center B cells within the $B220^{+}$ $CD138^{neg}$ B cell population on day 80 in the spleen. Symbols and bars represent the mean ± SEM (B,D-F) or individual mice (C). Number of biological replicates (n) = 5 (B-F) per experiment. Number of independent experiments (N) = 1 (A-F). Data sets were analyzed with Student's t test (C) and one-way ANOVA (D-F). *$P < 0.05$; **$P < 0.01$; ns, not significant.

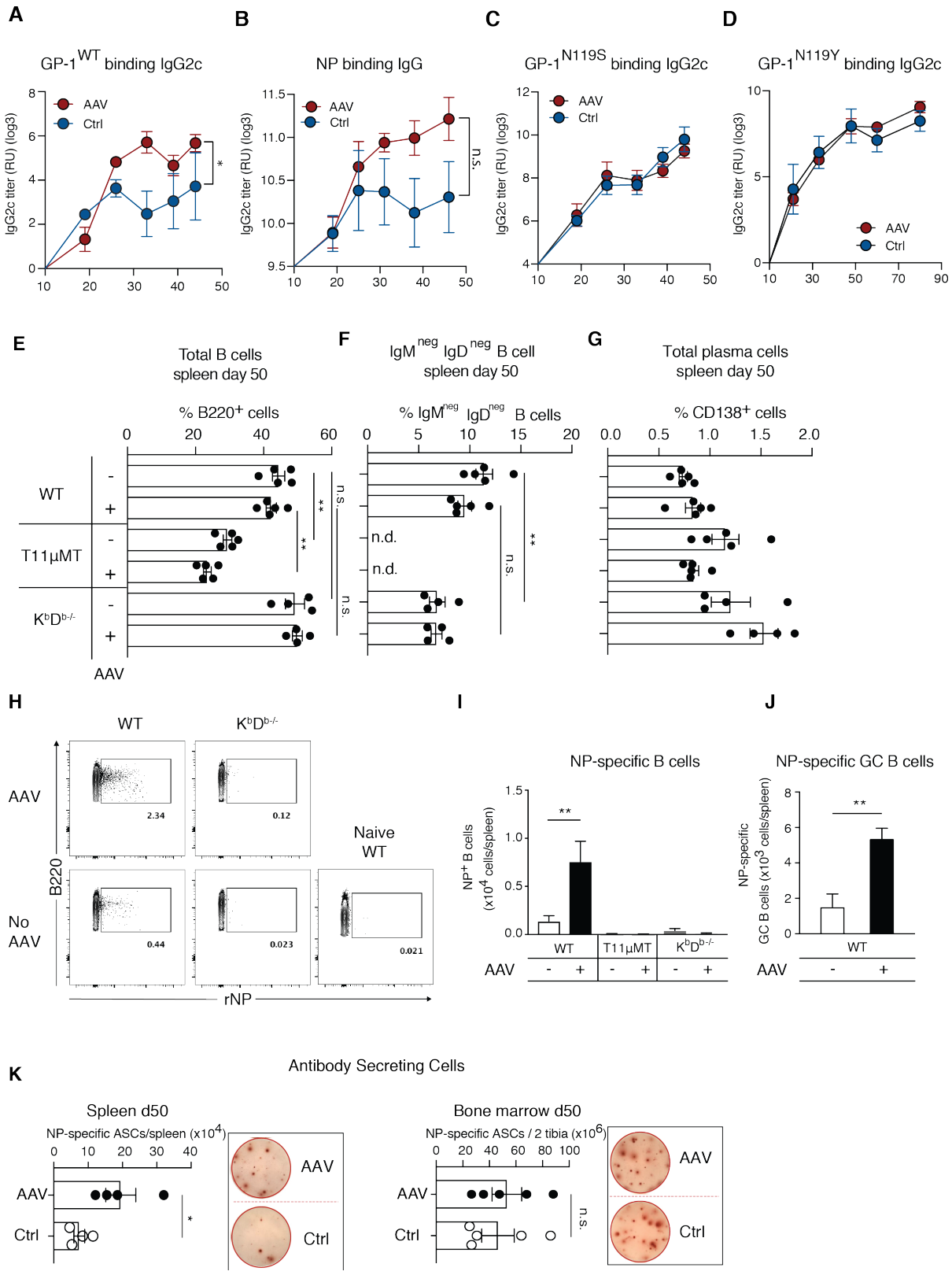

Figure 1.4: VIT-treated mice mount stronger virus-specific antibody, B cell and ASC responses.

We infected WT mice with LCMV Docile and administered VIT 20 days later, analogously to the experiment described in Fig. 2. LCMV GP-1^{WT} binding IgG2c titers (A), LCMV

nucleoprotein- (NP-) binding IgG2c responses (B), LCMV GP-1^{N119S}- (C) and LCMV GP-1^{N119Y}-binding (D) IgG2c titers were measured by ELISA over time. On day 50 we sacrificed the mice and measured the frequency of total B220^{+} B cells amongst viable lymphocytes (E), IgM^{neg}IgD^{neg} B cells (F) and CD138^{+} ASCs in the spleen (G). (H) Representative flow cytometry plots gated on B220^{+} CD138^{neg} IgM^{neg} IgD^{neg} B cells binding to recombinant LCMV nucleoprotein (rNP). (I) Absolute numbers of rNP-binding B220^{+} CD138^{neg} IgM^{neg} IgD^{neg} B cells in the spleen. (J) Absolute numbers of rNP-binding germinal center (GL7^{+} CD38^{neg}) B220^{+} CD138^{neg} IgM^{neg} IgD^{neg} B cells in the spleen. (K) LCMV NP-specific antibody secreting cells were enumerated in the spleen (left panel) and in bone marrow (BM, right panel) by ELISpot assay. Representative assay wells are displayed (A-D, I-K) or individual mice. Symbols in (A-D) and bars in (E-G, I-K) represent mean ± SEM, symbols in (E-G) show individual animals. (H) shows representative flow cytometry plots. Number of biological replicates (n) = 5 per experiment (A-G). Number of independent experiments (N) = 2 (A-G and K) and N=3 (H-J). Student's t test of the AUC values from individual mice between day 24 and day 44 was used to analyze the data from (A-D). Data sets were analyzed with one-way ANOVA (E-G), unpaired two-tailed Student's t test (I-K). *$P < 0.05$; **$P < 0.01$; ns, not significant. n.d., not determined.

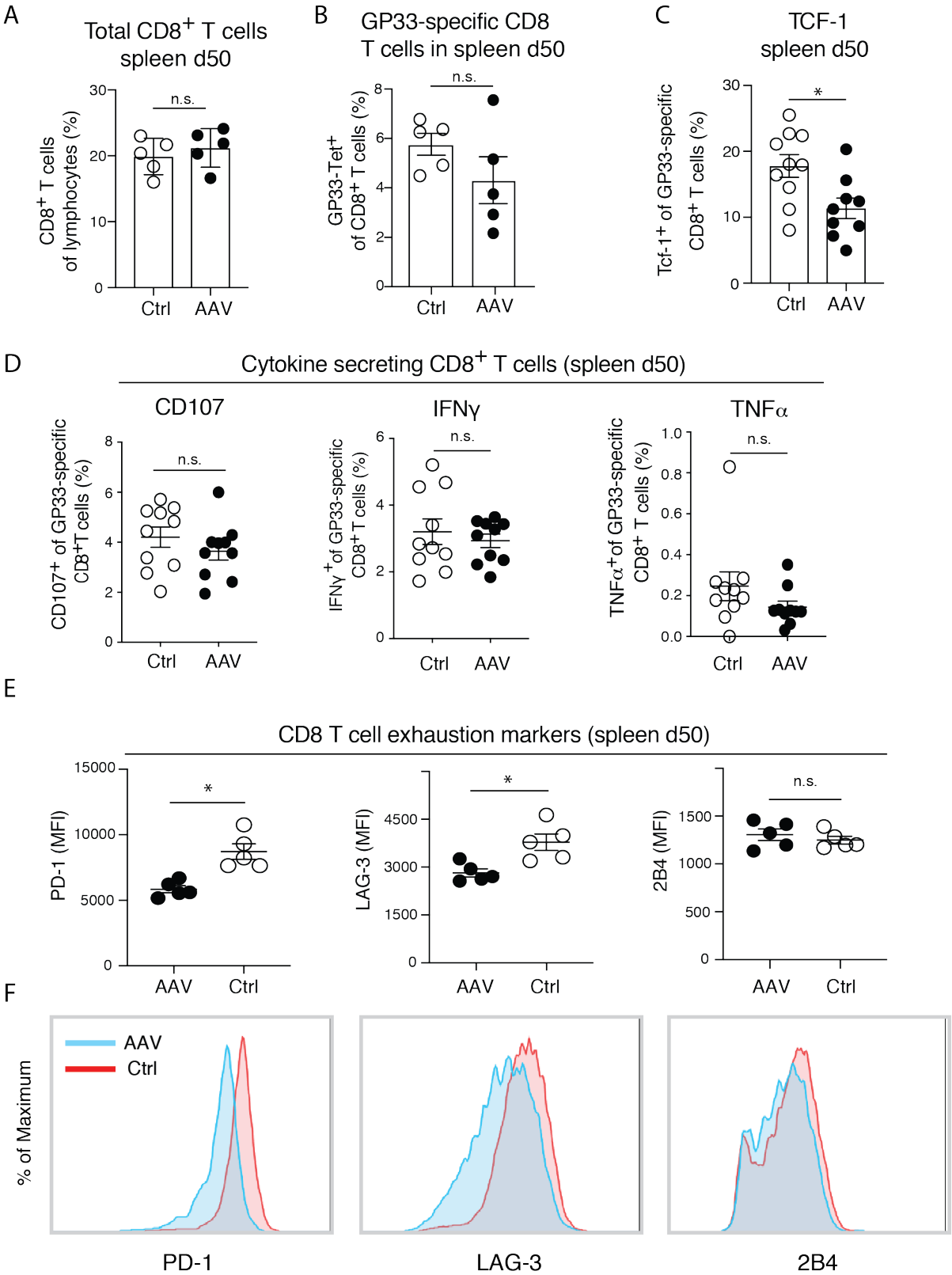

Figure 1.5: VIT reduces inhibitory receptor expression on antiviral CD8 T cells.

WT mice with LCMV Docile, followed by VIT or buffer control treatment on day 20, analogously to Fig. 2A. On day 50 the animals were sacrificed for T cell analysis in spleen. (A) $CD8^+$ T cells as a percentage of lymphocytes. (B) Percentage of virus-specific GP33-Tet^+ cells within the $CD8^+$ T cell compartment. (C) Percentage of Tcf-1^+ cells within GP33-Tet^+

$CD8^+$ T cell compartment. (D) We determined the frequency and functionality of GP33-specific $CD8^+$ T cells upon peptide stimulation by surface staining of CD107a and by intracellular cytokine staining for IFN-gamma (IFN-γ) and TNFα. (E) Expression levels of the exhaustion markers PD-1, LAG-3 and 2B4 on GP33-Tet^+ $CD8^+$ T cells. (F) The histogram plots from one representative animal in (E) are displayed. Bars represent mean ± SEM, symbols represent individual mice. Number of biological replicates (n) = 5 (A-E). Number of independent experiments (N) = 3 (A-F). Unpaired two-tailed Student's t test with $*P < 0.05$. ns, not significant.

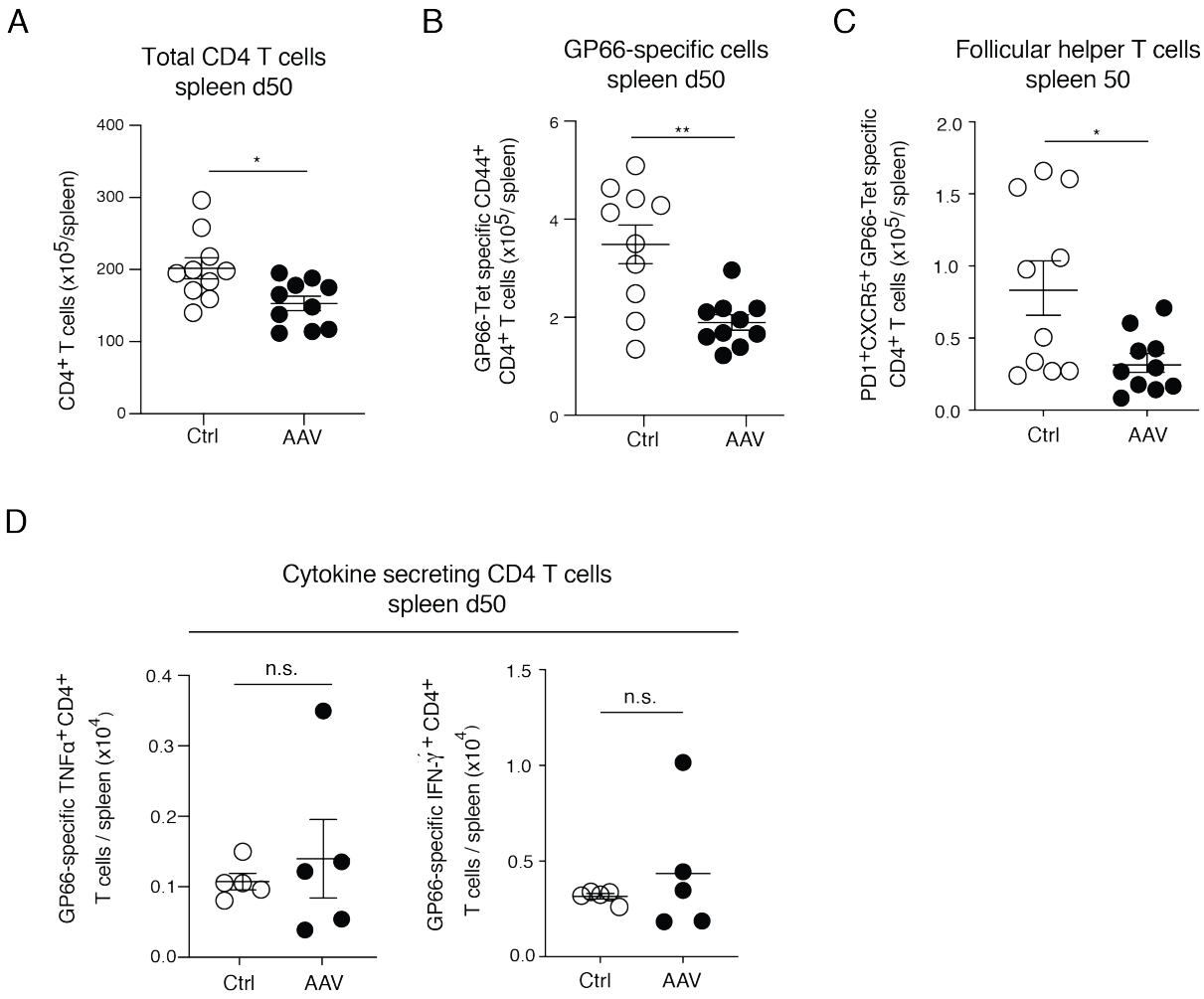

Figure 1.6: Reduced virus-specific total CD4 T cell and Tfh CD4 T cell responses upon VIT-mediated viral clearance.

We infected WT mice with LCMV Docile, followed by VIT or buffer control treatment on day 20, analogously to Fig. 2A. (A-C) Absolute numbers of $CD4^+$ T lymphocytes (A), $CD44^+$ GP66-Tet^+ T cells (B), and virus-specific Tfh (PD-1^+ $CXCR5^+$ $CD44^+$ GP66-Tet^+) $CD4^+$ T cells (C) were enumerated by flow cytometry. The numbers of GP61-80-specific IFN-γ- or TNFα-producing $CD4^+$ T cells were determined by intracellular cytokine assays (D). Symbols represent individual mice. Number of biological replicates (n) = 5 (A-D) per experiment. Number of independent experiments (N) = 2 (A-D). Unpaired two-tailed Student's t test with $*P < 0.05$; $**P < 0.01$. ns, not significant.

1.7 Supplementary Figures

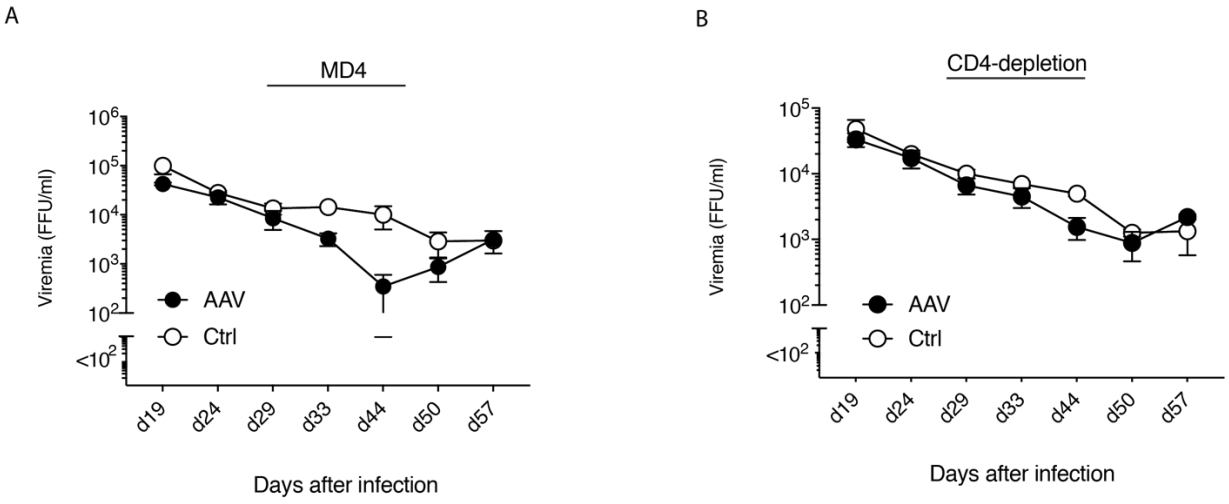

C

	Occurrence of N119 KL25 escape mutation (# mice with viral mutation / # mice tested)	
Mouse genotype	AAV	No treatment
MD4	3/3	0/2
CD4-depleted	3/3	0/3

Figure 1.S1: VIT fails to control chronic LCMV infection in CD4-depleted or BCR-restricted mice.

(A) We infected MD4 mice with LCMV Docile and 20 days later the mice were given either VIT (10^{11} GC) or PBS i.m. Viremia was assessed on the indicated time points. (B) anti-CD4 depletion antibody was administered i.p. to WT mice on days -3 and -1, and on day 0 the mice were infected with LCMV Docile. 20 days later the mice were given either VIT (10^{11} GC) or PBS i.m. Viremia was assessed on the indicated time points. (C) Table reporting the occurrence of the two commonly found viral escape mutations. Symbols and error bars in (A,B) represent means ± SEM. Number of biological replicates (n) = 2 (C) for MD4-VIT, for others (n) = 3 (A-C) . Number of independent experiments (N) = 1 for (A-C).

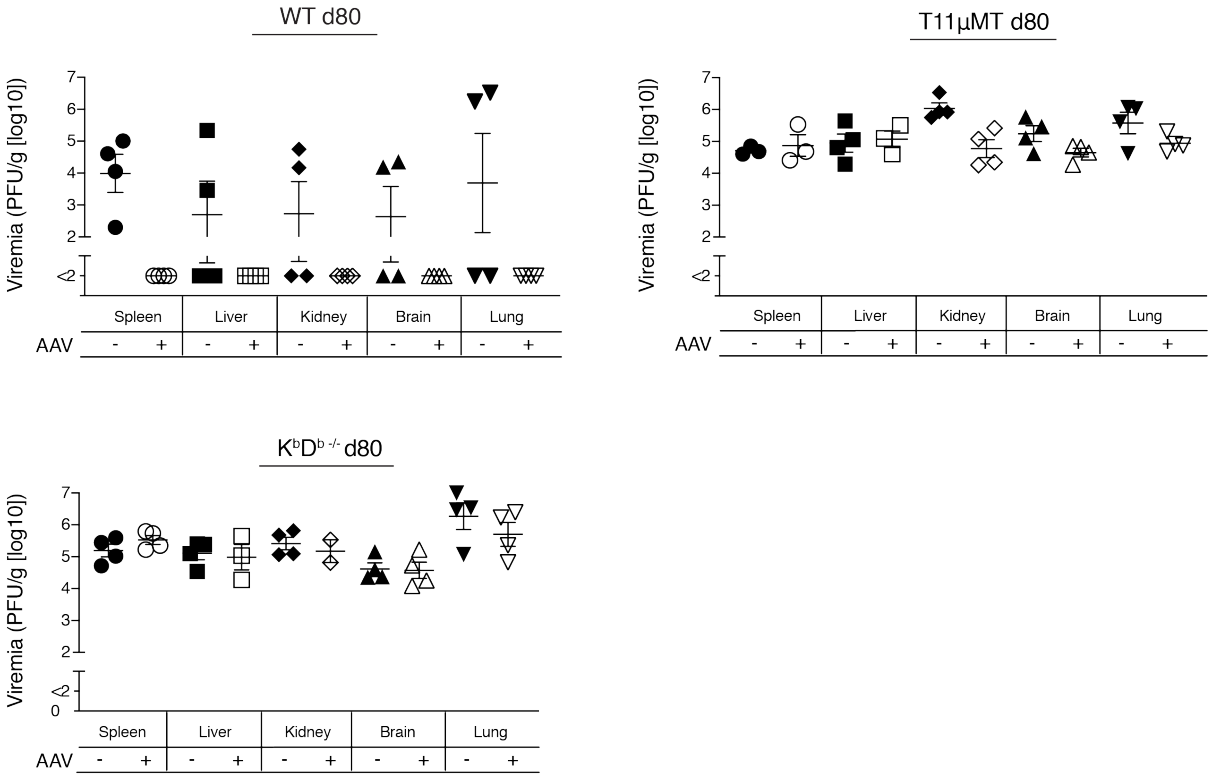

Figure 1.S2: VIT fails to clear chronic LCMV infection from the organs of mice lacking CD8 T cells or antiviral antibody responses.

Viral titers in the liver, spleen, kidney and lung of WT, $K^bD^{b-/-}$ and T11µMT mice on day 80 of the experiment displayed in Fig. 2. Symbols show individual mice, error bars represent means ± SEM. Number of independent experiments (*N*) = 2.

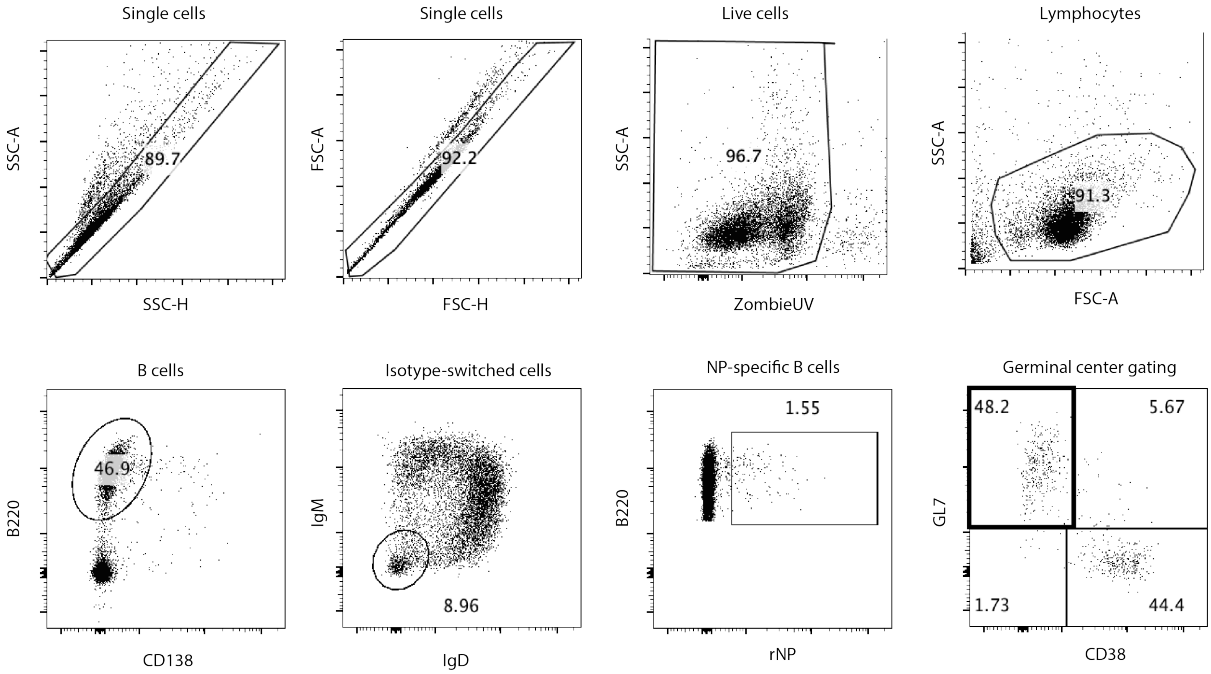

Figure 1.S3: Gating strategy to the FACS analysis in Figure 4E-J.

Single cells were gated in SSC-A / SSC-H plots followed by FSC-A / FSC-H gating. Then, Zombie-UV positive cells (dead cells) were excluded from further analysis. Next, lymphocytes were identified by their SSC-A / FSC-A profile. Subsequently, B cells ($B220^{+}$ $CD138^{neg}$) and, amongst B cells, isotype-switched cells (IgM^{neg} IgD^{neg}) were analyzed. rNP^{+} cells within this population were identified and, finally, GC cells ($GL7^{+}$ $CD38^{neg}$) within the rNP^{+} B cell population were gated.

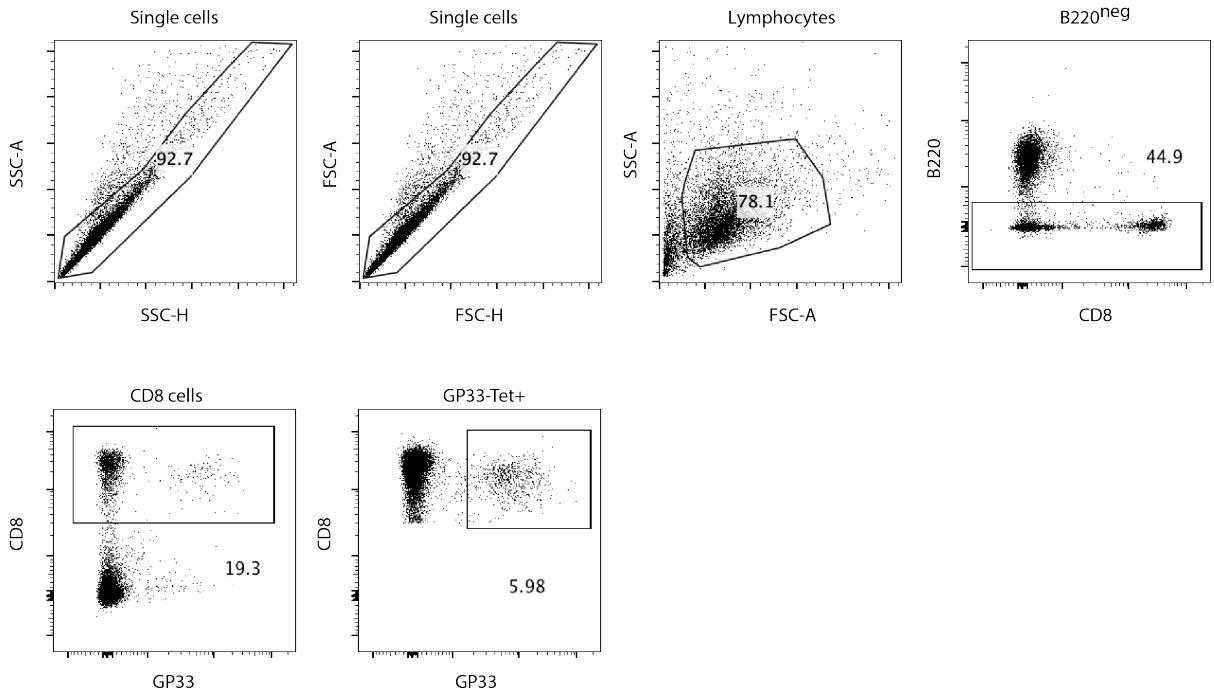

Figure 1.S4: Gating strategy to the FACS analysis in Figure 5A-F.

Single cells were gated on by using SSC-A and SSC-H gating followed by FSC-A and FSC-H gating. Lymphocytes were gated on according to SSC-A and FSC-A profile. This was followed by gating $B220^{neg}$ cells. Next, total $CD8^{+}$ cells within the $B220^{neg}$ population were gated Finally, GP33-Tet^{+} cells within the total CD8 population were gated.

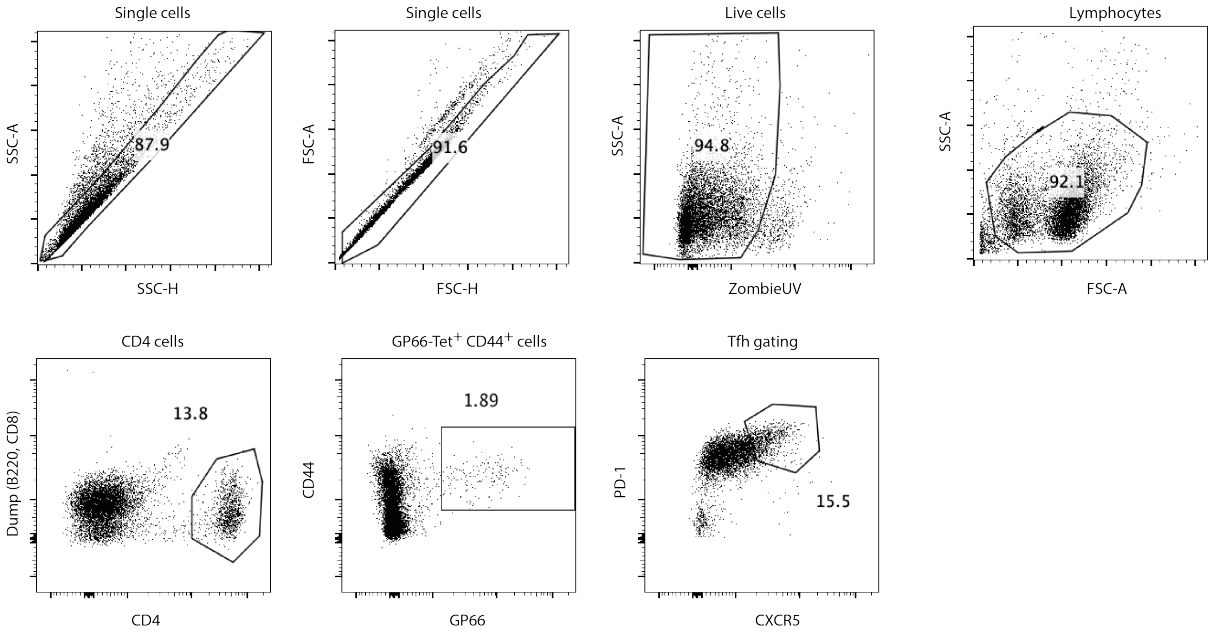

Figure 1.S5: Gating strategy to the FACS analysis in Figure 6A-D.

Single cells were gated by SSC-A / SSC-H followed by FSC-A / FSC-H. Then, Zombie-UV positive (dead cells) were excluded from further analysis. Lymphocytes were gated according to their SSC-A / FSC-A profile, followed by the identification of $CD4^+$ $CD8^{neg}$, $B220^{neg}$ cells (CD4 T cells) within the lymphocyte population. Next, $CD44^+$ GP66-Tet^+ cells within $CD4^+$ population were identified. Finally, $CXCR5^+$ $PD\text{-}1^+$ cells within the $CD44^+$ GP66-Tet^+ CD4 T cell population were gated as follicular helper T cells.

2. Interferon-driven decimation of antiviral B cells at the onset of chronic infection

Benedict Fallet[1*], Kerstin Narr[1*], Yusuf I. Ertuna[1], Melissa Remy[1], Rami Sommerstein[2], Karen Cornille[1], Mario Kreutzfeldt[2,3], Nicolas Page[2], Gert Zimmer[4], Tobias Straub[5], Hanspeter Pircher[5], Kevin Larimore[6,7], Philip D. Greenberg[6,7], Doron Merkler[2,3] & Daniel D. Pinschewer[1,#]

Affiliations

[1] Department of Biomedicine, Division of Experimental Virology, University of Basel, 4003 Basel, Switzerland.

[2] Department of Pathology and Immunology, Geneva Faculty of Medicine, 1211 Geneva 4, Switzerland.

[3] Division of Clinical Pathology, University Hospital Geneva, 1 rue Michel Servet, 1211 Geneva 4, Switzerland

[4] Institute of Virology and Immunology IVI, 3147 Mittelhäusern, Switzerland.

[5] Institute for Immunology, Department for Medical Microbiology and Hygiene, University Medical Center Freiburg, 79104 Freiburg, Germany

[6] Fred Hutchinson Cancer Research Center, University of Washington, Seattle, WA 98109, USA.

[7] Department of Immunology, University of Washington, Seattle, Washington, WA 98109, USA.

*B.F. and K.N. contributed equally to this work

#Correspondence: daniel.pinschewer@unibas.ch

2.1 Abstract

Immune subversion represents a hallmark of persistent infection, but microbial suppression of B cell responses remains mechanistically ill-defined. Adoptive transfer experiments in a chronic viral infection model evidenced the rapid and profound decimation of B cells that responded to virus or to concomitantly administered protein. Decimation affected naïve and memory B cells and resulted from biased differentiation into short-lived antibody-secreting cells. It was driven by type I interferon (IFN-I) signaling to several cell types including dendritic cells, T cells and myeloid cells. Durable B cell responses were restored upon IFN-I receptor blockade or, partially, when depleting myeloid cells or key IFN-I-induced cytokines. B cell decimation represents a molecular mechanism of humoral immune subversion and reflects an unsustainable "all-in" response of B cells in IFN-I-driven inflammation.

2.2 One-sentence summary

Interferon-driven inflammation at the onset of chronic viral infection orchestrates unsustainable antibody production and decimation of antiviral B cell populations.

2.3 Results and discussion

Humoral immunity represents a cornerstone of antimicrobial host defense and vaccine protection. Infection-induced suppression of humoral immune defense is therefore predicted to further microbial persistence and pathogenesis, with the potential to thwart B cell-based vaccination efforts. Perturbed or dysfunctional B cell compartments represent a hallmark of persistent microbial diseases including HIV, hepatitis B, hepatitis C, malaria, schistosomiasis and tuberculosis (Joosten et al., 2016; Labuda et al., 2013; Moir and Fauci, 2014; Oliviero et al., 2011; Weiss et al., 2009). Besides delayed and inadequate antibody responses to the causative agent itself (Chen et al., 1999; Cohen et al., 2011; Peacock et al., 1973), consequences can consist in a generalized suppression of vaccine responses and B cell memory (Cunnington and Riley, 2010; Malaspina et al., 2005; Wheatley et al., 2016). In comparison to T cell exhaustion, however, the molecular mechanisms leading to viral subversion of the B cell system have remained less well defined.

Here we compared B cell responses to protracted LCMV infection (rCl13) and to recombinant vesicular stomatitis virus (rVSV) vaccine vectors. The two viruses were engineered to express the same surface glycoprotein (GP) as neutralizing antibody target, but served as prototypic models of chronic viremic and acute infection, respectively (Fig. 2.1A). To study antiviral B cell responses in mice, we adoptively transferred oligoclonal, traceable ($CD45.1^+$) KL25H B cells, which contain ~2% GP-specific cells owing to an immunoglobulin heavy chain knock-in (Fig. 2.S1A). The transferred KL25H cells mounted only transient GP-specific antibody responses to rCl13, whereas rVSV-induced responses were durable and of higher titer (Fig. 2.1B). Moreover, KL25H B cell numbers at four weeks after rVSV immunization were ~20-fold higher than after rCl13 infection (Fig. 2.1C). We obtained analogous results, both in spleen and inguinal lymph nodes (iLN), when adoptively transferring quasi-monoclonal KL25HL B cells (~85% GP-specific, Fig. 2.S1A, B), which express the matching immunoglobulin light chain transgene in addition to the heavy chain knock-in (Fig. 2.1D, 2.S1C). Four weeks after infection, KL25HL B cells populated the germinal centers (GCs) of rVSV-immunized mice but not of rCl13-infected animals (Fig. 2.1E). When studying KL25HL B cells in the first week of rCl13 infection, they proliferated vigorously and acquired a blast-like morphology within the first three days, but disappeared almost completely by day 6 (Fig. 2.1F, G). On day three, the majority of proliferating ($CFSE^{low}$) KL25HL B cells in rCl13-infected mice were apoptotic ($7AAD^+AnnexinV^+$, Fig. 2.1H), whereas KL25HL B cells responding to rVSV remained mostly viable. These observations suggested a near-complete apoptotic loss (referred to as

"decimation") of virus-neutralizing KL25HL B cells within days after the onset of rCl13 infection. By analogy to T cells (Mueller and Ahmed, 2009a), high antigen loads in rCl13 but not rVSV infection could have accounted for antiviral B cell decimation. Counter to this hypothesis, adoptive transfer of KL25HL B cells into neonatally infected immunologically tolerant rCl13 carrier mice (Pircher et al., 1989a) resulted in robust B cell and plasmablast/plasma cell (antibody-secreting cell, ASC) formation despite high-level viremia (Fig. 2.1I and 2.S1D; B cells and ASCs jointly referred to as "B cell progeny"). Furthermore, KL25HL B cell transfer on day 3 of rCl13 infection, when viremia had set in, yielded ~20-fold more B cell progeny than transfer at the onset of infection (Fig. 2.1J, K (Zellweger et al., 2006)). Day 3 transfer of KL25HL B cells resulted also in substantially higher neutralizing antibody (nAb) responses and in a more potent antiviral effect than transfer on the day of infection (Fig. 2.1L, M).

These observations argued against antigen overload as the root cause of KL25HL B cell decimation, suggesting rather that the inflammatory milieu at the onset of infection was unfavorable to sustained B cell responses. Intriguingly, this 3-day time window coincided with the strong systemic type I interferon (IFN-I) response in rCl13 infection (Fig. 2.2A). Moreover, rCl13-induced serum IFN-I responses clearly exceeded those induced by rVSV, and IFN-I was below technical backgrounds in rCl13 carriers, altogether suggesting an inverse correlation between systemic IFN-I levels and sustained antiviral B cell responses. IFN-I transcriptome signatures characterize chronic hepatitis C virus, pathogenic immunodeficiency virus infection and chronic active tuberculosis (Berry et al., 2010; Bolen et al., 2013; Mandl et al., 2008; Rotger et al., 2011), and IFN-I can exert detrimental effects on antiviral T cell responses (Teijaro et al., 2013; Wilson et al., 2013). Hence we speculated that rCl13-induced IFN-I accounted for antiviral B cell decimation. Antibody-based blockade of the type I interferon receptor (αIFNAR) resulted in ~20-fold more KL25HL progeny on day 3 of rCl13 infection (Fig. 2.2B, C). By day 15, αIFNAR blockade yielded >100-fold higher numbers of KL25HL memory B cells (memB) and GC B cells, both in spleen and iLN, and comparably elevated KL25HL progeny were found in bone marrow (BM, Fig. 2.2D and 2.S2A). By immunohistochemistry we detected KL25HL B cells in GCs of IFNAR-blocked mice but not of control-treated animals (Fig. 2.2E). To investigate whether also antigen-experienced B cells were sensitive to IFN-I-driven decimation, we expanded KL25H B cells *in vivo* (~50% GP-specific, Fig. 2.S2B) and transferred them to naïve recipients, followed by rCl13 challenge. αIFNAR blockade yielded significantly more KL25H PCs and memB on day 8 and day 67

after rCl13 challenge, respectively (Fig. 2.2F and 2.S2C). Performing immunohistochemistry on day 67, we readily detected KL25H B cells in GCs of IFNAR-blocked but not control-treated recipients (Fig. 2.2G). We extended these adoptive transfer experiments to polyclonal LCMV-experienced B cells of GFP-transgenic mice. On day 7 after rCl13 challenge, IFNAR-blocked recipients contained ~30-fold higher numbers of LCMV nucleoprotein (NP) -binding GFP^+ memB cell progeny than control-treated animals (Fig. 2.2H and 2.S2D). Altogether, this documented that not only primary responses of LCMV-specific KL25H and KL25HL B cells but also recall responses of antigen-experienced LCMV-specific B cells, both oligoclonal (KL25H) and polyclonal, were subject to IFN-I-driven decimation. Next we tested whether B cells of unrelated specificity, when activated concomitantly with rCl13 infection ("activated bystander B cells"), were similarly affected. We transferred traceable ($CD45.2^+$) vesicular stomatitis virus glycoprotein (VSVG) -specific B cells (VI10) into syngeneic ($CD45.1^+$) wt recipients. Subsequent immunization with VSVG triggered robust proliferation (CFSE dilution) and expansion of virtually all VSVG-binding VI10 B cells. This response was markedly reduced by concomitant rCl13 infection but completely rescued by αIFNAR, extending the concept of IFN-I-driven decimation to activated bystander B cells (Fig. 2.2I). The use of (non-replicating) VSVG protein in these experiments corroborated that cognate antigen loads could not readily explain rCl13-driven B cell decimation.

αIFNAR prevented KL25HL B cell apoptosis as determined by flow cytometry (AnnexinV/7AAD binding) and by active caspase-3 staining in histology (Fig. 2.3A-C). To better understand IFN-I-driven B cell decimation, we performed whole genome RNA sequencing on KL25HL B cells recovered on day 3 of rCl13 infection. A pronounced antibody-secreting cell signature (Shi et al., 2015) in control-treated cells was largely reversed by αIFNAR blockade (Fig. 2.3D). This effect was also evident in αIFNAR-mediated suppression of ASC-related transcription factors (TF, Fig. 2.S3A). Conversely, IFNAR blockade promoted/restored TF expression profiles, which are typical for mature B cell stages prior to ASC differentiation, and modulated also GC B cell-specific TFs (Fig. 2.S3B, C). In line with its effects on the cells' ASC gene signature, αIFNAR altered the expression of 10 out of 13 genes, which have been linked to terminal B cell differentiation in human HIV infection (Fig. 2.S3D, (Moir et al., 2004)). Flow cytometric analyses corroborated that IFNAR blockade impeded rCl13-induced ASC differentiation. As hallmarks of ASC differentiation, most KL25HL B cells in control-treated recipients lost B220, CD22 and CD23 expression as they proliferated (Fig. 2.3E). When IFNAR was blocked, a significantly higher proportion of

KL25HL progeny cells retained these markers. Conversely, fewer KL25HL cells up-regulated the ASC marker CD138^{+}, and their intracellular IgM levels were lower (Fig. 2.3E). Altogether these observations indicated that IFNAR blockade prevented specific B cell decimation by countering short-lived plasmablast differentiation.

To differentiate between B cell-intrinsic and –extrinsic IFNAR effects on B cell decimation we used IFNAR-deficient and –sufficient KL25HL B cells for adoptive transfer. Both B cell types expanded vigorously when challenged with rCl13 in *ifnar*$^{-/-}$ recipients but yielded low progeny numbers when responding in wt recipients (Fig. 2.4A). This suggested B cell-extrinsic IFN-I effects as the root cause of rCl13-induced B cell decimation. We extended these observations to activated bystander B cells. IFNAR-deficient and –sufficient VI10 B cells responded similarly to VSVG protein immunization, and both responses were equally suppressed by concomitant rCl13 infection (Fig. 2.4B). When using reciprocal wt and *ifnar*$^{-/-}$ BM chimeras as recipients we found that hematopoietic IFNAR expression was decisive for KL25HL B cell decimation (Fig. 2.4C). To dissect how IFNAR signaling in various immune cell types contributed to B cell decimation we exploited cell type-specific IFNAR deletion models. KL25HL B cell progeny were significantly more numerous when recipients lacked IFNAR in either T cells, dendritic cells (DCs) or myeloid cells. IFNAR deletion in the recipient's B cells only modestly augmented KL25HL ASCs, and neither of the above cell-type specific IFNAR deletion models fully phenocopied plain *ifnar*$^{-/-}$ recipients (Fig. 2.4D). Taken together, IFNAR signaling in several cell types, namely in DCs, myeloid cells and T cells contributed to rCl13-induced B cell decimation. The essential antiviral role of IFN-I may preclude the success of αIFNAR-based immunomodulatory therapy ((Sandler et al., 2014; Teijaro et al., 2013; Wilson et al., 2013), Fig. 2.S4A). Also T cells and DCs are widely recognized as essential components of antiviral immune defense (Probst and van den Broek, 2005; Schmitz et al., 1999), but inhibition or depletion of myeloid cells can be pursued to combat persistent infection and cancer (Norris et al., 2013; Wesolowski et al., 2013). Hence we tested whether, by analogy to myeloid cell-specific IFNAR deficiency, myeloid cell depletion could rescue KL25HL B cell responses. Albeit less dramatically than αIFNAR, also αGr-1 (Ly6C/G) antibody depletion, a widely used means to deplete myeloid cells in mice, augmented KL25HL progeny (Fig 2.4E). Of note, αGr-1 depletion did not substantially affect viral loads or serum IFN-I kinetics (Fig. 2.S4A,B), attesting to the potential utility of myeloid cell-targeting strategies for countering B cell decimation. In accordance with earlier reports, however, αGr-1 depleted not only inflammatory monocytes (InfMo) and neutrophils but also eosinophils, plasmacytoid dendritic

cells (pDCs) and Ly6C^{high} CD8^{+} T cells (Fig. 2.S4C, D). Yet, the individual depletion of neutrophils, eosinophils or pDCs did not increase KL25HL B cell progeny, and *cd8*$^{-/-}$ mice yielded only modestly elevated numbers of KL25HL ASCs (Fig. 2.S4E). NK cell depletion (Crouse et al., 2014; Xu et al., 2014) did not augment KL25HL progeny either (Fig. 2.S4F). To address a potential role of InfMo in B cell decimation we used both InfMo-deficient *ccr2*$^{-/-}$ and *klf4*$^{fl/fl}$*xVav1-icre* mice recipients (Fig. 2.S4G-I and (Tussiwand et al., 2015)). Neither model phenocopied the αGr-1 effect, and αGr-1 depletion improved KL25HL progeny recovery also in InfMo-deficient *ccr2*$^{-/-}$ recipients (Fig 2.S4I). Hence, the B cell-sparing effect of αGr-1 depletion likely represented its combined impact on multiple myeloid and perhaps even non-myeloid cell subsets. Thus we speculated that both αGr-1 and αIFNAR countered antiviral B cell decimation by altering virus-induced inflammation. When profiling the expression of 248 inflammation-related genes in spleen, 128 were altered upon rCl13 infection, and αIFNAR attenuated or prevented a majority of these inflammatory gene expression changes (Fig. 2.4F, 2.S5A, B, Tbl. SI). αGr-1 exerted analogous albeit more modest effects, which were largely overlapping with those of αIFNAR. Similar results were obtained from BM, indicating that treatment-related anti-inflammatory effects were not confined to lymphoid organs (Fig. 2.S5C,D, Tbl. SI). In a serum cytokine panel analysis, 19 out of 31 tested chemokines and cytokines increased at 24 and 72 hours after rCl13 infection, respectively, and were at least 4-fold suppressed by αIFNAR (Fig. 2.4G, Table. SII). Nine of these 19 were also significantly suppressed, albeit less potently, in αGr-1-treated animals. Taken together, IFNAR deficiency and, to a lesser extent also αGr-1, modulated rCl13-induced systemic inflammation, and most if not all αGr-1 effects on inflammation were comprised in the αIFNAR effect.

These observations raised the possibility that the IFN-I-induced inflammatory milieu in rCl13 infection caused B cell decimation by altering B cell survival and/or differentiation signals. This hypothesis predicted that i) the supplementation of survival signals and also ii) the depletion of deleterious inflammatory mediators or blockade of death pathways should augment specific B cell responses in rCl13 infection. In line with prediction i), KL25HL B cell transfer and rCl13 infection yielded ~10-fold more progeny when performed in transgenic recipients overexpressing the B cell survival factor BAFF (Fig. 2.4H). In attempting to test prediction ii) we used knock-out mouse models and antibody depletion approaches to assess the individual contribution of IL-1β, IL-4, IL-6, IL-10, IL-12, TNF-α, iNOS and FasL to rCl13-induced KL25HL B cell decimation. KL25HL B cells yielded significantly more progeny when challenged with rCl13 in IL-10-deficient or TNF-α-blocked recipient mice (Fig. 2.4I).

Interestingly, IL-10 as well as TNF-α have been linked to B cell dysfunction in HIV-1 infection (Macchia et al., 1993; Muller et al., 1998). While we failed to detect a statistically significant individual role for IL-1β, IL-4, IL-6, IL-12, iNOS or FasL in B cell decimation (Fig. 2.S6A,B), contributive effects of some of these and other IFN-I-induced factors and pathways (Kacani et al., 1997; Moir et al., 2004; Muller et al., 1998) remain likely, and may vary between infection settings. Accordingly, only their combined suppression alongside with IL-10 and TNF-α may account for the potent B cell-sparing effect of IFNAR blockade.

IFN-I driven B cell decimation reflects apparently an "all in" strategy of the humoral immune system when facing antigen in a highly inflammatory context. In acute life-threatening infections, this ASC differentiation bias may augment survival chances by maximizing early immunoglobulin production. It thus seems desirable from an evolutionary standpoint. Conversely, B cell decimation puts at risk the sustainability of humoral responses, both of naïve and immunized hosts, when confronted with persistence-prone pathogens. Repertoire replenishment by new bone marrow emigrants (Osmond, 1993; Zellweger et al., 2006) and GC-driven evolution of low-affinity clones are predicted to eventually compensate for early repertoire decimation. But these processes take time, and the sustained IFN-I transcriptome signatures in active tuberculosis, chronic hepatitis C virus and pathogenic immunodeficiency virus infection raise the possibility that B cell decimation extends into the chronic phase of infection (Berry et al., 2010; Bolen et al., 2013; Mandl et al., 2008; Rotger et al., 2011). In summary, IFN-I-driven B cell decimation offers a molecular mechanism for humoral immune subversion under conditions of microbial inflammation.

2.4 Materials and Methods

2.4.1 Viruses, virus titrations, infections and immunizations

Reverse genetically engineered LCMV strain Clone 13 expressing the LCMV strain WE glycoprotein (rCl13) has been described (Penaloza-MacMaster et al., 2015a). A recombinant vesicular stomatitis virus vector expressing the LCMV strain WE glycoprotein instead of VSVG (rVSV) was generated following established procedures and strategies (Kalhoro et al., 2009). rCl13 and rVSV were grown on BHK-21 cells and were titrated in viral stocks and blood samples as previously described (Pinschewer et al., 2004). Unless specified otherwise, rCl13 and rVSV were administered to mice intravenously (i.v.) at doses of $2x10^6$ and $8x10^6$ plaque-forming units (PFU), respectively. Adult infections were performed 30 min. after

adoptive B cell transfer. To establish an immunologically tolerant neonatal rCl13 carrier status, mice were administered $6x10^5$ PFU rCl13 into the skull within 24 hours after birth. VSV glycoprotein (VSVG) for immunization was produced in SF9 cells using a recombinant baculovirus as previously described (Burkhart et al., 1994). For VSVG immunization, 20 µg whole cell lysate was administered to mice i.v..

2.4.2 Flow cytometry and FACS sorting

To prepare single cell suspensions, tibiae were flushed and spleens were enzymatically digested using collagenase D (Roche) and DNAseI (Sigma-Aldrich). All cell media were adjusted to mouse osmolarity (Williams et al., 1972). Single cell suspensions were stained with fluorophore- or biotin-conjugated antibodies to detect the following markers and molecules: CD138 (clone 281-2), B220 (clone RA3-6B2), IgD (clone 11-26c.2a), CD45.1 (clone A20), CD45.2 (clone 104), CD22 (clone OX-97), CD23 (clone B3B4), CD8a (clone 53-6.7), Ly-6C (clone HK1.4), CD11b (clone M1/70), CD11c (clone HL3), CCR3 (clone J073E5), SiglecH (clone 551), NK1.1 (clone PK136), Thy1.2 (clone 30-H12) and CD19 (clone 6D5) from BioLegend; IgM (clone II/41), GL-7 (clone GL-7) and Ly-6G (clone 1A8) from eBioscience; CD95 (clone Jo2) and SiglecF (clone E50-2440) from BD Biosciences. Biotin-conjugated antibodies were detected using fluorophore-conjugated streptavidin (BioLegend). Dead cells were excluded using the Zombie UV™ Fixable viability kit (BioLegend). AnnexinV/7AAD staining (BD Biosciences) was performed to detect apoptotic cells by flow cytometry. To label GP-binding B cells for flow cytometric detection we used a recombinant fusion protein (GP-Strep-tag, (Sommerstein et al., 2015b)) consisting of the GP extracellular domain, fused to a C-terminal streptag (Twin-Strep-tag, IBA GmbH). Detection was performed using Strep-Tactin-PE (IBA Biosciences). To label VSVG-binding VI10 cells we used a recombinant fusion protein consisting of the VSVG ectodomain (sVSVG), fused to a C-terminal trimerization motif derived from T4 fibritin (foldon). sVSVG-binding cells were identified using Alexa647-labelled anti-VSVG antibody VI7 (Kalinke et al., 1996). GP-Strep-tag and sVSVG were produced by transient transfection in HEK-293 cells. For the identification of NP-binding B cells in flow cytometry we used bacterially derived and Alexa647-labelled recombinant NP (Sommerstein et al., 2015b). The cells were measured on Gallios (Beckman Coulter) and LSRFortessa (Becton Dickinson, BD) flow cytometers and data were analyzed with FlowJo software (Tree Star). For sorting of KL25HL B cells progeny, labeled with CFSE

prior to transfer and rCl13 challenge, splenocyte suspensions were stained with antibodies to B220, CD45.1 and CD45.2. We sorted $CD45.1^{+}CD45.2^{-}CFSE^{lo}B220^{int/hi}$ cells directly into TRI Reagent LS (Sigma-Aldrich) using an FACSAria II (Becton Dickinson, BD) cell sorter at the Flow Cytometry Core Facility of the University of Basel. RNA was extracted using the Direct-zol™ RNA MicroPrep kit (Zymo research).

2.4.3 Immunohistochemistry and image analysis

For immunohistochemical staining, tissues were fixed in HEPES-glutamic acid buffer-mediated organic solvent protection effect (HOPE, DCS Innovative) fixative as previously described (Bergthaler et al., 2007) and embedded in paraffin. Immunostaining was performed on 3 µm thick sections using antibodies against active caspase-3 (9661T, Cell Signaling) and CD45.1 (clone A20, FITC-labeled, BioLegend). Bound caspase-3 antibodies were visualized using tyramide signal amplification (Thermo-Fisher). Bound CD45.1 antibody was visualized using rabbit anti-FITC antibody followed by incubation with Alexa-fluor goat-anti-rabbit antibody (Life-Technologies). Germinal centers were visualized using FITC-labeled Peanut agglutinin (PNA; Life technologies). Nuclei were stained with 4',6-diamidino-2-phenylindole (DAPI, Invitrogen).

Stained sections were scanned using a Panoramic Digital Slide Scanner 250 FLASH II (3DHISTECH) at 200x magnification. For representative images, contrast was linearly enhanced using the tools “levels”, “curves”, “brightness” and “contrast” in Photoshop CS6 (Adobe).

Whole slide images were analyzed with a custom made rule-set using Developer Definiens XD software (Definiens, Munich). Briefly, the regions of interests (ROIs) were drawn manually and CD45.1 as well as caspase-3 signal was automatically detected based on corresponding spectral channels in conjunction with the DAPI signal. Following detection, CD45.1+ cells were classified into caspase-3-positive and, -negative cells depending on cellular collocalisation with caspase-3. The total ROI area and cell quantification results were exported in CSV-format for further analysis.

2.4.4 Whole-genome RNA sequencing and low-density inflammatory gene expression profiling

For RNA sequencing of sorted KL25HL B cells, RNA was extracted using the Direct-zol™ RNA MicroPrep kit (Zymo research) according to the manufacturer's instructions. Library preparation was performed with a TruSeq kit (Illumina) according to the provider's protocol and sequencing was performed by 50 bp single-end reads on an Illumina HiSeq 2000 at the Microarray and Deep-Sequencing Core Facility, University Medical Center, Göttingen, Germany. Analysis was performed at the Bioinformatics Core Facility of the University of Basel as follow: Reads were mapped against the mouse genome (version mm9; NCBI build 37) using the spliced-read aligner STAR (Dobin et al., 2013). Raw reads and mapping quality was assessed by the qQCReport function from the R package QuasR (Gaidatzis et al., 2015; Team, 2015). Expression of RefSeq genes (UCSC version downloaded 2013-07-25) was quantified by counting reads mapping into exons using the qCount function of QuasR. The R package edgeR (McCarthy et al., 2012) was used for detecting differentially expressed genes between conditions. P-values for the contrasts of interest were calculated by likelihood ratio tests and adjusted for multiple testing by controlling the expected FDR.

For low density inflammatory gene expression profiling, spleen and BM from naïve mice and from rCl13-infected mice treated with αGr-1, αIFNAR or control antibody were harvested on day 3. RNA was extracted using Direct-zol™ RNA MicroPrep kit (Zymo research) according to the manufacturer's instructions. Expression profiling was done using the nCounter Nanostring Mouse Inflammation v2 assay (NanoString Technologies) at the iGE3 genomics platform of the University of Geneva. Analysis was performed at the Bioinformatics Core Facility of the University of Basel as follow: Raw counts were scale-normalized using the TMM method of the R package limma (Law et al., 2014). The transformed counts (log-CPM values) were subsequently used for linear modelling. Differential gene expression between conditions was evaluated using the lmFit and eBayes functions of limma. P-values of the moderated t-tests were adjusted for multiple testing by controlling the expected false discovery rate (FDR).

Heatmaps were generated using the ComplexHeatmap R package (Gu, 2016). Heatmaps employing the Nanostring data show genes with an absolute log2-fold change (log2FC) bigger than 0.5 and an FDR-controlled p-value smaller than 0.05. No thresholding was used for heatmaps showing pre-defined gene lists.

2.4.5 Mice

KL25L transgenic mice were generated using a construct as schematically described in Fig. S1B. It encoded for the rearranged KL25 V and J segments as well as for the light chain kappa constant domain. Additionally, for the efficient screening of transgene-expressing founder mice by FACS, a downstream internal ribosome entry site (IRES) controlled expression of a cell surface reporter protein consisting of the Thy1.1 ectodomain fused to the transmembrane and cytoplasmic domains of the mouse PDGF receptor. The complete expression cassette was released from the vector using appropriate restriction enzymes and was purified and injected into C57BL/6 embryos using standard techniques.

KL25H and VI10 mice carry an immunoglobulin heavy chain knock-in (KI) derived from the neutralizing GP-specific and VSVG-specific KL25 and VI10 antibodies, respectively (Hangartner et al., 2003). KL25H and KL25L mice were intercrossed to obtain KL25HL mice, and were brought onto a CD45.1 congenic background for adoptive transfer experiments. Intercrosses of KL25HL and VI10 mice with *ifnar*$^{-/-}$ (Muller et al., 1994) mice yielded KL25HL x *ifnar*$^{-/-}$ (CD45.1) and VI10 x *ifnar*$^{-/-}$ (CD45.2) mice, respectively.

Wt C57BL/6J mice were purchased from Charles River Laboratories, iNOS-deficient *nos2*$^{-/-}$ (Laubach et al., 1995) and *Fasl*^{gld} mutant mice (Roths et al., 1984) on C57BL/6 background were bought from the Jackson Laboratories. *ccr2*$^{-/-}$ mice (Boring et al., 1997) were generously provided by S. LeibundGut-Landmann, *ifnar*$^{fl/fl}$ mice (Prinz et al., 2008) by U. Kalinke, *Baff-tg* mice (Kreuzaler et al., 2012) by T. Rolink, *klf4*$^{fl/fl}$ *x Vav1-icre* mice (Tussiwand et al., 2015) by R. Tussiwand, *il1β*$^{-/-}$ mice (Horai et al., 1998) by N. Schaeren-Wiemers, *il4*$^{-/-}$ mice (Kuhn et al., 1991) by A. Teubner and *il6*$^{-/-}$ mice (Kopf et al., 1994) by M. Recher. *cd19-cre* mice (Rickert et al., 1997) were kindly provided by A. Oxenius with authorization from the MGC foundation. CD45.1-congenic C57BL/6, *il10*$^{-/-}$(Kuhn et al., 1993), *cd8*$^{-/-}$(Fung-Leung et al., 1991), *il12p40*$^{-/-}$ (Magram et al., 1996), *cd4-cre* (Lee et al., 2001), *cd11c-cre* (Caton et al., 2007), *LysM-cre* (Clausen et al., 1999), *ifnar*$^{-/-}$ (Muller et al., 1994) and *ubc-gfp* mice (Schaefer et al., 2001) were from the Swiss Immunological Mouse Repository (SwImMR). *ifnar*$^{fl/fl}$ mice were crossed onto B cell-specific (*cd19-cre*), dendritic cell-specific (*cd11c-cre)*, myeloid cell-specific (*LysM-cre*) and T cell-specific (*cd4-cre*) Cre deleter strains to obtain the respective "B-*ifnar*$^{-/-}$" (*cd19-cre x ifnar*$^{fl/fl}$), "DC-*ifnar*$^{-/-}$" (*cd11c-cre x ifnar*$^{fl/fl}$), "myeloid-*ifnar*$^{-/-}$" (*LysM-cre x ifnar*$^{fl/fl}$) and "T-*ifnar*$^{-/-}$" (*cd4-cre x ifnar*$^{fl/fl}$) strains.

2.4.6 Animal experiments

All mice were kept under specific-pathogen-free (SPF) conditions for colony maintenance and experiments, and were housed at the Laboratory Animal Services Center (LASC) of the University of Zurich and at the Universities of Geneva and Basel. Experiments were performed at the Universities of Geneva and Basel, in accordance with the Swiss law for animal protection and with authorization by the respective Cantonal authorities.

2.4.7 *In vivo* cell depletion and antibody blockade

IFNAR-blocking antibody (MAR1-5A3, BioXCell) was administered intraperitoneally (i.p.) at a dose of 1 mg on day -1 of infection. TNF-α-blocking antibody (XT3.11; BioXCell) was given at doses of 500 µg i.p. on day -1 and day 1 of infection. To deplete myeloid cells, we administered 500 µg of anti-Gr-1 (Ly6C/G) antibody (RB6-8C5, BioXCell) each on day -2.5 and day -0.5 of infection i.p.. Depletion of neutrophils was performed by means of a single i.p. injection of 1mg anti-Ly6G antibody (1A8, BioXCell) on day -1 of infection. Eosinophils were depleted by i.p. injections of 20 µg anti-SiglecF (clone 238047, R&D Systems) on day -1 and day 1 of infection. The obtained results were independently confirmed in experiments relying on the combined administration of 500 µg anti-IL5 antibody (Trfk5, BioXCell) and 250 µg of anti-CCR3 antibody (6S2-19-4 (Grimaldi et al., 1999), generously provided by Dr. J. J. Lee) each on day -2.5 and day -0.5 of infection. Plasmacytoid dendritic cell depletion was performed by administering 500 µg of anti-mPDCA-1 antibody (JF05-1C2.4.1, Miltenyi Biotec) i.v. on day -1 and day 0 of infection. MOPC-21 mouse IgG1, LTF-2 rat IgG2b, HPRN rat IgG1 and 2A3 rat IgG2a (all from BioXCell) were administered as isotype control antibodies.

2.4.8 Generation of bone marrow-chimeric mice

To generate bone marrow chimeric mice, wt and *ifnar*$^{-/-}$ recipients were lethally irradiated with a fractionated dose of twice 5.5 gray (Gy) at a 6-hour interval. One day later, the recipients were given 100 µg of anti-Thy1 antibody (clone T24, BioXcell) intraperitoneally to deplete remaining T cells and were reconstituted with ~10^7 wt or *ifnar*$^{-/-}$ BM cells. The animals were then rested for eight weeks before entering cell transfer and infection experiments.

2.4.9 Adoptive cell transfer and fluorescent cell labeling

For adoptive transfer of naïve B cells and subsequent analysis by flow cytometry, splenocyte suspensions (2-4x10^6 per recipient) in balanced salt solution were administered i.v. For histological assessments, MACS-purified B cells (Miltenyi Biotec Pan B cell isolation kit, for untouched B cells) were also used. Syngeneic C57BL/6J mice served as recipients, except for long-term (>1 week) transfer of KL25HL cells, which were performed in KL25L recipients to avoid anti-idiotypic responses. To assess *in vivo* proliferation, splenocyte populations were labeled with Carboxyfluorescein succinimidyl ester (CFSE, Sigma-Aldrich) or CellTraceViolet (CTV, Life Technologies) according to the manufacturer's instructions.

2.4.10 Generation of antigen-experienced KL25H B cells for adoptive transfer

To generate antigen-experienced GP-specific KL25H B cells, a sequential *in vivo* transfer system was used. We infected C57BL/6J primary recipients with 200 PFU rCl13 i.v. and six days later we transferred 2-4x10^6 MACS-purified untouched naïve B cells from CD45.1^+ KL25H mice (purified with the Pan B cell isolation kit of Miltenyi Biotec according to the provider instructions). ≥3 weeks later we sacrificed the primary recipients and purified antigen-experienced KL25H B cells from spleen, which at this stage were enriched to ~50% GP-binding by FACS (Fig S2B). These antigen-experienced KL25H B cells were isolated using the Pan B cell isolation kit, followed by CD45.2 MACS-based negative selection (both from Miltenyi Biotec) according to the manufacturer's instructions. 2-4x10^4 CD45.1^+ KL25H memory B cells (≥95% CD45.1^+B220$^+$) were transferred intravenously into naïve C57BL/6J wt secondary recipient mice to study the cells' behavior upon rCl13 challenge.

2.4.11 Generation of polyclonal LCMV-experienced B cells for adoptive transfer

To generate polyclonal LCMV-specific memory B cells, we infected GFP-transgenic UBC-GFP mice (Schaefer et al., 2001) with 10^5 PFU rCl13 i.v.. Fourty days later we isolated untouched splenic B cells using the Pan B cell isolation kit (Miltenyi Biotec) according to the provider's instructions. Upon CTV labeling, 2x10^6 of these LCMV-experienced B cells (>95%

pure) were transferred into naïve syngeneic C57BL/6J recipients to study their behavior upon rCl13 challenge.

2.4.12 Antibody, interferon-α and cytokine/chemokine panel measurements

To assess GP-specific serum antibodies in ELISA we used a recombinant fusion protein consisting of the outer globular GP-1 domain, fused to the human IgG1 constant domain (GP1-Fc) as described previously (Eschli et al., 2007a). To discriminate responses of adoptively transferred KL25H B cells from endogenous responses in ELISA, background GP-1 antibody titers in control mice without KL25H cell transfer were determined and were subtracted.

GP-specific neutralizing antibodies (nAbs) were measured by immunofocus reduction assays using rCl13 as a test article (Battegay et al., 1991a). IFN-α concentrations in mouse sera were determined by ELISA using the VeriKine Mouse Interferon Alpha ELISA Kit (PBL Assay Science). To profile inflammatory responses in mouse serum we used a laser bead-based 31-plex cytokine and chemokine array (Eve Biotechnologies).

2.4.13 Statistical analysis

For comparison of one parameter between two groups, unpaired two-tailed Student's *t* tests were performed. One-way analysis of variance (ANOVA) was used to compare one parameter between multiple groups, two-way ANOVA for comparison of multiple parameters between two or more groups. ANOVA was followed by Bonferroni's post-test for multiple comparisons. Dunnett's post-test was used to compare multiple groups to a control group. With the exception of percentages, values were log-converted to obtain a near-normal distribution for statistical analysis. Data were analyzed using Graphpad Prism software (version 6.0h). *P* values >0.05 were considered not significant (ns), *p* values <0.05 were considered significant (*,#) and *p* values <0.01 highly significant (**,##).

2.5 Figures

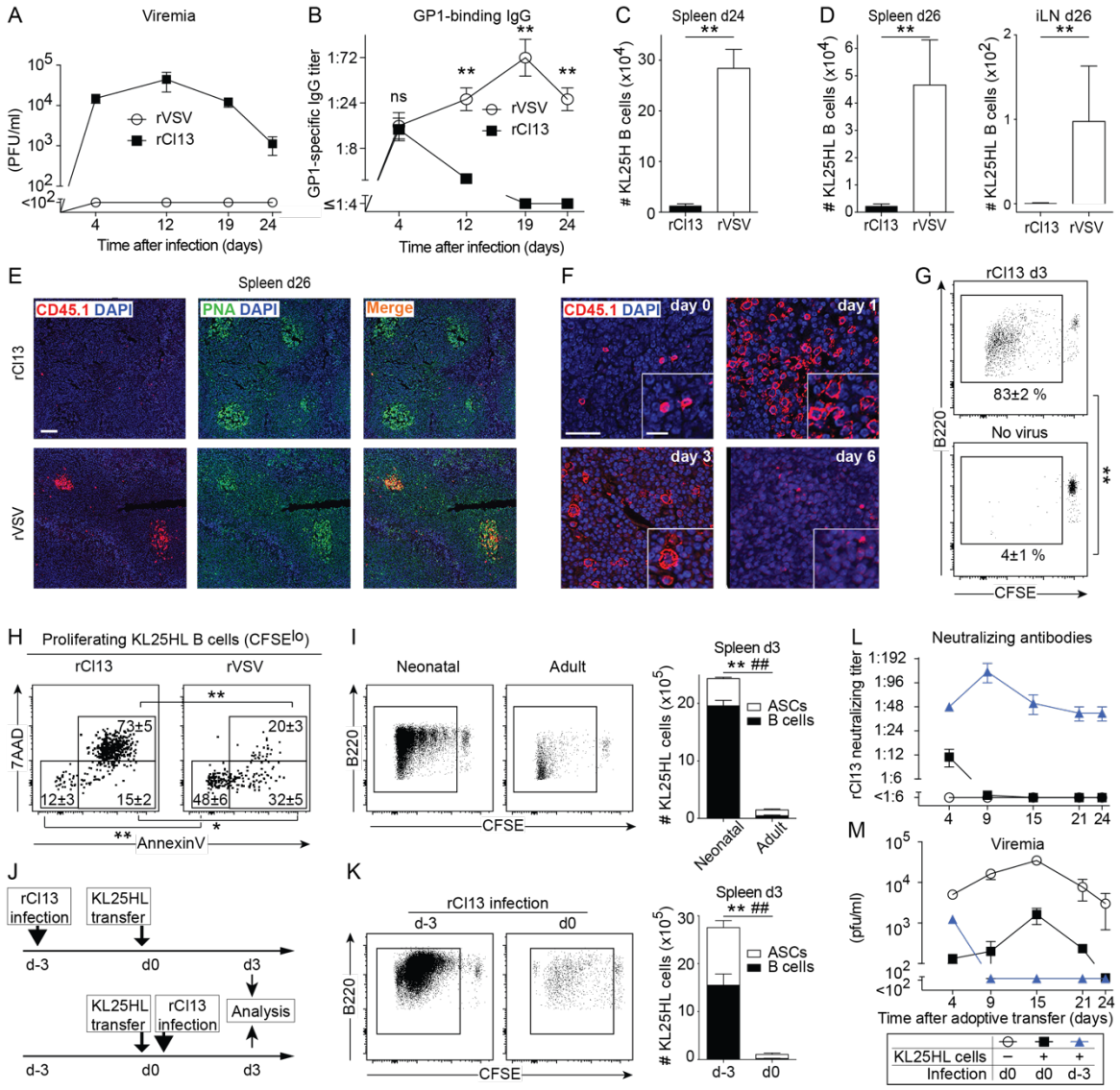

Figure 2.1: Decimation of naïve and memory B cells in rCl13 but not rVSV infection.

A-H: We adoptively transferred KL25H (A-C) or KL25HL cells (D-H) into naïve syngeneic recipients, followed by rCl13 or rVSV challenge. On the indicated days, viremia (A) and KL25H-derived GP1-binding IgG (B) were determined. Progeny B cells were enumerated by flow cytometry in spleen and iLN (C,D). KL25HL B cells (CD45.1$^+$) in germinal centers (E, bar 100 µm) and their abortive expansion following rCl13 infection (F, bars 50 µm, inset 20 µm) by histology. Proliferation (CFSE dilution) of d3 rCl13-challenged but not unchallenged KL25HL B cells (G). Apoptotic (AnnexinV/7AAD$^+$) KL25HL B cells on d3 of rCl13 or rVSV challenge (H). I: Proliferation and resulting KL25HL B cell progeny in neonatally infected rCl13 carriers or adult rCl13-infected mice. J-M: Upon KL25HL transfer and rCl13 infection, timed as outlined (J), we measured KL25HL B cell proliferation and expansion (K), nAb responses (L) and viremia (M). Symbols and bars represent means±SEM. *n*= 3-4, *N*=2-3. FACS plots are gated on CD45.1$^+$B220$^+$ lymphocytes. B cells and ASCs gating is shown in Fig. S1D. Numbers in FACS plots indicate percentages (mean±SEM). *,#: $p<0.05$; **,##: $p<0.01$. *,** compare B cells; #,## compare ASCs.

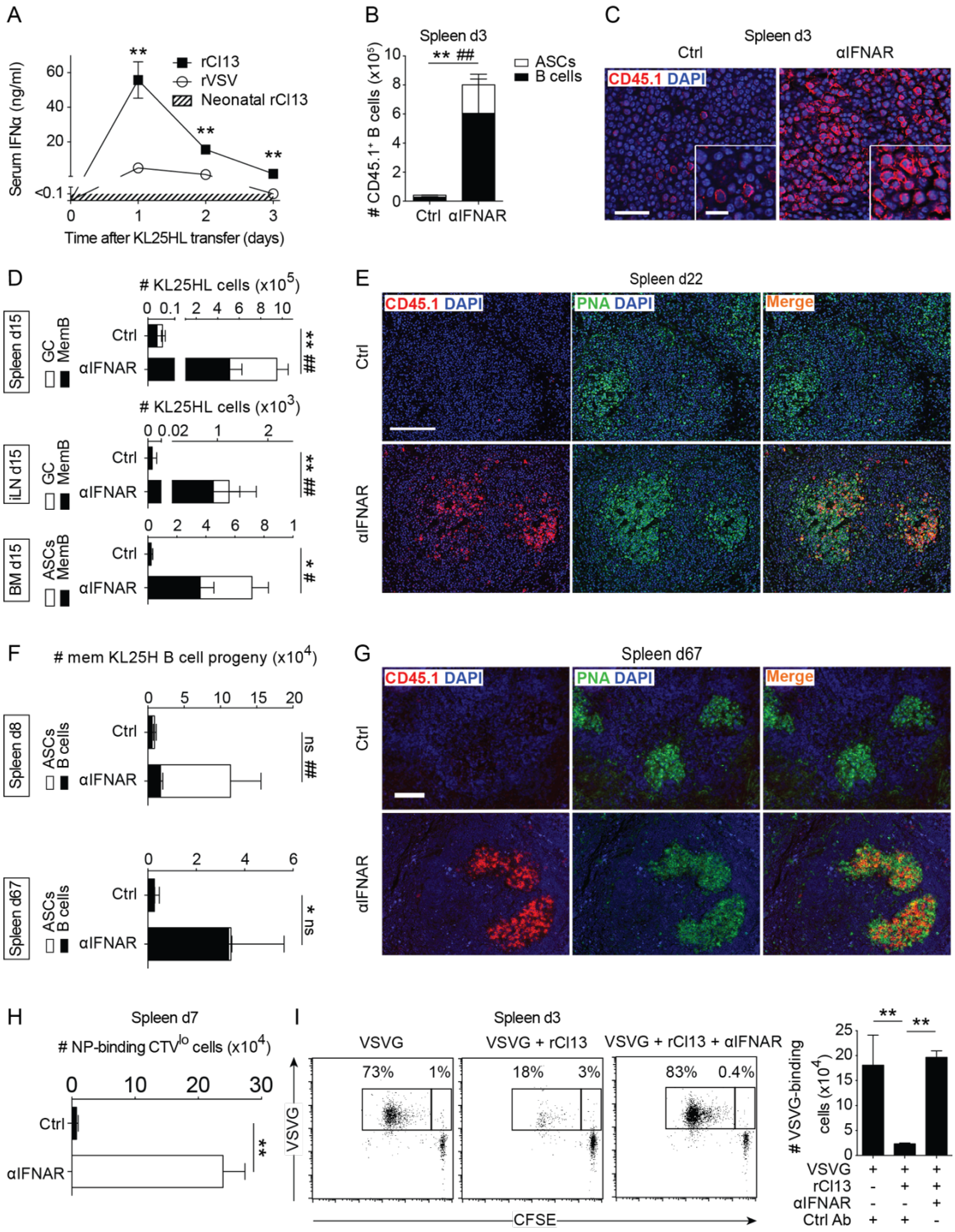

Figure 2.2: IFNAR blockade restores B cell expansion and GC differentiation in rCl13 infection.

A: Serum IFN-α in KL25HL cell recipients, infected with rCl13 at birth or on d0, or infected with rVSV on d0.
B-G: We transferred naïve KL25HL cells (B-E), antigen-experienced KL25H B cells (F-G) or antigen-experienced polyclonal GFP$^+$ B cells (H) to αIFNAR- or control-treated wt recipients, followed by rCl13 infection. B cell progeny in the indicated organs were detected by FACS (B,D,F,H) and histology (C,E,G). Note progeny of naïve KL25HL cells (E) and of antigen-experienced KL25H cells (G) in GCs of IFNAR-blocked recipients. Magnification bars: 50 µm, inset 20 µm (C); 200 µm (E); 100 µm (G). Numbers in (H) represent LCMV-NP-binding,

proliferated (CellTraceViolet/CTV^{lo}) polyclonal donor (GFP^{+}) B cell progeny (CTV^{lo}GFP^{+}LCMV-NP^{+} lymphocytes, compare Fig. S2D).
I: We transferred naïve VI10 cells to αIFNAR- or control-treated recipients, followed by VSVG immunization, alone or in combination with rCl13 infection. Proliferated (CFSE^{lo}) VSVG-binding VI10 B cells were enumerated by FACS. Plots are gated on CD45.2^{+}B220^{+} lymphocytes. Bars represent the mean±SEM. *n*= 3-4, *N*=2-3. ns: not significant; *,#: $p<0.05$; **,##: $p<0.01$. *,** compare total or GC B cells; #,## compare ASCs or memB, respectively.

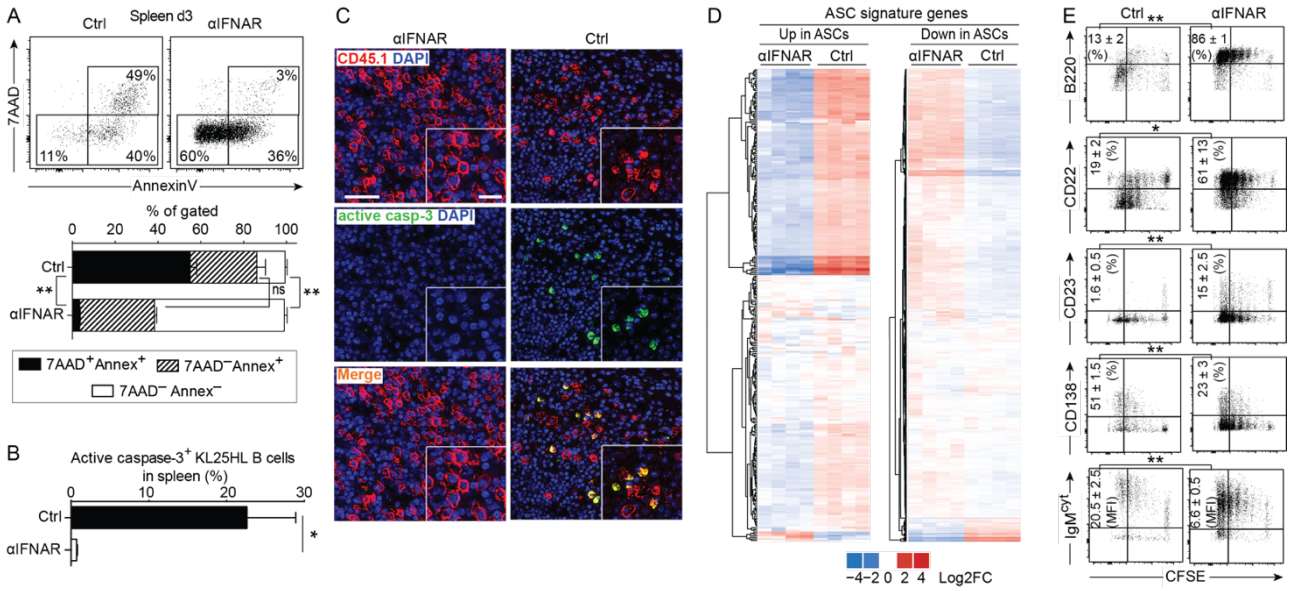

Figure 2.3: IFN-I-induced short-lived plasmablast differentiation in rCl13 infection.

We transferred naïve KL25HL cells to αIFNAR- or control-treated recipients, followed by rCl13 infection and analysis in spleen on day 3. Apoptotic KL25HL B cell were identified in FACS based on AnnexinV/7AAD-binding (A) and by histology based on expression of active caspase-3 (B,C, magnification bar 50 µm, inset 20 µm). Proliferated KL25HL B cell progeny ($CD45.1^+B220^+CFSE^{lo}$) were FACS-sorted and total RNA was processed for RNAseq (D). Heat maps show expression profiles of ASC signature genes known to be upregulated (left) or downregulated (right) upon ASC differentiation, respectively (Shi et al., 2015). Plasmablast differentiation of proliferated ($CFSE^{lo}$) KL25HL B cell progeny was determined by flow cytometry (E). Numbers in FACS plots indicate the percentage of cells falling into the respective gate (A, representative FACS plots, gated as shown in Fig. S1D), the percentage of $CFSE^{lo}$ cells expressing the respective marker (E) or the MFI of cytoplasmic IgM within $IgM^{cyt+}CFSE^{lo}$ cells. Numbers and bars show means±SEM. n=3-4, *N*=2-3 (A-C,E). ns: not significant; *: $p<0.05$; **: $p<0.01$.

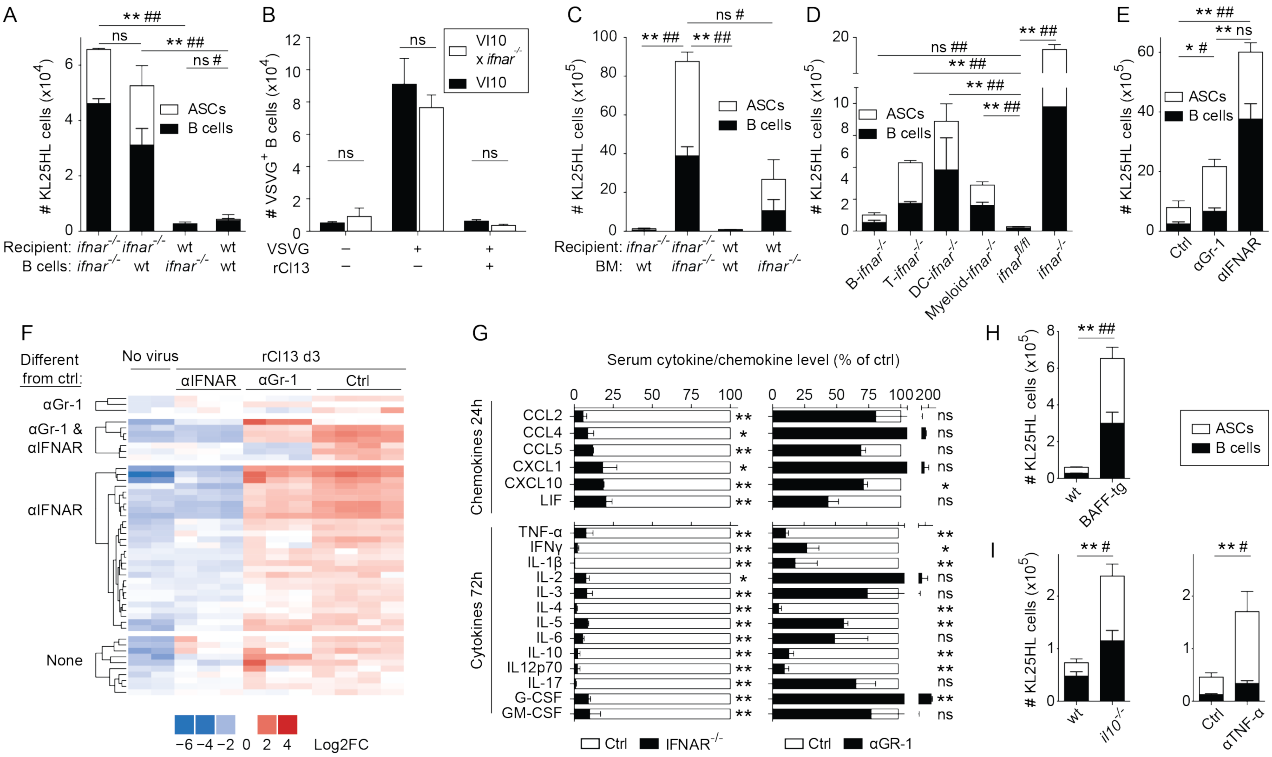

Figure 2.4: Impact of cell type-specific IFNAR signaling, IFN-I-induced inflammation and BAFF overexpression on rCl13-induced B cell decimation.

A: We transferred KL25HL cells, either wt or *ifnar*$^{-/-}$, into wt or *ifnar*$^{-/-}$ recipients and enumerated splenic KL25HL B cell progeny on d3 after rCl13.
B: We transferred VI10 cells into wt recipients, followed by VSVG immunization and rCl13 infection as indicated, and enumerated splenic VSVG-binding VI10 B cells on d3.
C-D: We transferred KL25HL cells into reciprocal wt and *ifnar*$^{-/-}$ BM chimeras (C) or into recipients with cell type-specific, conditional or complete IFNAR deficiency (D) and enumerated splenic KL25HL B cell progeny on d3 after rCl13.
E: We transferred KL25HL cells into wt recipients, treated with αGr-1, αIFNAR or control, and enumerated splenic KL25HL B cell progeny on d3 after rCl13.
F: Low density inflammatory gene expression profiling in spleen of naïve or d3 rCl13-infected KL25HL recipients. Heat maps shows the 48 genes significantly up-regulated upon rCl13 infection.
G: Serum chemokines and cytokines were profiled at 24h and 72h after rCl13, respectively. *ifnar*$^{-/-}$ and αGr-1-treated wt mice are expressed as percentage of control-treated wt mice. Only those 19/31 profiled chemokines and cytokines are displayed, which were ≥4-fold lower in *ifnar*$^{-/-}$ than wt controls (Tbl. SII).
H-I: We transferred KL25HL cells into BAFF-transgenic (H), *il-10*$^{-/-}$ or into wt recipients, treated with αTNF-α or control (I), and enumerated splenic KL25HL B cell progeny on d3 after rCl13.
B cells and ASCs were gated as shown in Fig. S1D. Bars show means±SEM. n=3-4. *N*=2-3 (A-E, H). ns: not significant; *,#: $p<0.05$; **,##: $p<0.01$. *,** compare B cells; #,## compare ASCs.

2.6 Supplementary Figures and Tables

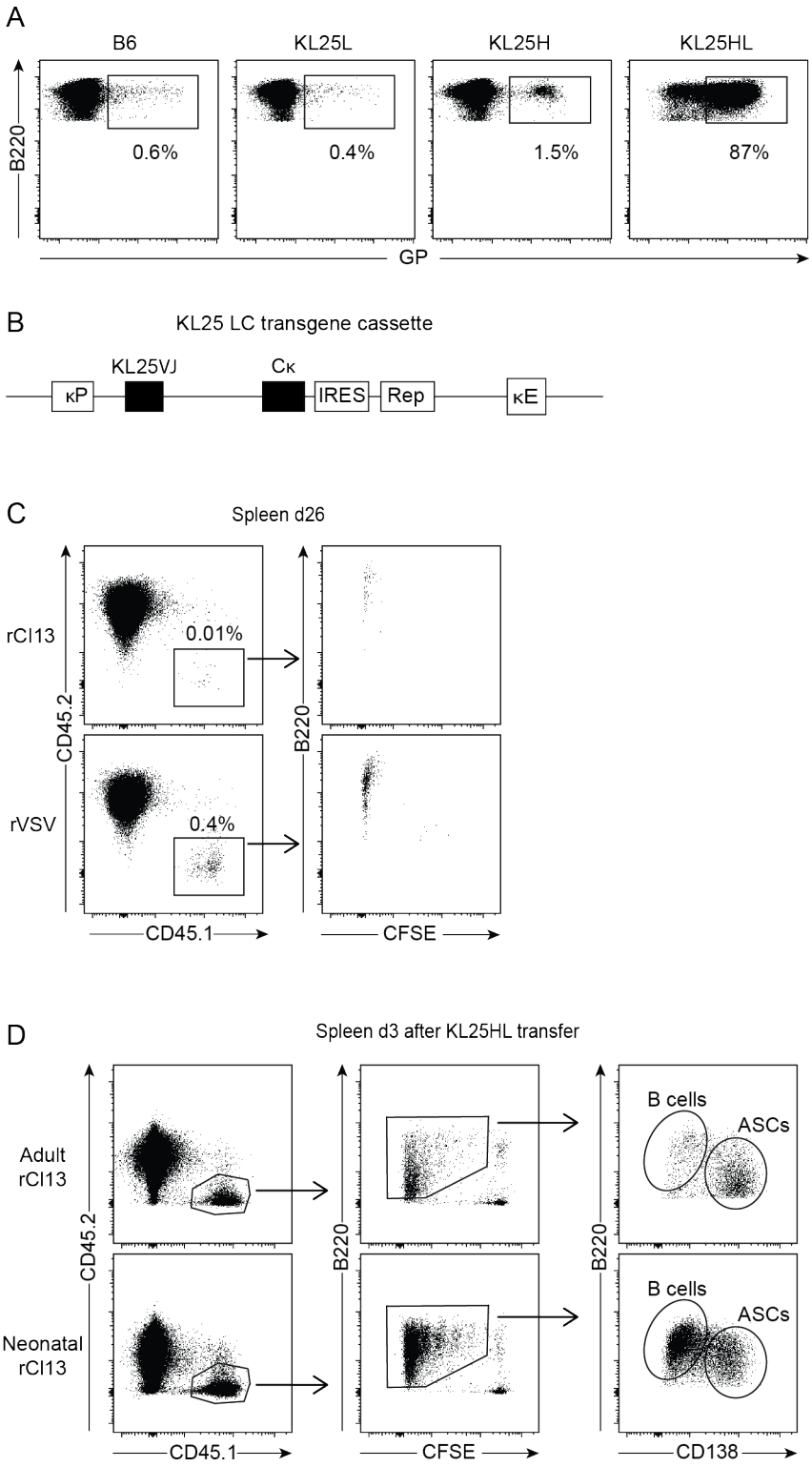

Figure 2.S1: Characterization of KL25H and KL25HL mice, and FACS gating strategy pursued to analyze the respective B cell progeny in adoptive transfer experiments.

A: GP-binding by B cells in peripheral blood of wt, KL25L (KL25 antibody light chain transgenic), KL25H (KL25 antibody heavy chain knock-in) and KL25HL mice (cross of

KL25L and KL25H). Numbers in plots indicate the percentage of GP-binding cells amongst total B cells (gated on $B220^+$ lymphocytes).
B: KL25 light chain (LC) transgene construct. κP: Genomic immunoglobulin kappa (Igκ) chain promoter; KL25VJ: rearranged KL25 V and J segments, including leader and intron; Cκ: light chain kappa constant domain; IRES: internal ribosome entry site; Rep: cell surface reporter protein consisting in the murine Thy1.1 ectodomain fused to the transmembrane and cytoplasmic domains of the mouse PDGF receptor; κE: genomic Igκ locus enhancer element.
C: Gating strategy to Fig. 1D. We adoptively transferred CFSE-labeled KL25HL cells into naïve syngeneic recipients, followed by rCl13 or rVSV challenge and measured KL25HL progeny B cells on day 26. FACS plots on the left are pre-gated on B cells ($B220^+$ lymphocytes). Percentages of gated cells are indicated. Representative FACS plots are shown.
D: Gating strategy to enumerate "KL25HL B cell progeny", i.e. progeny KL25HL B cells and ASCs. On d0 we transferred KL25HL cells into adult syngeneic recipients, infected with rCl13 since birth (i.e. as neonates) or on the day of cell transfer (d0) and assessed B cell progeny (B cells and ASCs) on day 3. FACS plots on the left are pre-gated on lymphocytes. Representative FACS plots are shown.

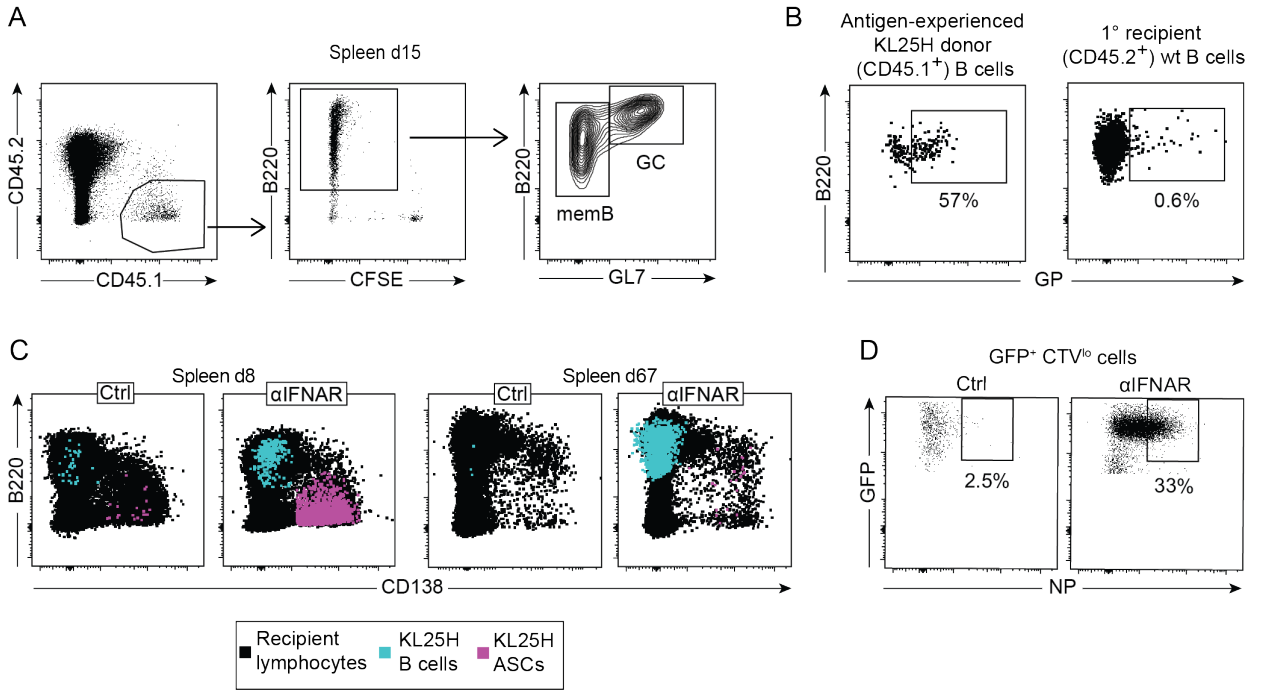

Figure 2.S2: Characterization of KL25H and KL25HL mice, and FACS gating strategy pursued to analyze the respective B cell progeny in adoptive transfer experiments.

A: Gating strategy to enumerate memB and GC B cells in Fig. 2D. We adoptively transferred CFSE-labeled KL25HL cells into naïve syngeneic recipients, treated with αIFNAR or control antibody, followed by rCl13 infection and analysis on day 15. FACS plots on the left are pre-gated on lymphocytes. Representative FACS plots are shown.
B: Characterization of antigen-experienced KL25H B cells as used for adoptive transfer in Fig. 2F,G. LCMV-reactive KL25H B cells were expanded *in vivo*, and 3-4 weeks later were purified from spleen (see Materials and Methods). Such antigen-experienced KL25H cells from 10 primary recipients were pooled for adoptive transfer into secondary recipients. An aliquot thereof was analyzed for purity (~95% $CD45.1^+B220^+$, not shown) and was compared to B cells of the primary $CD45.2^+$ recipient (from the MACS flow-through) for GP-binding. Note the infection-induced enrichment of GP-binding KL25H donor B cells from ~2% at baseline (Fig. S1A) to >50% on the day of secondary transfer. Plots are gated on either $CD45.1^+$ or $CD45.2^+$ $B220^+$ lymphocytes, as indicated. Numbers show the percentage of gated cells. N=3.
C: Illustrative FACS plots to Fig. 2F. On the indicated days after rCl13 challenge, progeny B cells and ASCs of antigen-experienced KL25H B cell were gated as outlined in Fig. S1D. These populations were superimposed on the recipient's lymphocytes for display.
D: Illustrative FACS plot to Fig. 2H. GFP-transgenic polyclonal LCMV-experienced B cells were generated *in vivo* and purified from spleen (see Materials and Methods). On d7 after transfer into naïve recipients and rCl13 challenge we analyzed NP-binding by adoptively transferred (GFP^+) B cell progeny. A representative FACS plot is shown, gated on $CTV^{lo}GFP^+$ lymphocytes.

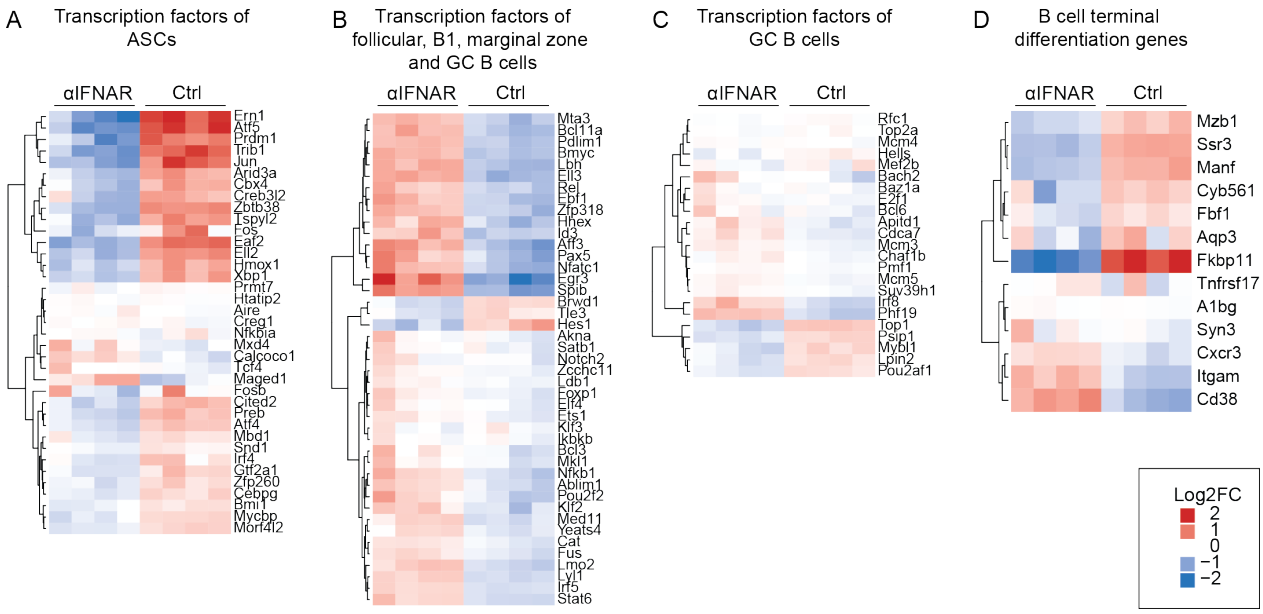

Figure 2.S3: IFNAR blockade alters transcription factor and terminal differentiation profiles of B cells in rCl13 infection.

We transferred naïve KL25HL cells to αIFNAR- or control-treated recipients, followed by rCl13 infection. On day 3, proliferated ($CFSE^{lo}$) KL25HL B cells were sorted from spleen and RNA was processed for RNAseq (same samples as in Fig. 3D). Heat maps show transcription factors associated with the indicated B cell differentiation stages (A-C, (Shi et al., 2015)) and genes associated with terminal B cell differentiation in HIV patients (D, (Moir et al., 2004)).

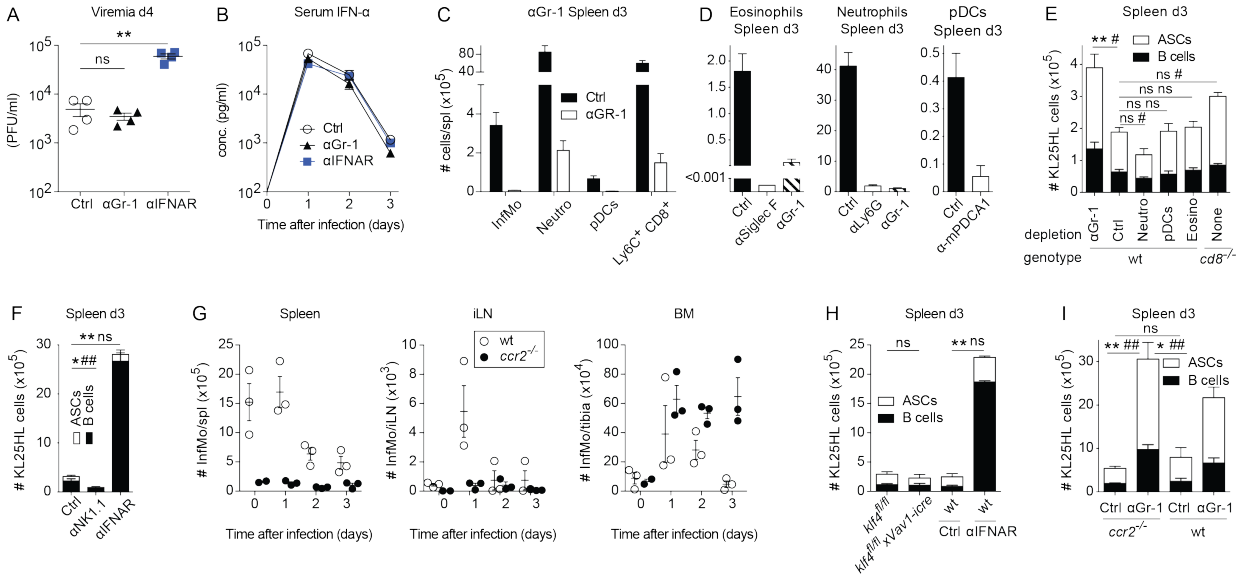

Figure 2.S4: Effects of depletion antibodies on serum IFN-α, virus loads, myeloid cell population and KL25HL B cell recovery, and impact of genetic InfMo deficiency on KL25HL B cell recovery.

A-B: We treated wt mice with αGr-1, αIFNAR or control antibody and infected them with rCl13. Viremia (A) and IFN-α concentrations in serum (B) were assessed on the indicated days.
C-E: We adoptively transferred KL25HL cells into wt (C,D) or wt and *cd8*$^{-/-}$ recipients (E), followed by rCl13 infection. Recipients were treated with either αGR-1 (pan-myeloid depletion), αSiglecF (selective eosinophil depletion), αLy6G (selective neutrophil depletion), α-mPDCA1 (selective pDC depletion) or control antibody. C,D: We enumerated InfMo (Thy1.2^{-}NK1.1^{-}CD19^{-}CD11b^{+}Ly6G^{-}Ly6C^{hi}, (Rose et al., 2012)), neutrophils (Thy1.2^{-} NK1.1^{-}CD19^{-}CD11b^{+}Ly6G^{hi}Ly6C^{int} cells (Rose et al., 2012)), pDCs (Thy1.2^{-}NK1.1^{-}CD19^{-} CD11b^{-}Ly6C^{+}Siglec-H^{+}B220^{+}CD11c^{+}) and Ly6C^{+} CD8^{+} T cells (CD8^{+}Ly6C^{+} lymphocytes) on d3 in spleen (C,D). Note that cell type-specific agents depleted their respective cell population similarly efficiently as αGr-1. KL25HL B cell progeny in spleen on d3 were enumerated (E) based on the gating strategy shown in Fig. S1D.
F: We adoptively transferred KL25HL cells into wt recipients, treated with NK cell-depleting antibody (αNK1.1), αIFNAR or control antibody, followed by rCl13 infection. KL25HL B cell progeny were enumerated on day 3 in spleen as in (E).
G: *ccr2*$^{-/-}$ and wt control mice were infected with rCl13 and InfMo numbers in spleen, iLN and BM were determined in spleen over time as described for (C,D).
H: We transferred KL25HL cells into *klf4*$^{fl/fl}$ *x Vav1-icre* and control *klf4*$^{fl/fl}$ followed by rCl13 infection. Groups of wt mice treated with αIFNAR or control antibody, served as high- and low-control groups, respectively. KL25HL B cell progeny were enumerated from spleen on d3 as in (E).
I: We adoptively transferred KL25HL cells into *ccr2*$^{-/-}$ and wt mice, treated with αGR-1 or control antibody as indicated, followed by rCl13 infection. KL25HL B cell progeny were enumerated from spleen on d3 as in (E). Same data set as Fig. 4E.
Symbols and bars represent means±SEM. *n*=3-4. *N*=2 (A-F, H-I). ns: not significant; *,#: $p<0.05$; **,##: $p<0.01$. *,** compare B cells; #,## compare ASCs.

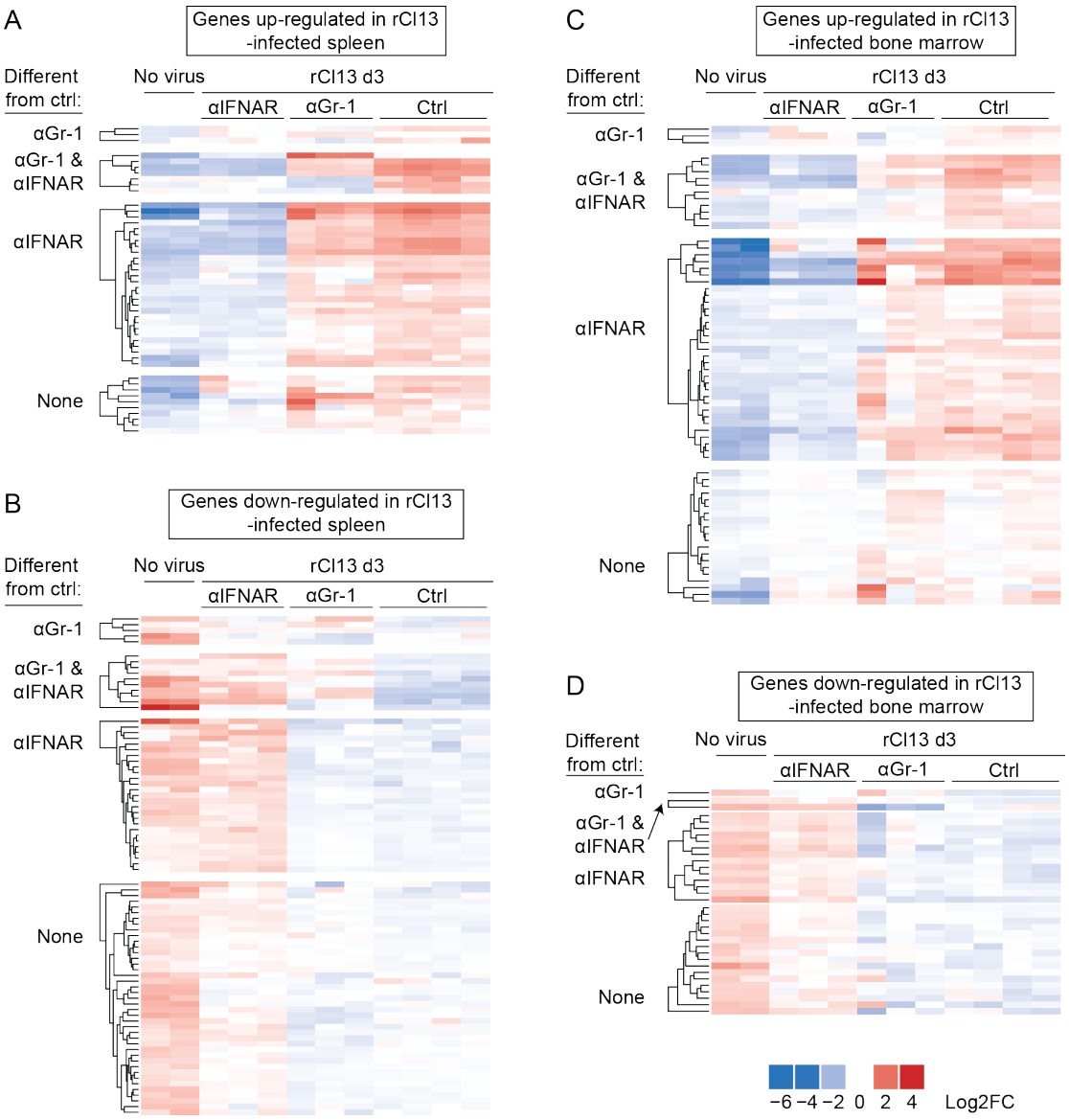

Figure 2.S5: Impact of αGr-1 and αIFNAR on inflammatory gene expression profiles in spleen and bone marrow.

We transferred KL25HL cells into wt recipients, treated with αGR-1, αIFNAR or control antibody, followed by rCl13 infection. Additional animals were left uninfected (no virus). On day 3 we processed spleen and BM for low-density expression profiling of 248 inflammatory genes. Heat maps show all those genes, which were significantly different between rCl13-infected control-treated mice and uninfected animals. Genes, which were up- (A,C) or down-regulated (B,D) in spleen (A,B) and BM (C,D) are shown separately, and were grouped according to whether αGR-1, αIFNAR or both treatments interfered with the infection-induced gene expression change. Columns represent individual mice, lanes individual genes (individually listed in Tbl. SI). Same data set as Fig. 4F.

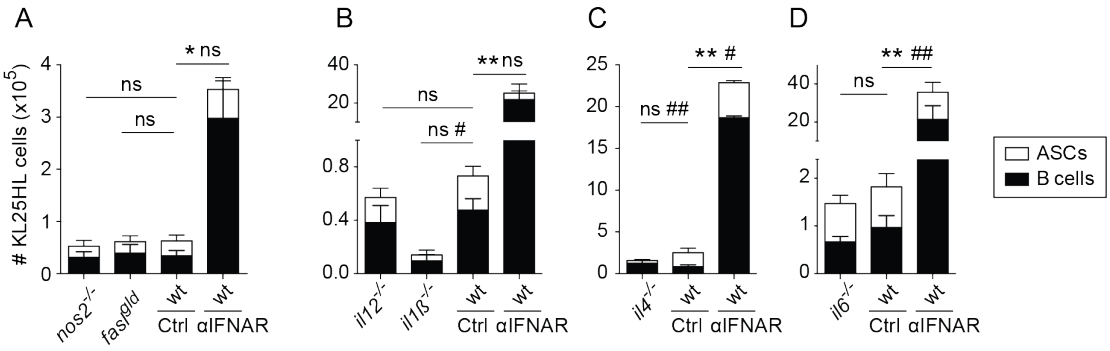

Figure 2.S6: Individual impact of iNOS, FasL, IL-1β, IL-4, IL-6 and IL-12 on KL25HL B cell decimation.

A-D. We transferred KL25HL cells into wt, iNOS-deficient *nos*2$^{-/-}$,FasL-mutant *fasl*^{gld} , *il12p40*$^{-/-}$, *il1β* $^{-/-}$, *il4*$^{-/-}$ and *il6*$^{-/-}$ mice, followed by rCl13 infection. Groups of wt mice treated with αIFNAR or control antibody, served as high- and low-control groups, respectively. KL25HL B cell progeny in spleen on d3 were enumerated based on the gating strategy shown in Fig. S1D. B, same data set as Fig. 4I. C, same data set as Fig. S4H. Bars represent means±SEM. *n*=3-4, *N*=2. ns: not significant; *,#: $p<0.05$; **,##: $p<0.01$. *,** compare B cells; #,## compare ASCs.

Table SI: Profound impact of IFNAR blockade and, more limited but largely overlapping, of αGr-1 depletion on inflammatory gene expression profiles in spleen and BM.

Gene expression change[1]	Different from ctrl Ab in:	EntrezID	Symbol	GeneName	no virus vs rCl13 + ctrl Ab[6]		rCl13 + αIFNAR vs rCl13 + ctrl Ab[7]		rCl13 + αGR-1 vs rCl13 + ctrl Ab[8]	
					log2FC	adj.P.Val	log2FC	adj.P.Val	log2FC	adj.P.Val
up-regulated in rCl13-infected spleen[2]	αGR-1[9]	16163	Il13	interleukin 13	0.91	0.03	-0.68	0.07	**-1.05**	**0.01**
		18783	Pla2g4a	phospholipase A2, group IVA (cytosolic, calcium-dependent)	0.70	0.00	0.05	0.78	**0.51**	**0.01**
		16362	Irf1	interferon regulatory factor 1	1.15	0.00	-0.47	0.04	**-0.59**	**0.02**
	αGR-1 & αIFNAR[10]	17392	Mmp3	matrix metallopeptidase 3	2.22	0.00	**-0.63**	**0.00**	**2.04**	**0.00**
		12768	Ccr1	chemokine (C-C motif) receptor 1	1.45	0.00	**-1.07**	**0.01**	**-1.90**	**0.00**
		15958	Ifit2	interferon-induced protein with tetratricopeptide repeats 2	3.31	0.00	**-3.15**	**0.00**	**-0.83**	**0.00**
		15959	Ifit3	interferon-induced protein with tetratricopeptide repeats 3	2.94	0.00	**-2.97**	**0.00**	**-0.71**	**0.03**
		16176	Il1b	interleukin 1 beta	0.82	0.02	**-1.01**	**0.00**	**-1.84**	**0.00**
		227288	Cxcr1	chemokine (C-X-C motif) receptor 1	0.73	0.03	**-1.11**	**0.00**	**-1.30**	**0.00**
		231655	Oasl1	2'-5' oligoadenylate synthetase-like 1	2.46	0.00	**-2.89**	**0.00**	**-0.75**	**0.01**
	αIFNAR[11]	12263	C2	complement component 2 (within H-2S)	1.42	0.01	**-1.39**	**0.00**	0.21	0.72
		12267	C3ar1	complement component 3a receptor 1	1.35	0.00	**-0.95**	**0.01**	0.35	0.43
		13163	Daxx	Fas death domain-associated protein	0.55	0.00	**-0.96**	**0.00**	-0.31	0.10
		14103	Fasl	Fas ligand (TNF superfamily, member 6)	0.83	0.04	**-1.11**	**0.00**	-0.16	0.75
		14962	Cfb	complement factor B	2.24	0.00	**-0.89**	**0.00**	0.47	0.10
		15945	Cxcl10	chemokine (C-X-C motif) ligand 10	2.04	0.00	**-1.62**	**0.00**	-0.77	0.16
		15957	Ifit1	interferon-induced protein with tetratricopeptide repeats 1	2.78	0.00	**-2.99**	**0.00**	-0.43	0.19
		15977	Ifnb1	interferon beta 1, fibroblast	1.19	0.00	**-0.67**	**0.02**	-0.22	0.49
		15978	Ifng	interferon gamma	1.37	0.00	**-1.03**	**0.00**	-0.59	0.09
		16153	Il10	interleukin 10	1.36	0.00	**-1.22**	**0.00**	-0.16	0.64
		16168	Il15	interleukin 15	0.64	0.02	**-0.71**	**0.00**	-0.09	0.80
		16181	Il1rn	interleukin 1 receptor antagonist	1.97	0.00	**-0.84**	**0.02**	0.10	0.84
		17392	Mmp3	matrix metallopeptidase 3	2.22	0.00	**-0.63**	**0.00**	2.04	0.00
		17857	Mx1	MX dynamin-like GTPase 1	0.64	0.01	**-1.29**	**0.00**	-0.31	0.18
		17858	Mx2	MX dynamin-like GTPase 2	1.41	0.00	**-2.93**	**0.00**	-0.47	0.07
		20296	Ccl2	chemokine (C-C motif) ligand 2	4.23	0.00	**-2.20**	**0.00**	0.06	0.93
		20302	Ccl3	chemokine (C-C motif) ligand 3	2.38	0.00	**-0.91**	**0.00**	0.30	0.34
		20303	Ccl4	chemokine (C-C motif) ligand 4	1.87	0.00	**-1.22**	**0.00**	-0.12	0.80
		20306	Ccl7	chemokine (C-C motif) ligand 7	5.67	0.00	**-3.10**	**0.00**	-0.05	0.94
		20846	Stat1	signal transducer and activator of transcription 1	1.53	0.00	**-0.63**	**0.01**	-0.36	0.16
		20847	Stat2	signal transducer and activator of transcription 2	1.31	0.00	**-1.51**	**0.00**	-0.37	0.10
		50909	C1ra	complement component 1, r subcomponent A	0.78	0.00	**-0.92**	**0.00**	0.20	0.35
		54123	Irf7	interferon regulatory factor 7	3.13	0.00	**-2.91**	**0.00**	-0.09	0.75
		76933	Ifi27l2a	interferon, alpha-inducible protein 27 like 2A	2.05	0.00	**-2.29**	**0.00**	-0.08	0.88
		99899	Ifi44	interferon-induced protein 44	4.18	0.00	**-3.46**	**0.00**	-0.06	0.88
		170743	Tlr7	toll-like receptor 7	0.62	0.00	**-1.00**	**0.00**	0.06	0.80
		246728	Oas2	2'-5' oligoadenylate synthetase 2	2.54	0.00	**-3.12**	**0.00**	-0.55	0.10
		246730	Oas1a	2'-5' oligoadenylate synthetase 1A	2.23	0.00	**-2.22**	**0.00**	-0.25	0.44
		625018	C4a	complement component 4A (Rodgers blood group)	0.75	0.01	**-1.02**	**0.00**	0.27	0.37
	none[12]	13198	Ddit3	DNA-damage inducible transcript 3	0.80	0.00	-0.49	0.05	0.33	0.23
		14825	Cxcl1	chemokine (C-X-C motif) ligand 1	2.04	0.03	-1.39	0.10	0.85	0.40
		16193	Il6	interleukin 6	1.05	0.03	-0.32	0.48	0.06	0.91
		16476	Jun	jun proto-oncogene	0.76	0.01	-0.43	0.10	0.16	0.63
		17329	Cxcl9	chemokine (C-X-C motif) ligand 9	2.16	0.01	-0.39	0.62	-0.13	0.89
		19225	Ptgs2	prostaglandin-endoperoxide synthase 2	3.12	0.00	-0.56	0.24	-0.30	0.62
		20307	Ccl8	chemokine (C-C motif) ligand 8	2.45	0.00	-0.96	0.08	1.19	0.05
		20310	Cxcl2	chemokine (C-X-C motif) ligand 2	1.17	0.04	-0.55	0.30	0.19	0.80
		60440	Iigp1	interferon inducible GTPase 1	2.66	0.00	-0.47	0.34	-0.53	0.35
		257632	Nod2	nucleotide-binding oligomerization domain containing 2	0.58	0.05	-0.32	0.24	-0.41	0.18

Gene expression change[1]	Different from ctrl Ab in:	EntrezID	Symbol	Gene Name	no virus vs rCl13 + ctrl Ab[6]		rCl13 + αIFNAR vs rCl13 + ctrl Ab[7]		rCl13 + αGR-1 vs rCl13 + ctrl Ab[8]	
					log2FC	adj.P.Val	log2FC	adj.P.Val	log2FC	adj.P.Val
down-regulated in rCl13-infected spleen[3]	αGR-1[9]	16196	Il7	interleukin 7	-1.57	0.00	0.15	0.72	**1.38**	**0.00**
		21812	Tgfbr1	transforming growth factor, beta receptor I	-0.79	0.00	0.47	0.00	**0.60**	**0.00**
		53603	Tslp	thymic stromal lymphopoietin	-0.61	0.05	0.45	0.11	**0.86**	**0.01**
		21947	Cd40lg	CD40 ligand	-1.37	0.00	-0.50	0.13	**-0.72**	**0.05**
		12053	Bcl6	B cell leukemia/lymphoma 6	-1.36	0.00	0.15	0.53	**-0.53**	**0.04**
	αGR-1 & αIFNAR[10]	11936	Fxyd2	FXYD domain-containing ion transport regulator 2	-2.27	0.00	**1.64**	**0.00**	**0.90**	**0.03**
		12274	C6	complement component 6	-1.14	0.01	**1.17**	**0.00**	**1.41**	**0.00**
		12771	Ccr3	chemokine (C-C motif) receptor 3	-2.45	0.00	**2.25**	**0.00**	**2.09**	**0.00**
		15289	Hmgb1	high mobility group box 1	-0.50	0.00	**1.15**	**0.00**	**0.58**	**0.00**
		17346	Mknk1	MAP kinase-interacting serine/threonine kinase 1	-0.61	0.00	**0.55**	**0.00**	**0.64**	**0.00**
		17533	Mrc1	mannose receptor, C type 1	-2.21	0.00	**1.75**	**0.00**	**1.78**	**0.00**
		18829	Ccl21a	chemokine (C-C motif) ligand 21A (serine)	-3.65	0.00	**0.64**	**0.01**	**0.57**	**0.04**
		19224	Ptgs1	prostaglandin-endoperoxide synthase 1	-1.19	0.00	**0.75**	**0.00**	**0.89**	**0.00**
		20299	Ccl22	chemokine (C-C motif) ligand 22	-2.36	0.00	**0.94**	**0.01**	**1.04**	**0.01**
		93671	Cd163	CD163 antigen	-3.01	0.00	**2.31**	**0.00**	**1.04**	**0.00**
	αIFNAR[11]	11687	Alox15	arachidonate 15-lipoxygenase	-0.99	0.01	**0.88**	**0.01**	-0.19	0.67
		11848	Rhoa	ras homolog gene family, member A	-0.64	0.00	**0.61**	**0.00**	0.40	0.03
		11909	Atf2	activating transcription factor 2	-0.60	0.00	**0.51**	**0.00**	0.28	0.02
		12048	Bcl2l1	BCL2-like 1	-1.05	0.00	**0.73**	**0.01**	0.38	0.18
		14784	Grb2	growth factor receptor bound protein 2	-0.90	0.00	**0.53**	**0.01**	0.14	0.56
		14969	H2-Eb1	histocompatibility 2, class II antigen E beta	-1.36	0.00	**0.69**	**0.00**	-0.14	0.62
		16160	Il12b	interleukin 12b	-1.39	0.00	**0.96**	**0.00**	0.56	0.13
		16189	Il4	interleukin 4	-0.95	0.00	**0.62**	**0.02**	-0.09	0.81
		16194	Il6ra	interleukin 6 receptor, alpha	-1.57	0.00	**0.92**	**0.04**	0.04	0.94
		17134	Mafg	v-maf musculoaponeurotic fibrosarcom oncog. fam., prot. G (avian)	-0.98	0.00	**0.92**	**0.00**	0.13	0.63
		18751	Prkcb	protein kinase C, beta	-1.24	0.00	**0.61**	**0.02**	0.18	0.55
		19219	Ptger4	prostaglandin E receptor 4 (subtype EP4)	-1.03	0.00	**0.67**	**0.00**	0.25	0.10
		20416	Shc1	src homology 2 domain-containing transforming protein C1	-0.58	0.00	**0.86**	**0.00**	0.36	0.06
		22154	Tubb5	tubulin, beta 5 class I	-0.54	0.02	**0.86**	**0.00**	0.11	0.68
		26398	Map2k4	mitogen-activated protein kinase kinase 4	-0.57	0.00	**0.72**	**0.00**	0.36	0.02
		26409	Map3k7	mitogen-activated protein kinase kinase kinase 7	-0.53	0.00	**0.64**	**0.00**	0.28	0.02
		26416	Mapk14	mitogen-activated protein kinase 14	-1.15	0.00	**0.81**	**0.00**	0.38	0.05
		26419	Mapk8	mitogen-activated protein kinase 8	-0.84	0.00	**0.63**	**0.00**	0.30	0.03
		53791	Tlr5	toll-like receptor 5	-1.58	0.00	**1.06**	**0.00**	0.25	0.49
		54473	Tollip	toll interacting protein	-0.61	0.00	**0.64**	**0.00**	0.30	0.01
		71609	Tradd	TNFRSF1A-associated via death domain	-0.91	0.00	**0.52**	**0.04**	-0.08	0.81
		73086	Rps6ka5	ribosomal protein S6 kinase, polypeptide 5	-1.47	0.00	**0.68**	**0.01**	0.20	0.48
		97165	Hmgb2	high mobility group box 2	-0.57	0.03	**1.38**	**0.00**	0.21	0.47
		237310	Il22ra2	interleukin 22 receptor, alpha 2	-3.13	0.00	**1.55**	**0.00**	0.08	0.88
		NA	Gpr44	NA	-0.72	0.04	**1.06**	**0.00**	0.14	0.75
		NA	Hras1	NA	-1.25	0.00	**1.04**	**0.00**	0.19	0.52
		329251	Ppp1r12b	protein phosphatase 1, regulatory (inhibitor) subunit 12B	-0.71	0.01	**0.89**	**0.00**	0.40	0.13
	none[12]	11684	Alox12	arachidonate 12-lipoxygenase	-1.89	0.01	0.77	0.27	0.76	0.35
		12504	Cd4	CD4 antigen	-1.19	0.00	-0.05	0.74	-0.02	0.90
		12767	Cxcr4	chemokine (C-X-C motif) receptor 4	-0.75	0.03	0.15	0.67	-0.55	0.13
		12773	Ccr4	chemokine (C-C motif) receptor 4	-1.01	0.01	0.44	0.24	-0.08	0.88
		12775	Ccr7	chemokine (C-C motif) receptor 7	-1.17	0.00	0.11	0.70	-0.57	0.06
		12912	Creb1	cAMP responsive element binding protein 1	-1.01	0.00	0.26	0.10	0.03	0.88
		13136	Cd55	CD55 molecule, decay accelerating factor for complement	-1.35	0.01	0.19	0.68	0.33	0.52
		13712	Elk1	ELK1, member of ETS oncogene family	-0.88	0.00	0.44	0.02	0.22	0.34
		14683	Gnas	GNAS (guanine nucleot. bind. Prot., alpha stim.) complex locus	-0.80	0.01	0.50	0.08	0.00	1.00
		14815	Nr3c1	nuclear receptor subfamily 3, group C, member 1	-0.72	0.00	0.12	0.43	0.05	0.82
		15139	Hc	hemolytic complement	-1.51	0.00	0.83	0.08	-0.19	0.78
		15962	Ifna1	interferon alpha 1	-0.62	0.00	0.15	0.44	-0.40	0.06
		16155	Il10rb	interleukin 10 receptor, beta	-0.61	0.00	0.17	0.27	0.35	0.04
		16177	Il1r1	interleukin 1 receptor, type I	-0.65	0.04	0.19	0.51	0.56	0.09

		16183	Il2	interleukin 2	-0.73	0.04	-0.22	0.51	-0.26	0.51
		16885	Limk1	LIM-domain containing, protein kinase	-0.64	0.00	0.40	0.01	0.21	0.18
		16994	Ltb	lymphotoxin B	-0.74	0.01	-0.20	0.43	-0.21	0.49
		17131	Smad7	SMAD family member 7	-1.24	0.00	-0.14	0.37	0.12	0.51
		17135	Mafk	v-maf musculoaponeurot. fibrosarcoma oncog. Fam., prot. K (avian)	-0.62	0.00	0.44	0.00	-0.25	0.13
		17195	Mbl2	mannose-binding lectin (protein C) 2	-0.83	0.01	0.10	0.76	-0.27	0.48
		17258	Mef2a	myocyte enhancer factor 2A	-0.55	0.03	0.26	0.25	0.37	0.15
		17261	Mef2d	myocyte enhancer factor 2D	-1.04	0.00	0.19	0.34	-0.08	0.80
		18021	Nfatc3	nuclear factor of activated T cells, cytoplasm., calcineurin dep. 3	-0.54	0.03	0.15	0.51	0.02	0.93
		18033	Nfkb1	nuclear factor of kappa light polypep. gene enha. in B cells 1, p105	-0.62	0.01	0.25	0.27	0.24	0.35
		19353	Rac1	RAS-related C3 botulinum substrate 1	-0.51	0.00	0.50	0.00	0.47	0.00
		19697	Rela	v-rel reticuloendotheliosis viral oncogene homolog A (avian)	-0.59	0.00	0.48	0.00	0.16	0.17
		19698	Relb	avian reticuloendotheliosis viral (v-rel) oncogene related B	-0.70	0.01	0.15	0.52	0.26	0.34
		19878	Rock2	Rho-associated coiled-coil containing protein kinase 2	-0.53	0.00	0.20	0.22	0.35	0.05
		21390	Tbxa2r	thromboxane A2 receptor	-1.30	0.00	-0.14	0.72	0.01	0.99
		21413	Tcf4	transcription factor 4	-0.51	0.00	0.14	0.35	0.45	0.01
		21803	Tgfb1	transforming growth factor, beta 1	-0.85	0.00	0.49	0.00	0.49	0.00
		22030	Traf2	TNF receptor-associated factor 2	-0.62	0.00	0.18	0.10	0.03	0.84
		26399	Map2k6	mitogen-activated protein kinase kinase 6	-1.52	0.00	0.44	0.11	0.26	0.42
		26401	Map3k1	mitogen-activated protein kinase kinase kinase 1	-0.80	0.00	0.15	0.40	-0.10	0.63
		26408	Map3k5	mitogen-activated protein kinase kinase kinase 5	-0.53	0.00	0.19	0.24	-0.05	0.81
		26417	Mapk3	mitogen-activated protein kinase 3	-0.90	0.01	0.54	0.09	0.36	0.34
		27056	Irf5	interferon regulatory factor 5	-1.00	0.00	0.32	0.27	0.17	0.64
		54131	Irf3	interferon regulatory factor 3	-0.94	0.00	0.45	0.11	-0.09	0.82
		11596	Ager	advanced glycosylation end product-specific receptor	-1.12	0.00	0.27	0.35	-0.35	0.32
		208727	Hdac4	histone deacetylase 4	-0.60	0.01	0.10	0.67	-0.25	0.34
		338372	Map3k9	mitogen-activated protein kinase kinase kinase 9	-1.11	0.03	0.05	0.92	0.16	0.81

Gene expression change[1]	Different from ctrl Ab in:	EntrezID	Symbol	Gene Name	no virus vs rCl13 + ctrl Ab[6]		rCl13 + αIFNAR vs rCl13 + ctrl Ab[7]		rCl13 + αGR-1 vs rCl13 + ctrl Ab[8]	
					log2FC	adj.P.Val	log2FC	adj.P.Val	log2FC	adj.P.Val
up-regulated in rCl13-infected bone marrow[4]	αGR-1[9]	12504	Cd4	CD4 antigen	0.92	0.00	-0.19	0.24	**-0.62**	**0.00**
		16362	Irf1	interferon regulatory factor 1	2.04	0.00	-0.40	0.09	**-0.81**	**0.00**
		257632	Nod2	nucleotide-binding oligomerization domain containing 2	1.21	0.00	0.11	0.75	**-0.88**	**0.01**
	αGR-1 & αIFNAR[10]	15958	Ifit2	interferon-induced protein with tetratricopeptide repeats 2	3.81	0.00	**-2.78**	**0.00**	**-0.95**	**0.00**
		15959	Ifit3	interferon-induced protein with tetratricopeptide repeats 3	3.97	0.00	**-2.47**	**0.00**	**-1.43**	**0.00**
		16153	Il10	interleukin 10	0.62	0.04	**-0.78**	**0.01**	**-0.99**	**0.00**
		17858	Mx2	MX dynamin-like GTPase 2	2.19	0.00	**-2.60**	**0.00**	**-0.60**	**0.04**
		20846	Stat1	signal transducer and activator of transcription 1	2.32	0.00	**-0.77**	**0.00**	**-0.77**	**0.00**
		20847	Stat2	signal transducer and activator of transcription 2	1.98	0.00	**-1.54**	**0.00**	**-0.86**	**0.00**
		21897	Tlr1	toll-like receptor 1	1.93	0.00	**-1.06**	**0.00**	**-0.70**	**0.00**
		54123	Irf7	interferon regulatory factor 7	3.46	0.00	**-2.27**	**0.00**	**-0.52**	**0.04**
		107607	Nod1	nucleotide-binding oligomerization domain containing 1	1.50	0.00	**-0.52**	**0.03**	**-0.89**	**0.00**
		170743	Tlr7	toll-like receptor 7	1.39	0.00	**-1.22**	**0.00**	**-0.63**	**0.00**
		231655	Oasl1	2'-5' oligoadenylate synthetase-like 1	3.25	0.00	**-3.30**	**0.00**	**-0.85**	**0.00**
	αIFNAR[11]	12259	C1qa	complement component 1, q subcomponent, alpha polypeptide	1.79	0.00	**-1.25**	**0.00**	-0.20	0.22
		12260	C1qb	complement component 1, q subcomponent, beta polypeptide	2.30	0.00	**-1.49**	**0.00**	-0.47	0.00
		12263	C2	complement component 2 (within H-2S)	1.37	0.01	**-0.94**	**0.05**	0.20	0.73
		12267	C3ar1	complement component 3a receptor 1	3.72	0.00	**-2.83**	**0.00**	-0.69	0.11
		12524	Cd86	CD86 antigen	1.17	0.00	**-0.93**	**0.00**	-0.22	0.21
		13163	Daxx	Fas death domain-associated protein	1.70	0.00	**-1.53**	**0.00**	-0.39	0.05
		14103	Fasl	Fas ligand (TNF superfamily, member 6)	1.82	0.00	**-0.89**	**0.02**	0.25	0.57
		14433	Gapdh	glyceraldehyde-3-phosphate dehydrogenase	1.02	0.00	**-0.62**	**0.00**	0.18	0.30
		14962	Cfb	complement factor B	5.52	0.00	**-2.37**	**0.00**	-0.45	0.14
		15945	Cxcl10	chemokine (C-X-C motif) ligand 10	5.17	0.00	**-3.03**	**0.00**	-1.03	0.07
		15957	Ifit1	interferon-induced protein with tetratricopeptide repeats 1	3.44	0.00	**-2.09**	**0.00**	-0.27	0.41
		16173	Il18	interleukin 18	1.39	0.00	**-1.39**	**0.00**	-0.42	0.04
		16476	Jun	jun proto-oncogene	1.73	0.00	**-1.49**	**0.00**	-0.05	0.88
		17329	Cxcl9	chemokine (C-X-C motif) ligand 9	5.67	0.00	**-1.65**	**0.03**	-0.40	0.65
		17857	Mx1	MX dynamin-like GTPase 1	1.18	0.00	**-1.02**	**0.00**	-0.07	0.82
		17869	Myc	myelocytomatosis oncogene	1.00	0.00	**-0.78**	**0.00**	0.30	0.21
		17874	Myd88	myeloid differentiation primary response gene 88	1.39	0.00	**-0.67**	**0.01**	-0.21	0.41
		20296	Ccl2	chemokine (C-C motif) ligand 2	5.84	0.00	**-3.87**	**0.00**	-0.93	0.16
		20302	Ccl3	chemokine (C-C motif) ligand 3	1.66	0.00	**-1.37**	**0.00**	-0.10	0.79
		20303	Ccl4	chemokine (C-C motif) ligand 4	2.24	0.00	**-1.32**	**0.00**	-0.41	0.30
		20306	Ccl7	chemokine (C-C motif) ligand 7	6.43	0.00	**-4.75**	**0.00**	-0.32	0.69
		21898	Tlr4	toll-like receptor 4	1.24	0.00	**-0.61**	**0.02**	-0.34	0.21
		50868	Keap1	kelch-like ECH-associated protein 1	0.81	0.00	**-0.64**	**0.00**	-0.02	0.91
		58861	Cysltr1	cysteinyl leukotriene receptor 1	2.12	0.00	**-1.23**	**0.02**	-0.44	0.44
		60440	Iigp1	interferon inducible GTPase 1	5.33	0.00	**-1.36**	**0.01**	-1.12	0.05
		76933	Ifi27l2a	interferon, alpha-inducible protein 27 like 2A	3.18	0.00	**-1.58**	**0.00**	-0.48	0.22
		81897	Tlr9	toll-like receptor 9	1.70	0.00	**-1.46**	**0.00**	-0.66	0.06
		99899	Ifi44	interferon-induced protein 44	5.47	0.00	**-4.20**	**0.00**	-0.35	0.26
		142980	Tlr3	toll-like receptor 3	1.46	0.00	**-1.06**	**0.00**	-0.27	0.28
		209488	Hsh2d	hematopoietic SH2 domain containing	1.10	0.00	**-0.96**	**0.00**	-0.49	0.04
		246728	Oas2	2'-5' oligoadenylate synthetase 2	2.97	0.00	**-1.57**	**0.00**	-0.48	0.17
		246730	Oas1a	2'-5' oligoadenylate synthetase 1A	3.36	0.00	**-1.82**	**0.00**	-0.38	0.21
		625018	C4a	complement component 4A (Rodgers blood group)	2.49	0.00	**-1.43**	**0.00**	-0.28	0.37
	none[12]	12608	Cebpb	CCAAT/enhancer binding protein (C/EBP), beta	1.34	0.00	-0.49	0.14	-0.45	0.22
		15251	Hif1a	hypoxia inducible factor 1, alpha subunit	0.74	0.00	-0.42	0.05	0.32	0.18
		16155	Il10rb	interleukin 10 receptor, beta	0.57	0.00	-0.32	0.05	-0.04	0.87
		16885	Limk1	LIM-domain containing, protein kinase	0.81	0.00	-0.27	0.07	0.27	0.10
		16992	Lta	lymphotoxin A	0.58	0.04	-0.02	0.94	-0.18	0.55
		17087	Ly96	lymphocyte antigen 96	0.86	0.00	-0.32	0.08	-0.15	0.46
		17164	Mapkapk2	MAP kinase-activated protein kinase 2	1.05	0.00	-0.28	0.11	0.03	0.88
		18033	Nfkb1	nuclear factor of kappa light polypept. gene enh. in B cells 1, p105	0.60	0.02	-0.11	0.70	0.40	0.12
		18783	Pla2g4a	phospholipase A2, group IVA (cytosolic, calcium-dependent)	0.78	0.00	-0.47	0.01	0.07	0.74

		19766	Ripk1	receptor (TNFRSF)-interacting serine-threonine kinase 1	0.61	0.00	-0.14	0.46	0.23	0.27
		20304	Ccl5	chemokine (C-C motif) ligand 5	2.50	0.00	-0.30	0.48	0.02	0.96
		20307	Ccl8	chemokine (C-C motif) ligand 8	3.60	0.00	-0.27	0.69	0.12	0.87
		20848	Stat3	signal transducer and activator of transcription 3	0.56	0.00	-0.17	0.26	0.01	0.96
		21899	Tlr6	toll-like receptor 6	0.85	0.00	-0.31	0.18	-0.49	0.06
		21926	Tnf	tumor necrosis factor	0.61	0.01	-0.18	0.45	-0.38	0.14
		24047	Ccl19	chemokine (C-C motif) ligand 19	1.48	0.02	0.20	0.78	1.10	0.10
		26395	Map2k1	mitogen-activated protein kinase kinase 1	0.76	0.00	-0.41	0.02	-0.09	0.65
		50909	C1ra	complement component 1, r subcomponent A	0.71	0.00	-0.02	0.94	0.42	0.05
		56221	Ccl24	chemokine (C-C motif) ligand 24	1.69	0.02	-0.28	0.72	-0.21	0.80
		110006	Gusb	glucuronidase, beta	1.10	0.00	-0.44	0.04	0.34	0.16

Gene expression change[1]	Different from ctrl Ab in:	EntrezID	Symbol	Gene Name	no virus vs rCl13 + ctrl Ab[6]		rCl13 + αIFNAR vs rCl13 + ctrl Ab[7]		rCl13 + αGR-1 vs rCl13 + ctrl Ab[8]	
					log2FC	adj.P.Val	log2FC	adj.P.Val	log2FC	adj.P.Val
down-regulated in rCl13-infected bone marrow[5]	αGR-1[9]	16177	Il1r1	interleukin 1 receptor, type I	-1.45	0.00	0.47	0.11	**1.08**	**0.00**
	αGR-1 & αIFNAR[10]	11687	Alox15	arachidonate 15-lipoxygenase	-0.94	0.02	**0.80**	**0.03**	**-2.16**	**0.00**
		15962	Ifna1	interferon alpha 1	-0.68	0.00	**0.67**	**0.00**	**0.52**	**0.03**
	αIFNAR[11]	11596	Ager	advanced glycosylation end product-specific receptor	-1.24	0.00	**0.99**	**0.00**	0.35	0.29
		12048	Bcl2l1	BCL2-like 1	-2.23	0.00	**1.27**	**0.00**	0.17	0.58
		13712	Elk1	ELK1, member of ETS oncogene family	-0.85	0.00	**0.51**	**0.01**	-0.42	0.06
		17134	Mafg	v-maf musculoaponeurotic fibrosarc. oncog. fam., protein G (avian)	-1.13	0.00	**0.67**	**0.00**	-0.12	0.64
		17392	Mmp3	matrix metallopeptidase 3	-0.71	0.00	**0.56**	**0.01**	0.11	0.64
		17906	Myl2	myosin, light polypeptide 2, regulatory, cardiac, slow	-1.53	0.00	**1.11**	**0.01**	-0.40	0.39
		18751	Prkcb	protein kinase C, beta	-0.79	0.01	**0.62**	**0.02**	-0.40	0.17
		18795	Plcb1	phospholipase C, beta 1	-0.77	0.03	**1.09**	**0.00**	0.12	0.76
		19222	Ptgir	prostaglandin I receptor (IP)	-0.91	0.00	**0.70**	**0.01**	0.42	0.14
		19224	Ptgs1	prostaglandin-endoperoxide synthase 1	-1.20	0.00	**0.65**	**0.01**	0.32	0.21
		26408	Map3k5	mitogen-activated protein kinase kinase kinase 5	-0.63	0.00	**0.61**	**0.00**	-0.09	0.64
		26417	Mapk3	mitogen-activated protein kinase 3	-0.72	0.04	**0.71**	**0.04**	-0.26	0.50
		53791	Tlr5	toll-like receptor 5	-1.32	0.00	**1.09**	**0.00**	-0.26	0.44
		97165	Hmgb2	high mobility group box 2	-1.31	0.00	**0.79**	**0.00**	0.09	0.79
	none[12]	11909	Atf2	activating transcription factor 2	-0.53	0.00	0.27	0.02	0.06	0.65
		12053	Bcl6	B cell leukemia/lymphoma 6	-0.53	0.04	0.47	0.05	-0.52	0.05
		12775	Ccr7	chemokine (C-C motif) receptor 7	-0.67	0.03	-0.05	0.89	-0.28	0.38
		14683	Gnas	GNAS (guanine nucleot. Bind. Prot., alpha stim.) complex locus	-0.83	0.01	0.50	0.09	-0.38	0.25
		14699	Gngt1	guanine nucleot. bind. protein (G prot.), gamma transd. Act. polyp. 1	-0.73	0.01	0.30	0.24	0.31	0.27
		16198	Il9	interleukin 9	-0.89	0.03	0.50	0.18	-0.09	0.87
		17135	Mafk	v-maf musculoaponeurotic fibrosarc. Oncog. Fam., prot. K (avian)	-0.88	0.00	0.26	0.08	-0.03	0.88
		17165	Mapkapk5	MAP kinase-activated protein kinase 5	-0.87	0.03	0.30	0.44	0.18	0.68
		18750	Prkca	protein kinase C, alpha	-1.47	0.01	0.84	0.13	0.53	0.40
		18829	Ccl21a	chemokine (C-C motif) ligand 21A (serine)	-0.73	0.01	0.15	0.58	-0.05	0.87
		21390	Tbxa2r	thromboxane A2 receptor	-0.87	0.04	0.72	0.07	0.36	0.41
		26401	Map3k1	mitogen-activated protein kinase kinase kinase 1	-0.53	0.01	0.16	0.37	-0.18	0.38
		73086	Rps6ka5	ribosomal protein S6 kinase, polypeptide 5	-0.77	0.01	0.48	0.05	0.05	0.88
		93671	Cd163	CD163 antigen	-1.86	0.00	0.50	0.09	-0.34	0.29
		329251	Ppp1r12b	protein phosphatase 1, regulatory (inhibitor) subunit 12B	-0.70	0.01	0.20	0.42	0.49	0.07
		338372	Map3k9	mitogen-activated protein kinase kinase kinase 9	-1.22	0.02	0.90	0.07	-0.55	0.30
		NA	Hras1	NA	-0.83	0.00	0.42	0.10	-0.14	0.65

[1] We transferred naïve KL25HL cells into wt recipients followed by rCl13 infection. Total RNA was extracted from spleen and BM on day 3 p.i. and processed for expression profiling of 248 inflammation-related genes. The table displays all those genes whose expression was significantly altered upon rCl13 infection (absolute $\log_2$ fold change (log2FC) >0.5 and adjusted *p* value (adj.P.Val) <0.05 when comparing gene expression in uninfected animals to rCl13-infected control-treated animals.

[2] The table shows 49 genes significantly up-regulated upon rCl13 infection in spleen. These data are displayed in form of a heat map in Fig. 4F.

[3] The table displays 83 genes significantly down-regulated upon rCl13 infection in spleen.

[4] The table displays 67 genes significantly up-regulated upon rCl13 infection in BM.

[5] The table displays 34 genes significantly down-regulated upon rCl13 infection in BM.

[6] Gene expression changes as $\log_2$ fold-change (log2FC) and adjusted *p* value (adj.P.Val) when comparing uninfected (no virus) and rCl13-infected control-treated mice.

[7] Gene expression changes as $\log_2$ fold-change (log2FC) and adjusted *p* value (adj.P.Val) when comparing rCL13 infected αIFNAR-treated mice and rCl13-infected control-treated mice.

[8] Gene expression changes as log_2 fold-change (log2FC) and adjusted *p* value (adj.P.Val) when comparing rCL13 infected αGr-1-treated mice and rCl13-infected control-treated mice.
[9] Genes whose expression was significantly altered in αGr-1-treated as compared to control-treated animals.
[10] Genes whose expression was significantly altered in both αGr-1-treated and αIFNAR-treated as compared to control-treated animals.
[11] Genes whose expression was significantly altered in αIFNAR-treated as compared to control-treated animals.
[12] Genes whose expression was not altered by αGr-1 nor αIFNAR treatment as compared to control-treated animals.

Table SII: Profound impact of IFNAR blockade and, to a more limited but largely overlapping extent, of αGr-1 depletion of inflammatory chemokine and cytokine responses in serum.

Chemokine[3]	Experimental group[1]					
	ctrl Ab[2]		αGR-1[2]		*ifnar*$^{-/-}$ [2]	
	mean	SEM	mean	SEM	mean	SEM
CCL2	3873.73	658.68	3118.46	1460.51	217.61	93.03
CCL3	226.09	3.47	432.50	34.29	82.84	8.55
CCL4	770.38	58.54	1257.12	64.58	63.90	31.97
CCL5	778.74	113.17	535.88	30.32	92.33	4.09
CCL11	987.74	41.62	891.78	33.50	526.14	52.38
CXCL1	465.31	117.45	677.78	231.09	95.51	37.41
CXCL2	231.37	5.84	165.34	24.87	153.95	35.92
CXCL5	16152.36	830.11	10648.70	1903.08	17578.23	1945.04
CXCL9	913.28	101.08	430.89	8.83	366.17	39.26
CXCL10	1173.96	136.86	832.50	36.37	217.87	7.57
LIF	6.99	0.50	4.60	0.46	1.75	0.20

Cytokine[3]	Experimental group[1]					
	ctrl Ab[2]		αGR-1[2]		*ifnar*$^{-/-}$ [2]	
	mean	SEM	mean	SEM	mean	SEM
TNF-α	68.29	9.97	7.01	1.59	5.20	3.04
IFN-γ	20.86	1.55	5.69	2.01	<0.64	N.A.
IL-1α	293.45	31.74	409.65	121.65	147.44	22.68
IL1-β	281.69	78.77	50.23	49.91	<0.64	N.A.
IL-2	16.85	9.45	25.56	14.58	1.16	0.46
IL-3	26.15	7.11	19.70	14.34	2.00	1.04
IL-4	25.43	5.47	0.99	0.67	<0.64	N.A.
IL-5	100.21	9.90	56.80	3.59	8.67	0.71
IL-6	115.56	30.20	57.10	30.71	6.27	1.08
IL-7	113.62	26.91	64.80	5.05	28.81	6.73
IL-9	85.86	35.49	133.78	71.19	18.83	3.52
IL-10	97.96	24.94	12.65	3.92	1.87	1.55
IL-12p40	74.39	42.89	182.91	168.07	26.94	3.87
IL-12p70	515.30	128.33	48.73	17.86	9.53	9.21
IL-13	85.90	23.17	47.53	13.93	71.33	10.73
IL-15	443.36	151.27	180.02	27.39	119.71	24.72
IL-17	31.33	1.91	20.79	4.92	<0.64	N.A.
G-CSF	6712.20	587.83	19290.09	905.23	606.98	97.00
GM-CSF	104.69	28.14	82.16	39.27	8.53	8.21
M-CSF	55.13	27.95	129.93	121.08	12.62	2.91
VEGF	1.19	0.47	3.72	1.85	<0.64	N.A.

[1] We infected mice with rCl13 and collected serum 24 and 72 hours later.

[2] The experimental groups consisted in wt mice, treated with αGr-1 or isotype control antibody, and in *ifnar*$^{-/-}$ mice.
[3] Chemokine concentrations (pg/ml) measured at 24 hours and cytokines measured at 72 hours after infection are displayed. To calculate means and SEM (*n*=3), individual values below detection limits were set to detection limit (0.64 pg/ml). A selection of these data is displayed in Fig. 4G.

2.7 Acknowledgments

We wish to thank S. Sammicheli, M. Kuka and M. Iannacone for long-standing and open exchange about their closely related work; C.A. Siegrist, P.H. Lambert, J.C. Weill, J. Luban, T. Rolink, R. Tussiwand and M. Recher for helpful discussions and comments on the manuscript; D. Labes, G. Salinas, T. Lingner, S. Iuthin, F. Ludewig, F. Geier, D. Chollet and S. Clement for cell sorting, gene expression profiling, biomathematical analyses and immunohistochemistry. RNAseq data are deposited with the National Center for Biotechnology Information Gene Expression Omnibus (GEO, accession number XXXXXX). This work was supported by the European Research Council (ERC grant No. 310962 to DDP) and by the Swiss National Science Foundation (stipendiary professorships No. PP00P3_135442/1 to DDP and No. PP00P3_152928 to DM).

II. Global Discussion and Perspectives

Perturbation of the immune responses during chronic viral infections leads to dysfunctionalities of adaptive immune responses. Immune system's efforts to cope with the foreign antigens or pathogens, at times, result in deletion or differentiation of immune cells. This discussion will focus on the two works included in this thesis to interrelate the subversive effects of chronic infection on adaptive immune compartments and the contribution of vectored antibody therapy on the control of the infection and therefore potential decrease or reversion of the subversive effects of the chronic infection.

II.1 Impacts of inflammatory milieu and VIT on virus specific B cell responses

Cytokine responses orchestrate the functionality and differentiation of distinct immune cell types. Type-I interferon (IFN-I) is a major regulatory cytokine inducing various immune functions. We and others have shown that at early stages of an infection, B cells decimate in the presence of IFN-I (Fallet et al., 2016; Moseman et al., 2016; Sammicheli et al., 2016). Deletion of these virus specific cells might be an effort of the immune system to stimulate the differentiation of plasmablasts and therefore promoting the increase in the early antibody production in the presence of an inflammatory milieu. In addition to the LCMV infection, many chronic infections exert sustained IFN-I transcriptome signatures including chronic HCV and active tuberculosis. The main aim of antibody therapies in controlling the chronic viral infections is naturally to suppress the viral loads. Suppression of the viral loads leads to the decline in inflammatory responses; therefore, the dysfunctional B cell and T cell compartments might be potentially reawakened or at least function more potently and robustly. Passive antibody immunizations were shown to enhance endogenous antibody responses in HIV and SHIV infections (Ng et al., 2010; Schoofs et al., 2016). In relation to this, our work contributes to the field with the side that AAV-mediated nAb expression enhances the virus-glycoprotein

specific antibody responses, and this enhancement effect is maintained over a long period of time. For infections where virus specific B cell responses undergo immune subversion, such immunotherapies might be evaluated with consideration. Chronic infections can result in B cell dysfunctionalities as seen in HIV-infected individuals (Titanji et al., 2005). Anti-retroviral therapy (ART), however, upon early administration was shown to preserve B cell functions (Moir et al., 2010). This might hint towards the idea that suppression of the viral antigen load as a consequence of ART, might enable the prevention of B cell dysfunctionality. With our therapy, our work shows that mice receiving VIT augments virus-specific B cell responses compared to untreated controls. Moreover, although the frequency of the GC cells among the NP-specific cells were comparable, number of NP-specific cells accumulated at the germinal centers were numerously higher in VIT-treated mice. Mechanisms to underpin the reasons for such an enhancement need to be further investigated. Emergence of quasi-species of viruses as a result of the VIT (and partial contribution from the endogenous antibody compartment) might trigger the formation of new B cell lineages exerting a polyclonal response to control these quasi-species of newly emerging viruses.

II.2 Necessity for the functional B cell and T cell compartments in the control of the viral escape variants

Not only B cell responses but T cell responses are known to be showing dysfunctional features, known as exhaustion. nAbs arise only in the late stages of the infection, and poor neutralizing antibodies are another correlate of various chronic infections, and the mechanisms interfering the neutralizing antibody responses during chronic infections still remain to be solved. Therefore, the functionality of several major immune compartments is impaired during chronic infections and regaining their functionality might play a role in the control of the infections where the antigen persists for a long term.

We have reported that the presence of the monotherapy led to the emergence of viral escape variants. Presence of an intact endogenous immune system is vital for the control of these escape variants, and we have shown viral clearance requires the involvement of both T and B cell responses. Restriction and control of viral escape variants by the means of combinatorial antibody therapy, to an extent, was reported previously (Barouch et al., 2013; Shingai et al., 2013). Therefore, to maximize the efficacy of the VIT in scenarios where the immune system is defective, combinatorial therapies with multiple nAbs can be considered for administration to assess the efficacy for the control of the infection. These aspects need further investigation. To our best knowledge, studies involving antibody therapies focus on clearance and antibody response measurements. There is significant need to understand the effects of these therapies on cellular players of the immune compartments. In this work, we address the synergy and impact of VIT on host cellular immune responses. We have previously shown that in the presence of IFN-I, virus specific cells undergo decimation. We have also suggested that IFN-I mediated B cell decimation includes involvement of various immune cell types such as dendritic cells (DCs), T cells and myeloid cells. Furthermore, in addition to IFN-I, IL-10 and TNF-α were shown to contribute to the decimation of B cells. In the absence or blockage of these cytokines, B cells were partially rescued. Virus-specific B cells survived in neonatally-infected carrier mice and IFN-I levels were detected to be very low in these mice. Interestingly, KL25HL-trangenic mice that were neonatally infected were shown to fail to clear the viral infection with LCMV (Seiler et al., 1999). Moreover, escape variant viruses, resistant to the KL25-binding, emerged in these carrier mice. Interestingly, carrier mice are known to be T cell tolerant mice (Pircher et al., 1989b). They can mount (although defective) low level antibody responses, but they were shown to lack virus specific T cell responses due to the presence of the virus in the course of thymic selection. Interestingly, our work shows VIT can only result

in viral clearance and control of the escape variants in the presence of intact B and T cells responses.

II.3 VIT-mediated clearance effect on Tfh compartment

Contribution and necessity of CD4 T cells for the control of chronic infections has been shown for several disease models including HBV and HCV, both in humans and mice models (Asabe et al., 2009; Matloubian et al., 1994; Planz et al., 1997; Shoukry et al., 2004). During chronic infections loss of antiviral Th1 cells can occur, and CD4 T cells show skewing into Tfh phenotype to mediate follicular helper functions (Brooks et al., 2005; Crawford et al., 2014; Oxenius et al., 2001). Probably for the decimation of the B cells, Tfh cells do not play a significant role as it is still too early for these cells to arise to provide helper functions. But, for the chronic phase of the infection, Tfh cells are known to accumulate in numbers compared to cleared infection or acute infection (Fahey et al., 2011). This is in parallel to our observations, since we detect lowered numbers of virus-specific Tfh cells in VIT receiving mice that clear the infection at the end time point. Moreover, CD4 T cells, 1 week after LCMV Clone 13 infection fail to produce IFNγ and TNF upon *ex vivo* stimulation (Brooks et al., 2005) and this continues even after viral clearance. We cannot assess whether VIT can alter or enhance Tfh mediated helper functions to B cells, further work can be useful to understand the effect of VIT on Tfh helper functions during chronic infections.

II.4 Potential combination therapies with VIT to regain exhausted T cell functionality

Exhaustion of CD8 T cells occur during chronic infections, possibly due to excess antigen loads (Gallimore et al., 1998; Moskophidis et al., 1993; Zajac et al., 1998) (Barber et al., 2006; Day et al., 2006; Mueller and Ahmed, 2009b; Pauken et al., 2016; Scott-Browne et al., 2016; Sen et al., 2016; Wherry et al., 2007). Our work shows, to our best knowledge for the first time, phenotypic reversion of exhausted CD8 T cells with VIT. CD8 T cells, after clearance, have

downregulated the expression of the inhibitory receptors, PD-1 and LAG-3, yet the *ex vivo* restimulation of the cells did not result in cytokine production. In HIV infection, ART was shown to reduce the expression of PD-1 in virus specific cells in HIV-infected individuals. Furthermore, long-term non-progressors (LTNPs) were shown to have low PD-1 expression on virus-specific T cells, and the cells from LTNPs are more potent and polyfunctional compared to their counterparts from progressive individuals (Day et al., 2006; Trautmann et al., 2006; Yi et al., 2010). Numerous *in vitro* and *in vivo* studies, in model animals from mice to chimpanzee show the promising effects of PD-1 blockade or anti-PD-L1 administration on the increase and functionality regaining of virus specific CD8 T cells (Day et al., 2006; Dyavar Shetty et al., 2012; Palmer et al., 2013; Petrovas et al., 2006; Trautmann et al., 2006; Velu et al., 2009). Therefore, possible additive effect of PD-1 blockade or anti-PD-L1 treatment in addition to VIT should be investigated to understand the effect of accelerated regain of T cell functionality on viral clearance dynamics. Such efforts can be valuable for potential development of treatments combining VIT and checkpoint inhibitors for the control of chronic viral infections. We have shown the involvement of T cell compartments in the decimation of virus specific B cells. Rather than being a direct-killer or effector, we believe CTLs contribute to the inflammatory milieu and this leads to the change in the splenic microarchitecture in the onset of the infection (Battegay et al., 1993; Odermatt et al., 1991). Furthermore, B cells adoptively transferred in *cd8*$^{-/-}$ and *cd4-cre x ifnar*$^{fl/fl}$ recipients were partially rescued, this suggests for a possible effect of CTLs but probably an indirect effect. Further experiments are needed to confirm that. The damage of CTLs to the splenic architecture in the early stages, and throughout the chronic infection might be one of the reasons why mice cannot mount nAb responses until late time points (around day 40). Especially for Docile infection we could not detect nAbs even on day 40. Therefore, using an antibody therapy, replacing the lacking nAb responses could work as a mechanism to lower excess antigen loads in the organs and the bone

marrow. This might give the possibility of emergence of new B cell lineages with alternative BCRs that will be responsive to emerging quasi-species of the viruses in the presence of an antibody pressure. In the absence of the contribution of an antibody therapy, viremia will be protracted, but will be cleared eventually.

III. References

Ahmed, R., A. Salmi, L.D. Butler, J.M. Chiller, and M.B. Oldstone. 1984. Selection of genetic variants of lymphocytic choriomeningitis virus in spleens of persistently infected mice. Role in suppression of cytotoxic T lymphocyte response and viral persistence. *The Journal of Experimental Medicine* 160:521-540.

Aiuti, A., L. Biasco, S. Scaramuzza, F. Ferrua, M.P. Cicalese, C. Baricordi, F. Dionisio, A. Calabria, S. Giannelli, M.C. Castiello, M. Bosticardo, C. Evangelio, A. Assanelli, M. Casiraghi, S. Di Nunzio, L. Callegaro, C. Benati, P. Rizzardi, D. Pellin, C. Di Serio, M. Schmidt, C. Von Kalle, J. Gardner, N. Mehta, V. Neduva, D.J. Dow, A. Galy, R. Miniero, A. Finocchi, A. Metin, P.P. Banerjee, J.S. Orange, S. Galimberti, M.G. Valsecchi, A. Biffi, E. Montini, A. Villa, F. Ciceri, M.G. Roncarolo, and L. Naldini. 2013. Lentiviral Hematopoietic Stem Cell Gene Therapy in Patients with Wiskott-Aldrich Syndrome. *Science* 341:1233151.

Alba, R., A. Bosch, and M. Chillon. 2005. Gutless adenovirus: last-generation adenovirus for gene therapy. *Gene Therapy* 12:S18-S27.

ALEXANDER, H.E. 1943. EXPERIMENTAL BASIS FOR TREATMENT OF HAEMOPHILUS INFLUENZAE INFECTIONS. *JAMA Pediatrics* 66:160-171.

Alexander, H.E., and M. Heidelberger. 1940. CHEMICAL STUDIES ON BACTERIAL AGGLUTINATION : V. AGGLUTININ AND PRECIPITIN CONTENT OF ANTISERA TO HAEMOPHILUS INFLUENZA, TYPE B. *The Journal of experimental medicine* 71:1-11.

Allen, C.D.C., T. Okada, H.L. Tang, and J.G. Cyster. 2007. Imaging of Germinal Center Selection Events During Affinity Maturation. *Science* 315:528-531.

Armbruster, C., G.M. Stiegler, B.A. Vcelar, W. Jäger, U. Köller, R. Jilch, C.G. Ammann, M. Pruenster, H. Stoiber, and H.W.D. Katinger. 2004. Passive immunization with the anti-HIV-1 human monoclonal antibody (hMAb) 4E10 and the hMAb combination 4E10/2F5/2G12. *Journal of Antimicrobial Chemotherapy* 54:915-920.

Asabe, S., S.F. Wieland, P.K. Chattopadhyay, M. Roederer, R.E. Engle, R.H. Purcell, and F.V. Chisari. 2009. The Size of the Viral Inoculum Contributes to the Outcome of Hepatitis B Virus Infection. *Journal of Virology* 83:9652-9662.

Atchison, R.W., B.C. Casto, and W.M. Hammon. 1965. Adenovirus-Associated Defective Virus Particles. *Science* 149:754-755.

Balazs, A.B., J.D. Bloom, C.M. Hong, D.S. Rao, and D. Baltimore. 2013. Broad protection against influenza infection by vectored immunoprophylaxis in mice. *Nature Biotechnology* 31:647.

Balazs, A.B., J. Chen, C.M. Hong, D.S. Rao, L. Yang, and D. Baltimore. 2012. Antibody-based protection against HIV infection by vectored immunoprophylaxis. *Nature* 481:81-84.

Balazs, A.B., Y. Ouyang, C.M. Hong, J. Chen, S.M. Nguyen, D.S. Rao, D.S. An, and D. Baltimore. 2014. Vectored immunoprophylaxis protects humanized mice from mucosal HIV transmission. *Nature Medicine* 20:296.

Balázs, M., F. Martin, T. Zhou, and J.F. Kearney. 2002. Blood Dendritic Cells Interact with Splenic Marginal Zone B Cells to Initiate T-Independent Immune Responses. *Immunity* 17:341-352.

Bar-On, Y., H. Gruell, T. Schoofs, J.A. Pai, L. Nogueira, A.L. Butler, K. Millard, C. Lehmann, I. Suárez, T.Y. Oliveira, T. Karagounis, Y.Z. Cohen, C. Wyen, S. Scholten, L. Handl, S. Belblidia, J.P. Dizon, J.J. Vehreschild, M. Witmer-Pack, I. Shimeliovich, K. Jain, K.

Fiddike, K.E. Seaton, N.L. Yates, J. Horowitz, R.M. Gulick, N. Pfeifer, G.D. Tomaras, M.S. Seaman, G. Fätkenheuer, M. Caskey, F. Klein, and M.C. Nussenzweig. 2018. Safety and antiviral activity of combination HIV-1 broadly neutralizing antibodies in viremic individuals. *Nature Medicine* 24:1701-1707.

Barber, D.L., E.J. Wherry, D. Masopust, B. Zhu, J.P. Allison, A.H. Sharpe, G.J. Freeman, and R. Ahmed. 2006. Restoring function in exhausted CD8 T cells during chronic viral infection. *Nature* 439:682-687.

Barouch, D.H., J.B. Whitney, B. Moldt, F. Klein, T.Y. Oliveira, J. Liu, K.E. Stephenson, H.-W. Chang, K. Shekhar, S. Gupta, J.P. Nkolola, M.S. Seaman, K.M. Smith, E.N. Borducchi, C. Cabral, J.Y. Smith, S. Blackmore, S. Sanisetty, J.R. Perry, M. Beck, M.G. Lewis, W. Rinaldi, A.K. Chakraborty, P. Poignard, M.C. Nussenzweig, and D.R. Burton. 2013. Therapeutic efficacy of potent neutralizing HIV-1-specific monoclonal antibodies in SHIV-infected rhesus monkeys. *Nature* 503:224.

Battegay, M., S. Cooper, A. Althage, J. Banziger, H. Hengartner, and R.M. Zinkernagel. 1991a. Quantification of lymphocytic choriomeningitis virus with an immunological focus assay in 24- or 96-well plates. *J Virol Methods* 33:191-198.

Battegay, M., S. Cooper, A. Althage, J. Bänziger, H. Hengartner, and R.M. Zinkernagel. 1991b. Quantification of lymphocytic choriomeningitis virus with an immunological focus assay in 24- or 96-well plates. *Journal of Virological Methods* 33:191-198.

Battegay, M., D. Moskophidis, A. Rahemtulla, H. Hengartner, T.W. Mak, and R.M. Zinkernagel. 1994. Enhanced establishment of a virus carrier state in adult CD4+ T-cell-deficient mice. *Journal of Virology* 68:4700-4704.

Battegay, M., D. Moskophidis, H. Waldner, M.A. Bründler, W.P. Fung-Leung, T.W. Mak, H. Hengartner, and R.M. Zinkernagel. 1993. Impairment and delay of neutralizing antiviral antibody responses by virus-specific cytotoxic T cells. *The Journal of Immunology* 151:5408-5415.

Behring, E.v., Shibasaburo Kitasato. 1890. Ueber Das Zustandekommen Der Diphtherie-Immunität Und Der Tetanus-Immunität Bei Thieren. *Deutsch. Med. Woch.* 49:1113-1114.

Bergthaler, A., L. Flatz, A. Verschoor, A.N. Hegazy, M. Holdener, K. Fink, B. Eschli, D. Merkler, R. Sommerstein, E. Horvath, M. Fernandez, A. Fitsche, B.M. Senn, J.S. Verbeek, B. Odermatt, C.-A. Siegrist, and D.D. Pinschewer. 2009. Impaired Antibody Response Causes Persistence of Prototypic T Cell–Contained Virus. *PLOS Biology* 7:e1000080.

Bergthaler, A., D. Merkler, E. Horvath, L. Bestmann, and D.D. Pinschewer. 2007. Contributions of the LCMV glycoprotein and polymerase to strain-specific differences in murine liver pathogenicity. *J Gen Virol* 88:592-603.

Berry, M.P., C.M. Graham, F.W. McNab, Z. Xu, S.A. Bloch, T. Oni, K.A. Wilkinson, R. Banchereau, J. Skinner, R.J. Wilkinson, C. Quinn, D. Blankenship, R. Dhawan, J.J. Cush, A. Mejias, O. Ramilo, O.M. Kon, V. Pascual, J. Banchereau, D. Chaussabel, and A. O'Garra. 2010. An interferon-inducible neutrophil-driven blood transcriptional signature in human tuberculosis. *Nature* 466:973-977.

Bolen, C.R., M.D. Robek, L. Brodsky, V. Schulz, J.K. Lim, M.W. Taylor, and S.H. Kleinstein. 2013. The blood transcriptional signature of chronic hepatitis C virus is consistent with an ongoing interferon-mediated antiviral response. *J Interferon Cytokine Res* 33:15-23.

Borducchi, E.N., J. Liu, J.P. Nkolola, A.M. Cadena, W.-H. Yu, S. Fischinger, T. Broge, P. Abbink, N.B. Mercado, A. Chandrashekar, D. Jetton, L. Peter, K. McMahan, E.T. Moseley, E.

Bekerman, J. Hesselgesser, W. Li, M.G. Lewis, G. Alter, R. Geleziunas, and D.H. Barouch. 2018. Antibody and TLR7 agonist delay viral rebound in SHIV-infected monkeys. *Nature* 563:360-364.

Boring, L., J. Gosling, S.W. Chensue, S.L. Kunkel, R.V. Farese, Jr., H.E. Broxmeyer, and I.F. Charo. 1997. Impaired monocyte migration and reduced type 1 (Th1) cytokine responses in C-C chemokine receptor 2 knockout mice. *J Clin Invest* 100:2552-2561.

Boutin, S., V. Monteilhet, P. Veron, C. Leborgne, O. Benveniste, M.F. Montus, and C. Masurier. 2010. Prevalence of Serum IgG and Neutralizing Factors Against Adeno-Associated Virus (AAV) Types 1, 2, 5, 6, 8, and 9 in the Healthy Population: Implications for Gene Therapy Using AAV Vectors. *Human Gene Therapy* 21:704-712.

Brooks, D.G., D.B. McGavern, and M.B.A. Oldstone. 2006. Reprogramming of antiviral T cells prevents inactivation and restores T cell activity during persistent viral infection. *The Journal of Clinical Investigation* 116:1675-1685.

Brooks, D.G., L. Teyton, M.B.A. Oldstone, and D.B. McGavern. 2005. Intrinsic Functional Dysregulation of CD4 T Cells Occurs Rapidly following Persistent Viral Infection. *Journal of Virology* 79:10514-10527.

Bründler, M.-A., P. Aichele, M. Bachmann, D. Kitamura, K. Rajewsky, and R.M. Zinkernagel. 1996. Immunity to viruses in B cell-deficient mice: Influence of antibodies on virus persistence and on T cell memory. *European Journal of Immunology* 26:2257-2262.

Buchlis, G., G.M. Podsakoff, A. Radu, S.M. Hawk, A.W. Flake, F. Mingozzi, and K.A. High. 2012. Factor IX expression in skeletal muscle of a severe hemophilia B patient 10 years after AAV-mediated gene transfer. *Blood* 119:3038-3041.

Burkhart, C., G. Freer, U. Steinhoff, Y. Li, D.H. Bishop, R.M. Zinkernagel, and H. Hengartner. 1994. Localization of T helper cell epitopes in the vesicular stomatitis virus: the nucleoprotein is responsible for serotype cross-reactive T help. *Viral Immunol* 7:103-111.

Burton, A.R., L.J. Pallett, L.E. McCoy, K. Suveizdyte, O.E. Amin, L. Swadling, E. Alberts, B.R. Davidson, P.T.F. Kennedy, U.S. Gill, C. Mauri, P.A. Blair, N. Pelletier, and M.K. Maini. 2018. Circulating and intrahepatic antiviral B cells are defective in hepatitis B. *The Journal of Clinical Investigation* 128:4588-4603.

Cartier, N., S. Hacein-Bey-Abina, C.C. Bartholomae, G. Veres, M. Schmidt, I. Kutschera, M. Vidaud, U. Abel, L. Dal-Cortivo, L. Caccavelli, N. Mahlaoui, V. Kiermer, D. Mittelstaedt, C. Bellesme, N. Lahlou, F. Lefrère, S. Blanche, M. Audit, E. Payen, P. Leboulch, B. l'Homme, P. Bougnères, C. Von Kalle, A. Fischer, M. Cavazzana-Calvo, and P. Aubourg. 2009. Hematopoietic Stem Cell Gene Therapy with a Lentiviral Vector in X-Linked Adrenoleukodystrophy. *Science* 326:818-823.

Casadevall, A., and M.D. Scharff. 1995. Return to the Past: The Case for Antibody-Based Therapies in Infectious Diseases. *Clinical Infectious Diseases* 21:150-161.

Caskey, M., F. Klein, J.C.C. Lorenzi, M.S. Seaman, A.P. West Jr, N. Buckley, G. Kremer, L. Nogueira, M. Braunschweig, J.F. Scheid, J.A. Horwitz, I. Shimeliovich, S. Ben-Avraham, M. Witmer-Pack, M. Platten, C. Lehmann, L.A. Burke, T. Hawthorne, R.J. Gorelick, B.D. Walker, T. Keler, R.M. Gulick, G. Fätkenheuer, S.J. Schlesinger, and M.C. Nussenzweig. 2015. Viraemia suppressed in HIV-1-infected humans by broadly neutralizing antibody 3BNC117. *Nature* 522:487.

Caskey, M., T. Schoofs, H. Gruell, A. Settler, T. Karagounis, E.F. Kreider, B. Murrell, N. Pfeifer, L. Nogueira, T.Y. Oliveira, G.H. Learn, Y.Z. Cohen, C. Lehmann, D. Gillor, I. Shimeliovich, C. Unson-O'Brien, D. Weiland, A. Robles, T. Kümmerle, C. Wyen, R.

Levin, M. Witmer-Pack, K. Eren, C. Ignacio, S. Kiss, A.P. West Jr, H. Mouquet, B.S. Zingman, R.M. Gulick, T. Keler, P.J. Bjorkman, M.S. Seaman, B.H. Hahn, G. Fätkenheuer, S.J. Schlesinger, M.C. Nussenzweig, and F. Klein. 2017. Antibody 10-1074 suppresses viremia in HIV-1-infected individuals. *Nature Medicine* 23:185.

Caton, M.L., M.R. Smith-Raska, and B. Reizis. 2007. Notch-RBP-J signaling controls the homeostasis of CD8- dendritic cells in the spleen. *J Exp Med* 204:1653-1664.

Cavacini, L.A., M.H. Samore, J. Gambertoglio, B. Jackson, M. Duval, A. Wisnewski, S. Hammer, C. Koziel, C. Trapnell, and M.R. Posner. 1998. Phase I Study of a Human Monoclonal Antibody Directed against the CD4-Binding Site of HIV Type 1 Glycoprotein 120. *AIDS Research and Human Retroviruses* 14:545-550.

Cavazzana-Calvo, M., E. Payen, O. Negre, G. Wang, K. Hehir, F. Fusil, J. Down, M. Denaro, T. Brady, K. Westerman, R. Cavallesco, B. Gillet-Legrand, L. Caccavelli, R. Sgarra, L. Maouche-Chrétien, F. Bernaudin, R. Girot, R. Dorazio, G.-J. Mulder, A. Polack, A. Bank, J. Soulier, J. Larghero, N. Kabbara, B. Dalle, B. Gourmel, G. Socie, S. Chrétien, N. Cartier, P. Aubourg, A. Fischer, K. Cornetta, F. Galacteros, Y. Beuzard, E. Gluckman, F. Bushman, S. Hacein-Bey-Abina, and P. Leboulch. 2010. Transfusion independence and HMGA2 activation after gene therapy of human β-thalassaemia. *Nature* 467:318.

Chen, C., Z. Yang, and X. Tang. 2018. Chemical modifications of nucleic acid drugs and their delivery systems for gene-based therapy. *Medicinal Research Reviews* 38:829-869.

Chen, M., M. Sallberg, A. Sonnerborg, O. Weiland, L. Mattsson, L. Jin, A. Birkett, D. Peterson, and D.R. Milich. 1999. Limited humoral immunity in hepatitis C virus infection. *Gastroenterology* 116:135-143.

Christensen, J.P., S.Ø. Kauffmann, and A.R. Thomsen. 2003. Deficient CD4⁺ T Cell Priming and Regression of CD8⁺ T Cell Functionality in Virus-Infected Mice Lacking a Normal B Cell Compartment. *The Journal of Immunology* 171:4733-4741.

Ciurea, A., L. Hunziker, P. Klenerman, H. Hengartner, and R.M. Zinkernagel. 2001. Impairment of Cd4⁺ T Cell Responses during Chronic Virus Infection Prevents Neutralizing Antibody Responses against Virus Escape Mutants. *The Journal of Experimental Medicine* 193:297-306.

Clausen, B.E., C. Burkhardt, W. Reith, R. Renkawitz, and I. Forster. 1999. Conditional gene targeting in macrophages and granulocytes using LysMcre mice. *Transgenic Res* 8:265-277.

Cohen, M.S., G.M. Shaw, A.J. McMichael, and B.F. Haynes. 2011. Acute HIV-1 Infection. *N Engl J Med* 364:1943-1954.

Corti, D., and A. Lanzavecchia. 2013. Broadly Neutralizing Antiviral Antibodies. *Annual Review of Immunology* 31:705-742.

Coutelier, J.P., J.T. van der Logt, F.W. Heessen, G. Warnier, and J. Van Snick. 1987. IgG2a restriction of murine antibodies elicited by viral infections. *The Journal of Experimental Medicine* 165:64-69.

Crawford, A., Jill M. Angelosanto, C. Kao, Travis A. Doering, Pamela M. Odorizzi, Burton E. Barnett, and E.J. Wherry. 2014. Molecular and Transcriptional Basis of CD4+ T Cell Dysfunction during Chronic Infection. *Immunity* 40:289-302.

Crouse, J., G. Bedenikovic, M. Wiesel, M. Ibberson, I. Xenarios, D. Von Laer, U. Kalinke, E. Vivier, S. Jonjic, and A. Oxenius. 2014. Type I interferons protect T cells against NK cell attack mediated by the activating receptor NCR1. *Immunity* 40:961-973.

Cunnington, A.J., and E.M. Riley. 2010. Suppression of vaccine responses by malaria: insignificant or overlooked? *Expert Rev Vaccines* 9:409-429.

Day, C.L., D.E. Kaufmann, P. Kiepiela, J.A. Brown, E.S. Moodley, S. Reddy, E.W. Mackey, J.D. Miller, A.J. Leslie, C. DePierres, Z. Mncube, J. Duraiswamy, B. Zhu, Q. Eichbaum, M. Altfeld, E.J. Wherry, H.M. Coovadia, P.J.R. Goulder, P. Klenerman, R. Ahmed, G.J. Freeman, and B.D. Walker. 2006. PD-1 expression on HIV-specific T cells is associated with T-cell exhaustion and disease progression. *Nature* 443:350-354.

de Jong, Y.P., M. Dorner, M.C. Mommersteeg, J.W. Xiao, A.B. Balazs, J.B. Robbins, B.Y. Winer, S. Gerges, K. Vega, R.N. Labitt, B.M. Donovan, E. Giang, A. Krishnan, L. Chiriboga, M.R. Charlton, D.R. Burton, D. Baltimore, M. Law, C.M. Rice, and A. Ploss. 2014. Broadly neutralizing antibodies abrogate established hepatitis C virus infection. *Science Translational Medicine* 6:254ra129-254ra129.

Deev, R., I. Plaksa, I. Bozo, N. Mzhavanadze, I. Suchkov, Y. Chervyakov, I. Staroverov, R. Kalinin, and A. Isaev. 2018. Results of 5-year follow-up study in patients with peripheral artery disease treated with PL-VEGF165 for intermittent claudication. *Therapeutic Advances in Cardiovascular Disease* 12:237-246.

Denard, J., J. Rouillon, T. Leger, C. Garcia, M.P. Lambert, G. Griffith, C. Jenny, J.-M. Camadro, L. Garcia, and F. Svinartchouk. 2018. AAV-8 and AAV-9 Vectors Cooperate with Serum Proteins Differently Than AAV-1 and AAV-6. *Molecular Therapy - Methods & Clinical Development* 10:291-302.

Diskin, R., F. Klein, J.A. Horwitz, A. Halper-Stromberg, D.N. Sather, P.M. Marcovecchio, T. Lee, A.P. West, H. Gao, M.S. Seaman, L. Stamatatos, M.C. Nussenzweig, and P.J. Bjorkman. 2013. Restricting HIV-1 pathways for escape using rationally designed anti–HIV-1 antibodies. *The Journal of Experimental Medicine* 210:1235-1249.

Dobin, A., C.A. Davis, F. Schlesinger, J. Drenkow, C. Zaleski, S. Jha, P. Batut, M. Chaisson, and T.R. Gingeras. 2013. STAR: ultrafast universal RNA-seq aligner. *Bioinformatics* 29:15-21.

Duan, D., P. Sharma, J. Yang, Y. Yue, L. Dudus, Y. Zhang, K.J. Fisher, and J.F. Engelhardt. 1998. Circular Intermediates of Recombinant Adeno-Associated Virus Have Defined Structural Characteristics Responsible for Long-Term Episomal Persistence in Muscle Tissue. *Journal of Virology* 72:8568-8577.

Duan, D., Z. Yan, Y. Yue, and J.F. Engelhardt. 1999. Structural Analysis of Adeno-Associated Virus Transduction Circular Intermediates. *Virology* 261:8-14.

Dyavar Shetty, R., V. Velu, K. Titanji, S.E. Bosinger, G.J. Freeman, G. Silvestri, and R.R. Amara. 2012. PD-1 blockade during chronic SIV infection reduces hyperimmune activation and microbial translocation in rhesus macaques. *The Journal of Clinical Investigation* 122:1712-1716.

Emini, E.A., W.A. Schleif, J.H. Nunberg, A.J. Conley, Y. Eda, S. Tokiyoshi, S.D. Putney, S. Matsushrta, K.E. Cobb, C.M. Jett, J.W. Eichberg, and K.K. Murthy. 1992. Prevention of HIV-1 infection in chimpanzees by gpl20 V3 domain-specific monoclonal antibody. *Nature* 355:728-730.

Emonet, S., J.-J. Lemasson, J.-P. Gonzalez, X. de Lamballerie, and R.N. Charrel. 2006. Phylogeny and evolution of old world arenaviruses. *Virology* 350:251-257.

Eschli, B., R.M. Zellweger, A. Wepf, K.S. Lang, K. Quirin, J. Weber, R.M. Zinkernagel, and H. Hengartner. 2007a. Early antibodies specific for the neutralizing epitope on the receptor binding subunit of the lymphocytic choriomeningitis virus glycoprotein fail to neutralize the virus. *J Virol* 81:11650-11657.

Eschli, B., R.M. Zellweger, A. Wepf, K.S. Lang, K. Quirin, J. Weber, R.M. Zinkernagel, and H. Hengartner. 2007b. Early Antibodies Specific for the Neutralizing Epitope on the Receptor Binding Subunit of the Lymphocytic Choriomeningitis Virus Glycoprotein Fail To Neutralize the Virus. *Journal of Virology* 81:11650-11657.

Fahey, L.M., E.B. Wilson, H. Elsaesser, C.D. Fistonich, D.B. McGavern, and D.G. Brooks. 2011. Viral persistence redirects CD4 T cell differentiation toward T follicular helper cells. *The Journal of Experimental Medicine* 208:987-999.

Fallet, B., K. Narr, Y.I. Ertuna, M. Remy, R. Sommerstein, K. Cornille, M. Kreutzfeldt, N. Page, G. Zimmer, F. Geier, T. Straub, H. Pircher, K. Larimore, P.D. Greenberg, D. Merkler, and D.D. Pinschewer. 2016. Interferon-driven deletion of antiviral B cells at the onset of chronic infection. *Science Immunology* 1:eaah6817.

Fang, J., J.-J. Qian, S. Yi, T.C. Harding, G.H. Tu, M. VanRoey, and K. Jooss. 2005. Stable antibody expression at therapeutic levels using the 2A peptide. *Nature Biotechnology* 23:584-590.

Ferrari, F.K., T. Samulski, T. Shenk, and R.J. Samulski. 1996. Second-strand synthesis is a rate-limiting step for efficient transduction by recombinant adeno-associated virus vectors. *Journal of Virology* 70:3227-3234.

Fisher, K.J., G.P. Gao, M.D. Weitzman, R. DeMatteo, J.F. Burda, and J.M. Wilson. 1996. Transduction with recombinant adeno-associated virus for gene therapy is limited by leading-strand synthesis. *Journal of virology* 70:520-532.

Flatz, L., A. Bergthaler, J.C. de la Torre, and D.D. Pinschewer. 2006. Recovery of an arenavirus entirely from RNA polymerase I/II-driven cDNA. *Proc Natl Acad Sci U S A* 103:4663-4668.

Freund, N.T., H. Wang, L. Scharf, L. Nogueira, J.A. Horwitz, Y. Bar-On, J. Golijanin, S.A. Sievers, D. Sok, H. Cai, J.C. Cesar Lorenzi, A. Halper-Stromberg, I. Toth, A. Piechocka-Trocha, H.B. Gristick, M.J. van Gils, R.W. Sanders, L.-X. Wang, M.S. Seaman, D.R. Burton, A. Gazumyan, B.D. Walker, A.P. West, P.J. Bjorkman, and M.C. Nussenzweig. 2017. Coexistence of potent HIV-1 broadly neutralizing antibodies and antibody-sensitive viruses in a viremic controller. *Science Translational Medicine* 9:eaal2144.

Fuchs, S.P., J.M. Martinez-Navio, M. Piatak, Jr., J.D. Lifson, G. Gao, and R.C. Desrosiers. 2015. AAV-Delivered Antibody Mediates Significant Protective Effects against SIVmac239 Challenge in the Absence of Neutralizing Activity. *PLOS Pathogens* 11:e1005090.

Fung-Leung, W.P., M.W. Schilham, A. Rahemtulla, T.M. Kundig, M. Vollenweider, J. Potter, W. van Ewijk, and T.W. Mak. 1991. CD8 is needed for development of cytotoxic T cells but not helper T cells. *Cell* 65:443-449.

Gaidatzis, D., A. Lerch, F. Hahne, and M.B. Stadler. 2015. QuasR: quantification and annotation of short reads in R. *Bioinformatics* 31:1130-1132.

Gallimore, A., A. Glithero, A. Godkin, A.C. Tissot, A. Plückthun, T. Elliott, H. Hengartner, and R. Zinkernagel. 1998. Induction and Exhaustion of Lymphocytic Choriomeningitis Virus–specific Cytotoxic T Lymphocytes Visualized Using Soluble Tetrameric Major Histocompatibility Complex Class I–Peptide Complexes. *The Journal of Experimental Medicine* 187:1383-1393.

Gao, G.-P., M.R. Alvira, L. Wang, R. Calcedo, J. Johnston, and J.M. Wilson. 2002. Novel adeno-associated viruses from rhesus monkeys as vectors for human gene therapy. *Proceedings of the National Academy of Sciences* 99:11854-11859.

Gardner, M.R., L.M. Kattenhorn, H.R. Kondur, M. von Schaewen, T. Dorfman, J.J. Chiang, K.G. Haworth, J.M. Decker, M.D. Alpert, C.C. Bailey, E.S. Neale, C.H. Fellinger, V.R.

Joshi, S.P. Fuchs, J.M. Martinez-Navio, B.D. Quinlan, A.Y. Yao, H. Mouquet, J. Gorman, B. Zhang, P. Poignard, M.C. Nussenzweig, D.R. Burton, P.D. Kwong, M. Piatak, J.D. Lifson, G. Gao, R.C. Desrosiers, D.T. Evans, B.H. Hahn, A. Ploss, P.M. Cannon, M.S. Seaman, and M. Farzan. 2015. AAV-expressed eCD4-Ig provides durable protection from multiple SHIV challenges. *Nature* 519:87.

Garside, P., E. Ingulli, R.R. Merica, J.G. Johnson, R.J. Noelle, and M.K. Jenkins. 1998. Visualization of specific B and T lymphocyte interactions in the lymph node. *Science* 281:96-99.

Gautam, R., Y. Nishimura, A. Pegu, M.C. Nason, F. Klein, A. Gazumyan, J. Golijanin, A. Buckler-White, R. Sadjadpour, K. Wang, Z. Mankoff, S.D. Schmidt, J.D. Lifson, J.R. Mascola, M.C. Nussenzweig, and M.A. Martin. 2016. A single injection of anti-HIV-1 antibodies protects against repeated SHIV challenges. *Nature* 533:105.

Ginn, S.L., A.K. Amaya, I.E. Alexander, M. Edelstein, and M.R. Abedi. 2018. Gene therapy clinical trials worldwide to 2017: An update. *The Journal of Gene Medicine* 20:e3015.

Goodnow, C.C., J. Crosbie, S. Adelstein, T.B. Lavoie, S.J. Smith-Gill, R.A. Brink, H. Pritchard-Briscoe, J.S. Wotherspoon, R.H. Loblay, K. Raphael, R.J. Trent, and A. Basten. 1988. Altered immunoglobulin expression and functional silencing of self-reactive B lymphocytes in transgenic mice. *Nature* 334:676-682.

Green, L.L., M.C. Hardy, C.E. Maynard-Currie, H. Tsuda, D.M. Louie, M.J. Mendez, H. Abderrahim, M. Noguchi, D.H. Smith, Y. Zeng, N.E. David, H. Sasai, D. Garza, D.G. Brenner, J.F. Hales, R.P. McGuinness, D.J. Capon, S. Klapholz, and A. Jakobovits. 1994. Antigen–specific human monoclonal antibodies from mice engineered with human Ig heavy and light chain YACs. *Nature Genetics* 7:13-21.

Grieger, J.C., S.M. Soltys, and R.J. Samulski. 2016. Production of Recombinant Adeno-associated Virus Vectors Using Suspension HEK293 Cells and Continuous Harvest of Vector From the Culture Media for GMP FIX and FLT1 Clinical Vector. *Molecular Therapy* 24:287-297.

Grimaldi, J.C., N.X. Yu, G. Grunig, B.W. Seymour, F. Cottrez, D.S. Robinson, N. Hosken, W.G. Ferlin, X. Wu, H. Soto, A. O'Garra, M.C. Howard, and R.L. Coffman. 1999. Depletion of eosinophils in mice through the use of antibodies specific for C-C chemokine receptor 3 (CCR3). *J Leukoc Biol* 65:846-853.

Gu, Z. 2016. ComplexHeatmap: Making Complex Heatmaps. R package version 1.10.2. . *https://github.com/jokergoo/ComplexHeatmap*

Guan, X., Z. Guo, T. Wang, L. Lin, J. Chen, H. Tian, and X. Chen. 2017. A pH-Responsive Detachable PEG Shielding Strategy for Gene Delivery System in Cancer Therapy. *Biomacromolecules* 18:1342-1349.

Hacein-Bey-Abina, S., A. Garrigue, G.P. Wang, J. Soulier, A. Lim, E. Morillon, E. Clappier, L. Caccavelli, E. Delabesse, K. Beldjord, V. Asnafi, E. MacIntyre, L. Dal Cortivo, I. Radford, N. Brousse, F. Sigaux, D. Moshous, J. Hauer, A. Borkhardt, B.H. Belohradsky, U. Wintergerst, M.C. Velez, L. Leiva, R. Sorensen, N. Wulffraat, S. Blanche, F.D. Bushman, A. Fischer, and M. Cavazzana-Calvo. 2008. Insertional oncogenesis in 4 patients after retrovirus-mediated gene therapy of SCID-X1. *J Clin Invest* 118:3132-3142.

Halper-Stromberg, A., C.-L. Lu, F. Klein, Joshua A. Horwitz, S. Bournazos, L. Nogueira, Thomas R. Eisenreich, C. Liu, A. Gazumyan, U. Schaefer, Rebecca C. Furze, Michael S. Seaman, R. Prinjha, A. Tarakhovsky, Jeffrey V. Ravetch, and Michel C. Nussenzweig.

2014. Broadly Neutralizing Antibodies and Viral Inducers Decrease Rebound from HIV-1 Latent Reservoirs in Humanized Mice. *Cell* 158:989-999.

Hammon, W.M., L.L. Coriell, and J. Stokes, Jr. 1952. EVALUATION OF RED CROSS GAMMA GLOBULIN AS A PROPHYLACTIC AGENT FOR POLIOMYELITIS: 2. CONDUCT AND EARLY FOLLOW-UP OF 1952 TEXAS AND IOWA-NEBRASKA STUDIES. *JAMA* 150:750-756.

Hangartner, L., B.M. Senn, B. Ledermann, U. Kalinke, P. Seiler, E. Bucher, R.M. Zellweger, K. Fink, B. Odermatt, K. Burki, R.M. Zinkernagel, and H. Hengartner. 2003. Antiviral immune responses in gene-targeted mice expressing the immunoglobulin heavy chain of virus-neutralizing antibodies. *Proc Natl Acad Sci U S A* 100:12883-12888.

Hanna, E., C. Rémuzat, P. Auquier, and M. Toumi. 2017. Gene therapies development: slow progress and promising prospect. *Journal of Market Access & Health Policy* 5:1265293.

Harker, J.A., G.M. Lewis, L. Mack, and E.I. Zuniga. 2011. Late Interleukin-6 Escalates T Follicular Helper Cell Responses and Controls a Chronic Viral Infection. *Science* 334:825-829.

He, R., S. Hou, C. Liu, A. Zhang, Q. Bai, M. Han, Y. Yang, G. Wei, T. Shen, X. Yang, L. Xu, X. Chen, Y. Hao, P. Wang, C. Zhu, J. Ou, H. Liang, T. Ni, X. Zhang, X. Zhou, K. Deng, Y. Chen, Y. Luo, J. Xu, H. Qi, Y. Wu, and L. Ye. 2016. Follicular CXCR5-expressing CD8+ T cells curtail chronic viral infection. *Nature* 537:412.

Hoggan, M.D., N.R. Blacklow, and W.P. Rowe. 1966. Studies of small DNA viruses found in various adenovirus preparations: physical, biological, and immunological characteristics. *Proc Natl Acad Sci U S A* 55:1467-1474.

Horai, R., M. Asano, K. Sudo, H. Kanuka, M. Suzuki, M. Nishihara, M. Takahashi, and Y. Iwakura. 1998. Production of mice deficient in genes for interleukin (IL)-1alpha, IL-1beta, IL-1alpha/beta, and IL-1 receptor antagonist shows that IL-1beta is crucial in turpentine-induced fever development and glucocorticoid secretion. *J Exp Med* 187:1463-1475.

Horwitz, J.A., A. Halper-Stromberg, H. Mouquet, A.D. Gitlin, A. Tretiakova, T.R. Eisenreich, M. Malbec, S. Gravemann, E. Billerbeck, M. Dorner, H. Büning, O. Schwartz, E. Knops, R. Kaiser, M.S. Seaman, J.M. Wilson, C.M. Rice, A. Ploss, P.J. Bjorkman, F. Klein, and M.C. Nussenzweig. 2013. HIV-1 suppression and durable control by combining single broadly neutralizing antibodies and antiretroviral drugs in humanized mice. *Proceedings of the National Academy of Sciences* 110:16538-16543.

Hotchin, J., and H. Weigand. 1961. Studies of Lymphocytic Choriomeningitis in Mice. <*span class="subtitle">I. The Relationship Between Age at Inoculation and Outcome of Infection</span*> 86:392-400.

Hu, W.-S., and V.K. Pathak. 2000. Design of Retroviral Vectors and Helper Cells for Gene Therapy. *Pharmacological Reviews* 52:493-512.

Hur, E.M., S.N. Patel, S. Shimizu, D.S. Rao, P.N.P. Gnanapragasam, D.S. An, L. Yang, and D. Baltimore. 2012. Inhibitory effect of HIV-specific neutralizing IgA on mucosal transmission of HIV in humanized mice. *Blood* 120:4571-4582.

Im, S.J., M. Hashimoto, M.Y. Gerner, J. Lee, H.T. Kissick, M.C. Burger, Q. Shan, J.S. Hale, J. Lee, T.H. Nasti, A.H. Sharpe, G.J. Freeman, R.N. Germain, H.I. Nakaya, H.-H. Xue, and R. Ahmed. 2016. Defining CD8+ T cells that provide the proliferative burst after PD-1 therapy. *Nature* 537:417.

Janeway, C.A. 1945. Use of Concentrated Human Serum gamma-Globulin in the Prevention and Attenuation of Measles. *Bull N Y Acad Med* 21:202-222.

Johnson, P.R., B.C. Schnepp, J. Zhang, M.J. Connell, S.M. Greene, E. Yuste, R.C. Desrosiers, and K. Reed Clark. 2009. Vector-mediated gene transfer engenders long-lived neutralizing activity and protection against SIV infection in monkeys. *Nature Medicine* 15:901-906.

Johnson, S., A. Bergthaler, F. Graw, L. Flatz, W.V. Bonilla, C.-A. Siegrist, P.-H. Lambert, R.R. Regoes, and D.D. Pinschewer. 2015. Protective Efficacy of Individual CD8⁺ T Cell Specificities in Chronic Viral Infection. *The Journal of Immunology* 194:1755-1762.

Joosten, S.A., K.E. van Meijgaarden, F. Del Nonno, A. Baiocchini, L. Petrone, V. Vanini, H.H. Smits, F. Palmieri, D. Goletti, and T.H. Ottenhoff. 2016. Patients with Tuberculosis Have a Dysfunctional Circulating B-Cell Compartment, Which Normalizes following Successful Treatment. *PLoS Pathog* 12:e1005687.

Joseph, A., J.H. Zheng, K. Chen, M. Dutta, C. Chen, G. Stiegler, R. Kunert, A. Follenzi, and H. Goldstein. 2010. Inhibition of In Vivo HIV Infection in Humanized Mice by Gene Therapy of Human Hematopoietic Stem Cells with a Lentiviral Vector Encoding a Broadly Neutralizing Anti-HIV Antibody. *Journal of Virology* 84:6645-6653.

Kacani, L., H. Stoiber, and M.P. Dierich. 1997. Role of IL-15 in HIV-1-associated hypergammaglobulinaemia. *Clin Exp Immunol* 108:14-18.

Kalhoro, N.H., J. Veits, S. Rautenschlein, and G. Zimmer. 2009. A recombinant vesicular stomatitis virus replicon vaccine protects chickens from highly pathogenic avian influenza virus (H7N1). *Vaccine* 27:1174-1183.

Kalinke, U., E.M. Bucher, B. Ernst, A. Oxenius, H.P. Roost, S. Geley, R. Kofler, R.M. Zinkernagel, and H. Hengartner. 1996. The role of somatic mutation in the generation of the protective humoral immune response against vesicular stomatitis virus. *Immunity* 5:639-652.

Kaplon, H., and J.M. Reichert. 2019. Antibodies to watch in 2019. *mAbs* 11:219-238.

Kay, M.A., J.C. Glorioso, and L. Naldini. 2001. Viral vectors for gene therapy: the art of turning infectious agents into vehicles of therapeutics. *Nature Medicine* 7:33-40.

Kirn, D. 2001. Clinical research results with dl1520 (Onyx-015), a replication-selective adenovirus for the treatment of cancer: what have we learned? *Gene Therapy* 8:89-98.

Klein, F., A. Halper-Stromberg, J.A. Horwitz, H. Gruell, J.F. Scheid, S. Bournazos, H. Mouquet, L.A. Spatz, R. Diskin, A. Abadir, T. Zang, M. Dorner, E. Billerbeck, R.N. Labitt, C. Gaebler, P.M. Marcovecchio, R.-B. Incesu, T.R. Eisenreich, P.D. Bieniasz, M.S. Seaman, P.J. Bjorkman, J.V. Ravetch, A. Ploss, and M.C. Nussenzweig. 2012. HIV therapy by a combination of broadly neutralizing antibodies in humanized mice. *Nature* 492:118.

Klein, F., H. Mouquet, P. Dosenovic, J.F. Scheid, L. Scharf, and M.C. Nussenzweig. 2013. Antibodies in HIV-1 Vaccine Development and Therapy. *Science* 341:1199-1204.

Klein, F., L. Nogueira, Y. Nishimura, G. Phad, A.P. West, A. Halper-Stromberg, J.A. Horwitz, A. Gazumyan, C. Liu, T.R. Eisenreich, C. Lehmann, G. Fätkenheuer, C. Williams, M. Shingai, M.A. Martin, P.J. Bjorkman, M.S. Seaman, S. Zolla-Pazner, G.B. Karlsson Hedestam, and M.C. Nussenzweig. 2014. Enhanced HIV-1 immunotherapy by commonly arising antibodies that target virus escape variants. *The Journal of Experimental Medicine* 211:2361-2372.

Klein, M.A., R. Frigg, E. Flechsig, A.J. Raeber, U. Kalinke, H. Bluethmann, F. Bootz, M. Suter, R.M. Zinkernagel, and A. Aguzzi. 1997. A crucial role for B cells in neuroinvasive scrapie. *Nature* 390:687-690.

Ko, S.-Y., A. Pegu, R.S. Rudicell, Z.-y. Yang, M.G. Joyce, X. Chen, K. Wang, S. Bao, T.D. Kraemer, T. Rath, M. Zeng, S.D. Schmidt, J.-P. Todd, S.R. Penzak, K.O. Saunders, M.C. Nason, A.T. Haase, S.S. Rao, R.S. Blumberg, J.R. Mascola, and G.J. Nabel. 2014. Enhanced neonatal Fc receptor function improves protection against primate SHIV infection. *Nature* 514:642.

Köhler, G., and C. Milstein. 1975. Continuous cultures of fused cells secreting antibody of predefined specificity. *Nature* 256:495-497.

Kopf, M., H. Baumann, G. Freer, M. Freudenberg, M. Lamers, T. Kishimoto, R. Zinkernagel, H. Bluethmann, and G. Kohler. 1994. Impaired immune and acute-phase responses in interleukin-6-deficient mice. *Nature* 368:339-342.

Kormann, M.S.D., G. Hasenpusch, M.K. Aneja, G. Nica, A.W. Flemmer, S. Herber-Jonat, M. Huppmann, L.E. Mays, M. Illenyi, A. Schams, M. Griese, I. Bittmann, R. Handgretinger, D. Hartl, J. Rosenecker, and C. Rudolph. 2011. Expression of therapeutic proteins after delivery of chemically modified mRNA in mice. *Nature Biotechnology* 29:154-157.

Kreuzaler, M., M. Rauch, U. Salzer, J. Birmelin, M. Rizzi, B. Grimbacher, A. Plebani, V. Lougaris, I. Quinti, V. Thon, J. Litzman, M. Schlesier, K. Warnatz, J. Thiel, A.G. Rolink, and H. Eibel. 2012. Soluble BAFF levels inversely correlate with peripheral B cell numbers and the expression of BAFF receptors. *J Immunol* 188:497-503.

Kuhn, R., J. Lohler, D. Rennick, K. Rajewsky, and W. Muller. 1993. Interleukin-10-deficient mice develop chronic enterocolitis. *Cell* 75:263-274.

Kuhn, R., K. Rajewsky, and W. Muller. 1991. Generation and analysis of interleukin-4 deficient mice. *Science* 254:707-710.

Labuda, L.A., U. Ateba-Ngoa, E.N. Feugap, J.J. Heeringa, L.E. van der Vlugt, R.B. Pires, L. Mewono, P.G. Kremsner, M.C. van Zelm, A.A. Adegnika, M. Yazdanbakhsh, and H.H. Smits. 2013. Alterations in peripheral blood B cell subsets and dynamics of B cell responses during human schistosomiasis. *PLoS Negl Trop Dis* 7:e2094.

Laubach, V.E., E.G. Shesely, O. Smithies, and P.A. Sherman. 1995. Mice lacking inducible nitric oxide synthase are not resistant to lipopolysaccharide-induced death. *Proc Natl Acad Sci U S A* 92:10688-10692.

Laughlin, C.A., H. Westphal, and B.J. Carter. 1979. Spliced adenovirus-associated virus RNA. *Proc Natl Acad Sci U S A* 76:5567-5571.

Law, C.W., Y. Chen, W. Shi, and G.K. Smyth. 2014. voom: Precision weights unlock linear model analysis tools for RNA-seq read counts. *Genome Biol* 15:R29.

Lee, P.P., D.R. Fitzpatrick, C. Beard, H.K. Jessup, S. Lehar, K.W. Makar, M. Perez-Melgosa, M.T. Sweetser, M.S. Schlissel, S. Nguyen, S.R. Cherry, J.H. Tsai, S.M. Tucker, W.M. Weaver, A. Kelso, R. Jaenisch, and C.B. Wilson. 2001. A critical role for Dnmt1 and DNA methylation in T cell development, function, and survival. *Immunity* 15:763-774.

Leong, Y.A., Y. Chen, H.S. Ong, D. Wu, K. Man, C. Deleage, M. Minnich, B.J. Meckiff, Y. Wei, Z. Hou, D. Zotos, K.A. Fenix, A. Atnerkar, S. Preston, J.G. Chipman, G.J. Beilman, C.C. Allison, L. Sun, P. Wang, J. Xu, J.G. Toe, H.K. Lu, Y. Tao, U. Palendira, A.L. Dent, A.L. Landay, M. Pellegrini, I. Comerford, S.R. McColl, T.W. Schacker, H.M. Long, J.D. Estes,

M. Busslinger, G.T. Belz, S.R. Lewin, A. Kallies, and D. Yu. 2016. CXCR5+ follicular cytotoxic T cells control viral infection in B cell follicles. *Nature Immunology* 17:1187.

Lewis, A.D., R. Chen, D.C. Montefiori, P.R. Johnson, and K.R. Clark. 2002. Generation of Neutralizing Activity against Human Immunodeficiency Virus Type 1 in Serum by Antibody Gene Transfer. *Journal of Virology* 76:8769-8775.

Li, J., C.I. Lord, W. Haseltine, N.L. Letvin, and J. Sodroski. 1992. Infection of cynomolgus monkeys with a chimeric HIV-1/SIVmac virus that expresses the HIV-1 envelope glycoproteins. *Journal of acquired immune deficiency syndromes* 5:639-646.

Liu, D., H. Xu, C. Shih, Z. Wan, X. Ma, W. Ma, D. Luo, and H. Qi. 2014. T–B-cell entanglement and ICOSL-driven feed-forward regulation of germinal centre reaction. *Nature* 517:214.

Lock, M., M.R. Alvira, S.-J. Chen, and J.M. Wilson. 2013. Absolute Determination of Single-Stranded and Self-Complementary Adeno-Associated Viral Vector Genome Titers by Droplet Digital PCR. *Human Gene Therapy Methods* 25:115-125.

Lonberg, N., L.D. Taylor, F.A. Harding, M. Trounstine, K.M. Higgins, S.R. Schramm, C.-C. Kuo, R. Mashayekh, K. Wymore, J.G. McCabe, D. Munoz-O'Regan, S.L. O'Donnell, E.S.G. Lapachet, T. Bengoechea, D.M. Fishwild, C.E. Carmack, R.M. Kay, and D. Huszar. 1994. Antigen-specific human antibodies from mice comprising four distinct genetic modifications. *Nature* 368:856-859.

Louten, J., N. van Rooijen, and C.A. Biron. 2006. Type 1 IFN Deficiency in the Absence of Normal Splenic Architecture during Lymphocytic Choriomeningitis Virus Infection. *The Journal of Immunology* 177:3266-3272.

Lu, C.-L., D.K. Murakowski, S. Bournazos, T. Schoofs, D. Sarkar, A. Halper-Stromberg, J.A. Horwitz, L. Nogueira, J. Golijanin, A. Gazumyan, J.V. Ravetch, M. Caskey, A.K. Chakraborty, and M.C. Nussenzweig. 2016. Enhanced clearance of HIV-1–infected cells by broadly neutralizing antibodies against HIV-1 in vivo. *Science* 352:1001-1004.

Luo, X.M., E. Maarschalk, R.M. O'Connell, P. Wang, L. Yang, and D. Baltimore. 2009. Engineering human hematopoietic stem/progenitor cells to produce a broadly neutralizing anti-HIV antibody after in vitro maturation to human B lymphocytes. *Blood* 113:1422-1431.

Macchia, D., F. Almerigogna, P. Parronchi, A. Ravina, E. Maggi, and S. Romagnani. 1993. Membrane tumour necrosis factor-alpha is involved in the polyclonal B-cell activation induced by HIV-infected human T cells. *Nature* 363:464-466.

MacLaren, R.E., M. Groppe, A.R. Barnard, C.L. Cottriall, T. Tolmachova, L. Seymour, K.R. Clark, M.J. During, F.P.M. Cremers, G.C.M. Black, A.J. Lotery, S.M. Downes, A.R. Webster, and M.C. Seabra. 2014. Retinal gene therapy in patients with choroideremia: initial findings from a phase 1/2 clinical trial. *The Lancet* 383:1129-1137.

MacLennan, I.C.M., A. Gulbranson-Judge, K.M. Toellner, M. Casamayor-Palleja, E. Chan, D.M.Y. Sze, S.A. Luther, and H.A. Orbea. 1997. The changing preference of T and B cells for partners as T-dependent antibody responses develop. *Immunological Reviews* 156:53-66.

Magram, J., S.E. Connaughton, R.R. Warrier, D.M. Carvajal, C.Y. Wu, J. Ferrante, C. Stewart, U. Sarmiento, D.A. Faherty, and M.K. Gately. 1996. IL-12-deficient mice are defective in IFN gamma production and type 1 cytokine responses. *Immunity* 4:471-481.

Malaspina, A., S. Moir, S.M. Orsega, J. Vasquez, N.J. Miller, E.T. Donoghue, S. Kottilil, M. Gezmu, D. Follmann, G.M. Vodeiko, R.A. Levandowski, J.M. Mican, and A.S. Fauci.

2005. Compromised B cell responses to influenza vaccination in HIV-infected individuals. *J Infect Dis* 191:1442-1450.

Mandl, J.N., A.P. Barry, T.H. Vanderford, N. Kozyr, R. Chavan, S. Klucking, F.J. Barrat, R.L. Coffman, S.I. Staprans, and M.B. Feinberg. 2008. Divergent TLR7 and TLR9 signaling and type I interferon production distinguish pathogenic and nonpathogenic AIDS virus infections. *Nat Med* 14:1077-1087.

Manunta, M.D.I., A.D. Tagalakis, M. Attwood, A.M. Aldossary, J.L. Barnes, M.M. Munye, A. Weng, R.J. McAnulty, and S.L. Hart. 2017. Delivery of ENaC siRNA to epithelial cells mediated by a targeted nanocomplex: a therapeutic strategy for cystic fibrosis. *Scientific Reports* 7:700.

Matloubian, M., R.J. Concepcion, and R. Ahmed. 1994. CD4+ T cells are required to sustain CD8+ cytotoxic T-cell responses during chronic viral infection. *Journal of Virology* 68:8056-8063.

Matsushita, T., S. Elliger, C. Elliger, G. Podsakoff, L. Villarreal, G.J. Kurtzman, Y. Iwaki, and P. Colosi. 1998. Adeno-associated virus vectors can be efficiently produced without helper virus. *Gene Therapy* 5:938-945.

Maude, S.L., N. Frey, P.A. Shaw, R. Aplenc, D.M. Barrett, N.J. Bunin, A. Chew, V.E. Gonzalez, Z. Zheng, S.F. Lacey, Y.D. Mahnke, J.J. Melenhorst, S.R. Rheingold, A. Shen, D.T. Teachey, B.L. Levine, C.H. June, D.L. Porter, and S.A. Grupp. 2014. Chimeric Antigen Receptor T Cells for Sustained Remissions in Leukemia. *New England Journal of Medicine* 371:1507-1517.

Mays, L.E., L. Wang, J. Lin, P. Bell, A. Crawford, E.J. Wherry, and J.M. Wilson. 2014. AAV8 Induces Tolerance in Murine Muscle as a Result of Poor APC Transduction, T Cell Exhaustion, and Minimal MHCI Upregulation on Target Cells. *Molecular Therapy* 22:28-41.

McCafferty, J., A.D. Griffiths, G. Winter, and D.J. Chiswell. 1990. Phage antibodies: filamentous phage displaying antibody variable domains. *Nature* 348:552-554.

McCarthy, D.J., Y. Chen, and G.K. Smyth. 2012. Differential expression analysis of multifactor RNA-Seq experiments with respect to biological variation. *Nucleic Acids Res* 40:4288-4297.

Mesin, L., J. Ersching, and Gabriel D. Victora. 2016. Germinal Center B Cell Dynamics. *Immunity* 45:471-482.

Moir, S., C.M. Buckner, J. Ho, W. Wang, J. Chen, A.J. Waldner, J.G. Posada, L. Kardava, M.A. O'Shea, S. Kottilil, T.-W. Chun, M.A. Proschan, and A.S. Fauci. 2010. B cells in early and chronic HIV infection: evidence for preservation of immune function associated with early initiation of antiretroviral therapy. *Blood* 116:5571-5579.

Moir, S., and A.S. Fauci. 2014. B-cell exhaustion in HIV infection: the role of immune activation. *Curr Opin HIV AIDS* 9:472-477.

Moir, S., A. Malaspina, O.K. Pickeral, E.T. Donoghue, J. Vasquez, N.J. Miller, S.R. Krishnan, M.A. Planta, J.F. Turney, J.S. Justement, S. Kottilil, M. Dybul, J.M. Mican, C. Kovacs, T.W. Chun, C.E. Birse, and A.S. Fauci. 2004. Decreased survival of B cells of HIV-viremic patients mediated by altered expression of receptors of the TNF superfamily. *J Exp Med* 200:587-599.

Moseman, E.A., T. Wu, J.C. de la Torre, P.L. Schwartzberg, and D.B. McGavern. 2016. Type I interferon suppresses virus-specific B cell responses by modulating CD8⁺ T cell differentiation. *Science Immunology* 1:eaah3565.

Moskophidis, D., M. Battegay, M. van den Broek, E. Laine, U. Hoffmann-Rohrer, and R.M. Zinkernagel. 1995. Role of virus and host variables in virus persistence or immunopathological disease caused by a non-cytolytic virus. *Journal of General Virology* 76:381-391.

Moskophidis, D., F. Lechner, H. Pircher, and R.M. Zinkernagel. 1993. Virus persistence in acutely infected immunocompetent mice by exhaustion of antiviral cytotoxic effector T cells. *Nature* 362:758-761.

Mueller, S.N., and R. Ahmed. 2009a. High antigen levels are the cause of T cell exhaustion during chronic viral infection. *Proc Natl Acad Sci U S A* 106:8623-8628.

Mueller, S.N., and R. Ahmed. 2009b. High antigen levels are the cause of T cell exhaustion during chronic viral infection. *Proc Natl Acad Sci U S A* 106:8623-8628.

Muller, F., P. Aukrust, I. Nordoy, and S.S. Froland. 1998. Possible role of interleukin-10 (IL-10) and CD40 ligand expression in the pathogenesis of hypergammaglobulinemia in human immunodeficiency virus infection: modulation of IL-10 and Ig production after intravenous Ig infusion. *Blood* 92:3721-3729.

Muller, U., U. Steinhoff, L.F. Reis, S. Hemmi, J. Pavlovic, R.M. Zinkernagel, and M. Aguet. 1994. Functional role of type I and type II interferons in antiviral defense. *Science* 264:1918-1921.

Ndhlovu, Z.M., S.W. Kazer, T. Nkosi, F. Ogunshola, D.M. Muema, G. Anmole, S.A. Swann, A. Moodley, K. Dong, T. Reddy, M.A. Brockman, A.K. Shalek, T. Ndung'u, and B.D. Walker. 2019. Augmentation of HIV-specific T cell function by immediate treatment of hyperacute HIV-1 infection. *Science Translational Medicine* 11:eaau0528.

Nemerow, G.R., P.L. Stewart, and V.S. Reddy. 2012. Structure of human adenovirus. *Current Opinion in Virology* 2:115-121.

Ng, C.T., J.P. Jaworski, P. Jayaraman, W.F. Sutton, P. Delio, L. Kuller, D. Anderson, G. Landucci, B.A. Richardson, D.R. Burton, D.N. Forthal, and N.L. Haigwood. 2010. Passive neutralizing antibody controls SHIV viremia and enhances B cell responses in infant macaques. *Nature Medicine* 16:1117.

Nicolson, S.C., and R.J. Samulski. 2014. Recombinant Adeno-Associated Virus Utilizes Host Cell Nuclear Import Machinery To Enter the Nucleus. *Journal of Virology* 88:4132-4144.

Nishimura, Y., R. Gautam, T.-W. Chun, R. Sadjadpour, K.E. Foulds, M. Shingai, F. Klein, A. Gazumyan, J. Golijanin, M. Donaldson, O.K. Donau, R.J. Plishka, A. Buckler-White, M.S. Seaman, J.D. Lifson, R.A. Koup, A.S. Fauci, M.C. Nussenzweig, and M.A. Martin. 2017. Early antibody therapy can induce long-lasting immunity to SHIV. *Nature* 543:559.

Nolte, M.A., R. Arens, M. Kraus, M.H.J. van Oers, G. Kraal, R.A.W. van Lier, and R.E. Mebius. 2004. B Cells Are Crucial for Both Development and Maintenance of the Splenic Marginal Zone. *The Journal of Immunology* 172:3620-3627.

Nonnenmacher, M., and T. Weber. 2011. Adeno-Associated Virus 2 Infection Requires Endocytosis through the CLIC/GEEC Pathway. *Cell Host & Microbe* 10:563-576.

Norris, B.A., L.S. Uebelhoer, H.I. Nakaya, A.A. Price, A. Grakoui, and B. Pulendran. 2013. Chronic but not acute virus infection induces sustained expansion of myeloid suppressor cell numbers that inhibit viral-specific T cell immunity. *Immunity* 38:309-321.

Odermatt, B., M. Eppler, T.P. Leist, H. Hengartner, and R.M. Zinkernagel. 1991. Virus-triggered acquired immunodeficiency by cytotoxic T-cell-dependent destruction of

antigen-presenting cells and lymph follicle structure. *Proceedings of the National Academy of Sciences* 88:8252-8256.

Okada, T., M.J. Miller, I. Parker, M.F. Krummel, M. Neighbors, S.B. Hartley, A. O'Garra, M.D. Cahalan, and J.G. Cyster. 2005. Antigen-Engaged B Cells Undergo Chemotaxis toward the T Zone and Form Motile Conjugates with Helper T Cells. *PLOS Biology* 3:e150.

Oliviero, B., A. Cerino, S. Varchetta, E. Paudice, S. Pai, S. Ludovisi, M. Zaramella, G. Michelone, P. Pugnale, F. Negro, V. Barnaba, and M.U. Mondelli. 2011. Enhanced B-cell differentiation and reduced proliferative capacity in chronic hepatitis C and chronic hepatitis B virus infections. *J Hepatol* 55:53-60.

Osmond, D.G. 1993. The turnover of B-cell populations. *Immunol Today* 14:34-37.

Ou, R., S. Zhou, L. Huang, and D. Moskophidis. 2001. Critical Role for Alpha/Beta and Gamma Interferons in Persistence of Lymphocytic Choriomeningitis Virus by Clonal Exhaustion of Cytotoxic T Cells. *Journal of Virology* 75:8407-8423.

Oxenius, A., S. Fidler, M. Brady, S.J. Dawson, K. Ruth, P.J. Easterbrook, J.N. Weber, R.E. Phillips, and D.A. Price. 2001. Variable fate of virus-specific CD4+ T cells during primary HIV-1 infection. *European Journal of Immunology* 31:3782-3788.

Palmer, B.E., C.P. Neff, J. LeCureux, A. Ehler, M. DSouza, L. Remling-Mulder, A.J. Korman, A.P. Fontenot, and R. Akkina. 2013. In Vivo Blockade of the PD-1 Receptor Suppresses HIV-1 Viral Loads and Improves CD4⁺ T Cell Levels in Humanized Mice. *The Journal of Immunology* 190:211-219.

Parren, P.W.H.I., P.A. Marx, A.J. Hessell, A. Luckay, J. Harouse, C. Cheng-Mayer, J.P. Moore, and D.R. Burton. 2001. Antibody Protects Macaques against Vaginal Challenge with a Pathogenic R5 Simian/Human Immunodeficiency Virus at Serum Levels Giving Complete Neutralization In Vitro. *Journal of Virology* 75:8340-8347.

Pauken, K.E., M.A. Sammons, P.M. Odorizzi, S. Manne, J. Godec, O. Khan, A.M. Drake, Z. Chen, D.R. Sen, M. Kurachi, R.A. Barnitz, C. Bartman, B. Bengsch, A.C. Huang, J.M. Schenkel, G. Vahedi, W.N. Haining, S.L. Berger, and E.J. Wherry. 2016. Epigenetic stability of exhausted T cells limits durability of reinvigoration by PD-1 blockade. *Science* 354:1160-1165.

Peacock, D.B., J.V. Jones, and M. Gough. 1973. The immune response to thetaX 174 in man. I. Primary and secondary antibody production in normal adults. *Clin Exp Immunol* 13:497-513.

Penaloza-MacMaster, P., D.L. Barber, E.J. Wherry, N.M. Provine, J.E. Teigler, L. Parenteau, S. Blackmore, E.N. Borducchi, R.A. Larocca, K.B. Yates, H. Shen, W.N. Haining, R. Sommerstein, D.D. Pinschewer, R. Ahmed, and D.H. Barouch. 2015a. Vaccine-elicited CD4 T cells induce immunopathology after chronic LCMV infection. *Science* 347:278-282.

Penaloza-MacMaster, P., D.L. Barber, E.J. Wherry, N.M. Provine, J.E. Teigler, L. Parenteau, S. Blackmore, E.N. Borducchi, R.A. Larocca, K.B. Yates, H. Shen, W.N. Haining, R. Sommerstein, D.D. Pinschewer, R. Ahmed, and D.H. Barouch. 2015b. Vaccine-elicited CD4 T cells induce immunopathology after chronic LCMV infection. *Science* 347:278-282.

Pérarnau, B., M.-F. Saron, B.R. San Martin, N. Bervas, H. Ong, M.J. Soloski, A.G. Smith, J.M. Ure, J.E. Gairin, and F.A. Lemonnier. 1999. Single H2Kb, H2Db and double H2KbDb knockout mice: peripheral CD8+ T cell repertoire and antilymphocytic choriomeningitis virus cytolytic responses. *European Journal of Immunology* 29:1243-1252.

Perez, M., R.C. Craven, and J.C. de la Torre. 2003. The small RING finger protein Z drives arenavirus budding: Implications for antiviral strategies. *Proceedings of the National Academy of Sciences* 100:12978-12983.

Petrovas, C., J.P. Casazza, J.M. Brenchley, D.A. Price, E. Gostick, W.C. Adams, M.L. Precopio, T. Schacker, M. Roederer, D.C. Douek, and R.A. Koup. 2006. PD-1 is a regulator of virus-specific CD8⁺ T cell survival in HIV infection. *The Journal of Experimental Medicine* 203:2281-2292.

Pfau, C.J., J.K. Valenti, D.C. Pevear, and K.D. Hunt. 1982. Lymphocytic choriomeningitis virus killer T cells are lethal only in weakly disseminated murine infections. *The Journal of Experimental Medicine* 156:79-89.

Pinschewer, D.D., M. Perez, E. Jeetendra, T. Bächi, E. Horvath, H. Hengartner, M.A. Whitt, J.C. de la Torre, and R.M. Zinkernagel. 2004. Kinetics of protective antibodies are determined by the viral surface antigen. *J. Clin. Invest.* 114:988-993.

Pircher, H., K. Burki, R. Lang, H. Hengartner, and R.M. Zinkernagel. 1989a. Tolerance induction in double specific T-cell receptor transgenic mice varies with antigen. *Nature* 342:559-561.

Pircher, H., K. Bürki, R. Lang, H. Hengartner, and R.M. Zinkernagel. 1989b. Tolerance induction in double specific T-cell receptor transgenic mice varies with antigen. *Nature* 342:559-561.

Planz, O., S. Ehl, E. Furrer, E. Horvath, M.-A. Bründler, H. Hengartner, and R.M. Zinkernagel. 1997. A critical role for neutralizing-antibody-producing B cells, CD4⁺ T cells, and interferons in persistent and acute infections of mice with lymphocytic choriomeningitis virus: Implications for adoptive immunotherapy of virus carriers. *Proceedings of the National Academy of Sciences* 94:6874-6879.

Poignard, P., R. Sabbe, G.R. Picchio, M. Wang, R.J. Gulizia, H. Katinger, P.W.H.I. Parren, D.E. Mosier, and D.R. Burton. 1999. Neutralizing Antibodies Have Limited Effects on the Control of Established HIV-1 Infection In Vivo. *Immunity* 10:431-438.

Priddy, F.H., D.J.M. Lewis, H.C. Gelderblom, H. Hassanin, C. Streatfield, C. LaBranche, J. Hare, J.H. Cox, L. Dally, D. Bendel, D. Montefiori, E. Sayeed, J. Ackland, J. Gilmour, B.C. Schnepp, J.F. Wright, and P. Johnson. 2019. Adeno-associated virus vectored immunoprophylaxis to prevent HIV in healthy adults: a phase 1 randomised controlled trial. *The Lancet HIV* 6:e230-e239.

Prinz, M., H. Schmidt, A. Mildner, K.P. Knobeloch, U.K. Hanisch, J. Raasch, D. Merkler, C. Detje, I. Gutcher, J. Mages, R. Lang, R. Martin, R. Gold, B. Becher, W. Bruck, and U. Kalinke. 2008. Distinct and nonredundant in vivo functions of IFNAR on myeloid cells limit autoimmunity in the central nervous system. *Immunity* 28:675-686.

Probst, H.C., and M. van den Broek. 2005. Priming of CTLs by lymphocytic choriomeningitis virus depends on dendritic cells. *J Immunol* 174:3920-3924.

Richter, K., and A. Oxenius. 2013. Non-neutralizing antibodies protect from chronic LCMV infection independently of activating FcγR or complement. *European Journal of Immunology* 43:2349-2360.

Rickert, R.C., J. Roes, and K. Rajewsky. 1997. B lymphocyte-specific, Cre-mediated mutagenesis in mice. *Nucleic Acids Res* 25:1317-1318.

Rose, S., A. Misharin, and H. Perlman. 2012. A novel Ly6C/Ly6G-based strategy to analyze the mouse splenic myeloid compartment. *Cytometry A* 81:343-350.

Rotger, M., J. Dalmau, A. Rauch, P. McLaren, S.E. Bosinger, R. Martinez, N.G. Sandler, A. Roque, J. Liebner, M. Battegay, E. Bernasconi, P. Descombes, I. Erkizia, J. Fellay, B.

Hirschel, J.M. Miro, E. Palou, M. Hoffmann, M. Massanella, J. Blanco, M. Woods, H.F. Gunthard, P. de Bakker, D.C. Douek, G. Silvestri, J. Martinez-Picado, and A. Telenti. 2011. Comparative transcriptomics of extreme phenotypes of human HIV-1 infection and SIV infection in sooty mangabey and rhesus macaque. *J Clin Invest* 121:2391-2400.

Roths, J.B., E.D. Murphy, and E.M. Eicher. 1984. A new mutation, gld, that produces lymphoproliferation and autoimmunity in C3H/HeJ mice. *J Exp Med* 159:1-20.

Rowe, W.P., R.J. Huebner, L.K. Gilmore, R.H. Parrott, and T.G. Ward. 1953. Isolation of a Cytopathogenic Agent from Human Adenoids Undergoing Spontaneous Degeneration in Tissue Culture. *Proceedings of the Society for Experimental Biology and Medicine* 84:570-573.

Ruella, M., and S.S. Kenderian. 2017. Next-Generation Chimeric Antigen Receptor T-Cell Therapy: Going off the Shelf. *BioDrugs* 31:473-481.

Sakhuja, K., P.S. Reddy, S. Ganesh, F. Cantaniag, S. Pattison, P. Limbach, D.B. Kayda, M.J. Kadan, M. Kaleko, and S. Connelly. 2003. Optimization of the Generation and Propagation of Gutless Adenoviral Vectors. *Human Gene Therapy* 14:243-254.

Salimzadeh, L., N. Le Bert, C.-A. Dutertre, U.S. Gill, E.W. Newell, C. Frey, M. Hung, N. Novikov, S. Fletcher, P.T.F. Kennedy, and A. Bertoletti. 2018. PD-1 blockade partially recovers dysfunctional virus–specific B cells in chronic hepatitis B infection. *The Journal of Clinical Investigation* 128:4573-4587.

Salvato, M., E. Shimomaye, and M.B.A. Oldstone. 1989. The primary structure of the lymphocytic choriomeningitis virus L gene encodes a putative RNA polymerase. *Virology* 169:377-384.

Salvato, M., E. Shimomaye, P. Southern, and M.B.A. Oldstone. 1988. Virus-lymphocyte interactions IV. Molecular characterization of LCMV Armstrong (CTL+) small genomic segment and that of its variant, clone 13 (CTL−). *Virology* 164:517-522.

Salvato, M.S., and E.M. Shimomaye. 1989. The completed sequence of lymphocytic choriomeningitis virus reveals a unique RNA structure and a gene for a zinc finger protein. *Virology* 173:1-10.

Sammicheli, S., M. Kuka, P. Di Lucia, N.J. de Oya, M. De Giovanni, J. Fioravanti, C. Cristofani, C.G. Maganuco, B. Fallet, L. Ganzer, L. Sironi, M. Mainetti, R. Ostuni, K. Larimore, P.D. Greenberg, J.C. de la Torre, L.G. Guidotti, and M. Iannacone. 2016. Inflammatory monocytes hinder antiviral B cell responses. *Science Immunology* 1:eaah6789.

Sánchez, A.B., and J.C. de la Torre. 2006. Rescue of the prototypic Arenavirus LCMV entirely from plasmid. *Virology* 350:370-380.

Sandler, N.G., S.E. Bosinger, J.D. Estes, R.T. Zhu, G.K. Tharp, E. Boritz, D. Levin, S. Wijeyesinghe, K.N. Makamdop, G.Q. del Prete, B.J. Hill, J.K. Timmer, E. Reiss, G. Yarden, S. Darko, E. Contijoch, J.P. Todd, G. Silvestri, M. Nason, R.B. Norgren, Jr., B.F. Keele, S. Rao, J.A. Langer, J.D. Lifson, G. Schreiber, and D.C. Douek. 2014. Type I interferon responses in rhesus macaques prevent SIV infection and slow disease progression. *Nature* 511:601-605.

Saunders, K.O., L. Wang, M.G. Joyce, Z.-Y. Yang, A.B. Balazs, C. Cheng, S.-Y. Ko, W.-P. Kong, R.S. Rudicell, I.S. Georgiev, L. Duan, K.E. Foulds, M. Donaldson, L. Xu, S.D. Schmidt, J.-P. Todd, D. Baltimore, M. Roederer, A.T. Haase, P.D. Kwong, S.S. Rao, J.R. Mascola, and G.J. Nabel. 2015. Broadly Neutralizing Human Immunodeficiency Virus Type 1 Antibody Gene Transfer Protects Nonhuman Primates from Mucosal Simian-Human Immunodeficiency Virus Infection. *Journal of Virology* 89:8334-8345.

Saydaminova, K., X. Ye, H. Wang, M. Richter, M. Ho, H. Chen, N. Xu, J.-S. Kim, E. Papapetrou, M.C. Holmes, P.D. Gregory, D. Palmer, P. Ng, A. Ehrhardt, and A. Lieber. 2015. Efficient genome editing in hematopoietic stem cells with helper-dependent Ad5/35 vectors expressing site-specific endonucleases under microRNA regulation. *Molecular Therapy - Methods & Clinical Development* 2:14057.

Schaefer, B.C., M.L. Schaefer, J.W. Kappler, P. Marrack, and R.M. Kedl. 2001. Observation of antigen-dependent CD8+ T-cell/ dendritic cell interactions in vivo. *Cell Immunol* 214:110-122.

Scheid, J.F., H. Mouquet, N. Feldhahn, M.S. Seaman, K. Velinzon, J. Pietzsch, R.G. Ott, R.M. Anthony, H. Zebroski, A. Hurley, A. Phogat, B. Chakrabarti, Y. Li, M. Connors, F. Pereyra, B.D. Walker, H. Wardemann, D. Ho, R.T. Wyatt, J.R. Mascola, J.V. Ravetch, and M.C. Nussenzweig. 2009. Broad diversity of neutralizing antibodies isolated from memory B cells in HIV-infected individuals. *Nature* 458:636.

Schmitz, J.E., M.J. Kuroda, S. Santra, V.G. Sasseville, M.A. Simon, M.A. Lifton, P. Racz, K. Tenner-Racz, M. Dalesandro, B.J. Scallon, J. Ghrayeb, M.A. Forman, D.C. Montefiori, E.P. Rieber, N.L. Letvin, and K.A. Reimann. 1999. Control of viremia in simian immunodeficiency virus infection by CD8+ lymphocytes. *Science* 283:857-860.

Schoofs, T., F. Klein, M. Braunschweig, E.F. Kreider, A. Feldmann, L. Nogueira, T. Oliveira, J.C.C. Lorenzi, E.H. Parrish, G.H. Learn, A.P. West, P.J. Bjorkman, S.J. Schlesinger, M.S. Seaman, J. Czartoski, M.J. McElrath, N. Pfeifer, B.H. Hahn, M. Caskey, and M.C. Nussenzweig. 2016. HIV-1 therapy with monoclonal antibody 3BNC117 elicits host immune responses against HIV-1. *Science* 352:997-1001.

Schweier, O., U. Aichele, A.-F. Marx, T. Straub, J.S. Verbeek, D.D. Pinschewer, and H. Pircher. 2019. Residual LCMV antigen in transiently CD4+ T cell-depleted mice induces high levels of virus-specific antibodies but only limited B-cell memory. *European Journal of Immunology* 49:626-637.

Scott-Browne, J.P., I.F. López-Moyado, S. Trifari, V. Wong, L. Chavez, A. Rao, and R.M. Pereira. 2016. Dynamic Changes in Chromatin Accessibility Occur in CD8+ T Cells Responding to Viral Infection. *Immunity* 45:1327-1340.

Seiler, P., B.M. Senn, M.-A. Bründler, R.M. Zinkernagel, H. Hengartner, and U. Kalinke. 1999. In Vivo Selection of Neutralization-Resistant Virus Variants But No Evidence of B Cell Tolerance in Lymphocytic Choriomeningitis Virus Carrier Mice Expressing a Transgenic Virus-Neutralizing Antibody. *The Journal of Immunology* 162:4536-4541.

Sen, D.R., J. Kaminski, R.A. Barnitz, M. Kurachi, U. Gerdemann, K.B. Yates, H.-W. Tsao, J. Godec, M.W. LaFleur, F.D. Brown, P. Tonnerre, R.T. Chung, D.C. Tully, T.M. Allen, N. Frahm, G.M. Lauer, E.J. Wherry, N. Yosef, and W.N. Haining. 2016. The epigenetic landscape of T cell exhaustion. *Science* 354:1165-1169.

Shi, W., Y. Liao, S.N. Willis, N. Taubenheim, M. Inouye, D.M. Tarlinton, G.K. Smyth, P.D. Hodgkin, S.L. Nutt, and L.M. Corcoran. 2015. Transcriptional profiling of mouse B cell terminal differentiation defines a signature for antibody-secreting plasma cells. *Nat Immunol* 16:663-673.

Shibata, R., M. Kawamura, H. Sakai, M. Hayami, A. Ishimoto, and A. Adachi. 1991. Generation of a chimeric human and simian immunodeficiency virus infectious to monkey peripheral blood mononuclear cells. *Journal of Virology* 65:3514-3520.

Shingai, M., Y. Nishimura, F. Klein, H. Mouquet, O.K. Donau, R. Plishka, A. Buckler-White, M. Seaman, M. Piatak, J.D. Lifson, D. Dimitrov, M.C. Nussenzweig, and M.A. Martin.

2013. Antibody-mediated immunotherapy of macaques chronically infected with SHIV suppresses viraemia. *Nature* 503:277.
Shinnakasu, R., T. Inoue, K. Kometani, S. Moriyama, Y. Adachi, M. Nakayama, Y. Takahashi, H. Fukuyama, T. Okada, and T. Kurosaki. 2016. Regulated selection of germinal-center cells into the memory B cell compartment. *Nature Immunology* 17:861.
Shoukry, N.H., A.G. Cawthon, and C.M. Walker. 2004. Cell-Mediated Immunity and the Outcome of Hepatitis C Virus Infection. *Annual Review of Microbiology* 58:391-424.
Shulman, Z., A.D. Gitlin, J.S. Weinstein, B. Lainez, E. Esplugues, R.A. Flavell, J.E. Craft, and M.C. Nussenzweig. 2014. Dynamic signaling by T follicular helper cells during germinal center B cell selection. *Science* 345:1058-1062.
Solly, S.K., S. Trajcevski, C. Frisén, G.W. Holzer, E. Nelson, B. Clerc, E. Abordo-Adesida, M. Castro, P. Lowenstein, and D. Klatzmann. 2003. Replicative retroviral vectors for cancer gene therapy. *Cancer Gene Therapy* 10:30-39.
Sommerstein, R., L. Flatz, M.M. Remy, P. Malinge, G. Magistrelli, N. Fischer, M. Sahin, A. Bergthaler, S. Igonet, J. ter Meulen, D. Rigo, P. Meda, N. Rabah, B. Coutard, T.A. Bowden, P.-H. Lambert, C.-A. Siegrist, and D.D. Pinschewer. 2015a. Arenavirus Glycan Shield Promotes Neutralizing Antibody Evasion and Protracted Infection. *PLOS Pathogens* 11:e1005276.
Sommerstein, R., L. Flatz, M.M. Remy, P. Malinge, G. Magistrelli, N. Fischer, M. Sahin, A. Bergthaler, S. Igonet, J. Ter Meulen, D. Rigo, P. Meda, N. Rabah, B. Coutard, T.A. Bowden, P.H. Lambert, C.A. Siegrist, and D.D. Pinschewer. 2015b. Arenavirus Glycan Shield Promotes Neutralizing Antibody Evasion and Protracted Infection. *PLoS Pathog* 11:e1005276.
Sonntag, F., S. Bleker, B. Leuchs, R. Fischer, and J.A. Kleinschmidt. 2006. Adeno-Associated Virus Type 2 Capsids with Externalized VP1/VP2 Trafficking Domains Are Generated prior to Passage through the Cytoplasm and Are Maintained until Uncoating Occurs in the Nucleus. *Journal of Virology* 80:11040-11054.
Sonntag, F., K. Schmidt, and J.A. Kleinschmidt. 2010. A viral assembly factor promotes AAV2 capsid formation in the nucleolus. *Proceedings of the National Academy of Sciences* 107:10220-10225.
Steinitz, M., G. Klein, S. Koskimies, and O. Makel. 1977. EB virus-induced B lymphocyte cell lines producing specific antibody. *Nature* 269:420-422.
Straub, T., O. Schweier, M. Bruns, F. Nimmerjahn, A. Waisman, and H. Pircher. 2013. Nucleoprotein-specific nonneutralizing antibodies speed up LCMV elimination independently of complement and FcγR. *European Journal of Immunology* 43:2338-2348.
Streeck, H., Z.L. Brumme, M. Anastario, K.W. Cohen, J.S. Jolin, A. Meier, C.J. Brumme, E.S. Rosenberg, G. Alter, T.M. Allen, B.D. Walker, and M. Altfeld. 2008. Antigen Load and Viral Sequence Diversification Determine the Functional Profile of HIV-1–Specific CD8+ T Cells. *PLOS Medicine* 5:e100.
Suan, D., N.J. Kräutler, J.L.V. Maag, D. Butt, K. Bourne, J.R. Hermes, D.T. Avery, C. Young, A. Statham, M. Elliott, M.E. Dinger, A. Basten, S.G. Tangye, and R. Brink. 2017. CCR6 Defines Memory B Cell Precursors in Mouse and Human Germinal Centers, Revealing Light-Zone Location and Predominant Low Antigen Affinity. *Immunity* 47:1142-1153.e1144.
Team, R.C. 2015. R: A language and environment for statistical computing. R Foundation for Statistical Computing, Vienna, Austria. . *http://www.R-project.org/*

Teijaro, J.R., C. Ng, A.M. Lee, B.M. Sullivan, K.C. Sheehan, M. Welch, R.D. Schreiber, J.C. de la Torre, and M.B. Oldstone. 2013. Persistent LCMV infection is controlled by blockade of type I interferon signaling. *Science* 340:207-211.

Thomsen, A.R., J. Johansen, O. Marker, and J.P. Christensen. 1996. Exhaustion of CTL memory and recrudescence of viremia in lymphocytic choriomeningitis virus-infected MHC class II-deficient mice and B cell-deficient mice. *The Journal of Immunology* 157:3074-3080.

Titanji, K., F. Chiodi, R. Bellocco, D. Schepis, L. Osorio, C. Tassandin, G. Tambussi, S. Grutzmeier, L. Lopalco, and A. De Milito. 2005. Primary HIV-1 infection sets the stage for important B lymphocyte dysfunctions. *AIDS* 19:1947-1955.

Trautmann, L., L. Janbazian, N. Chomont, E.A. Said, S. Gimmig, B. Bessette, M.-R. Boulassel, E. Delwart, H. Sepulveda, R.S. Balderas, J.-P. Routy, E.K. Haddad, and R.-P. Sekaly. 2006. Upregulation of PD-1 expression on HIV-specific CD8+ T cells leads to reversible immune dysfunction. *Nature Medicine* 12:1198-1202.

Turtle, C.J., L.-A. Hanafi, C. Berger, T.A. Gooley, S. Cherian, M. Hudecek, D. Sommermeyer, K. Melville, B. Pender, T.M. Budiarto, E. Robinson, N.N. Steevens, C. Chaney, L. Soma, X. Chen, C. Yeung, B. Wood, D. Li, J. Cao, S. Heimfeld, M.C. Jensen, S.R. Riddell, and D.G. Maloney. 2016. CD19 CAR–T cells of defined CD4+:CD8+ composition in adult B cell ALL patients. *J Clin Invest* 126:2123-2138.

Tussiwand, R., B. Everts, G.E. Grajales-Reyes, N.M. Kretzer, A. Iwata, J. Bagaitkar, X. Wu, R. Wong, D.A. Anderson, T.L. Murphy, E.J. Pearce, and K.M. Murphy. 2015. Klf4 expression in conventional dendritic cells is required for T helper 2 cell responses. *Immunity* 42:916-928.

Utzschneider, D.T., M. Charmoy, V. Chennupati, L. Pousse, D.P. Ferreira, S. Calderon-Copete, M. Danilo, F. Alfei, M. Hofmann, D. Wieland, S. Pradervand, R. Thimme, D. Zehn, and W. Held. 2016. T Cell Factor 1-Expressing Memory-like CD8+ T Cells Sustain the Immune Response to Chronic Viral Infections. *Immunity* 45:415-427.

Utzschneider, D.T., A. Legat, S.A. Fuertes Marraco, L. Carrié, I. Luescher, D.E. Speiser, and D. Zehn. 2013. T cells maintain an exhausted phenotype after antigen withdrawal and population reexpansion. *Nature Immunology* 14:603.

van Lieshout, L.P., G. Soule, D. Sorensen, K.L. Frost, S. He, K. Tierney, D. Safronetz, S.A. Booth, G.P. Kobinger, X. Qiu, and S.K. Wootton. 2018. Intramuscular Adeno-Associated Virus–Mediated Expression of Monoclonal Antibodies Provides 100% Protection Against Ebola Virus Infection in Mice. *The Journal of Infectious Diseases* 217:916-925.

Vandenberghe, L.H., L. Wang, S. Somanathan, Y. Zhi, J. Figueredo, R. Calcedo, J. Sanmiguel, R.A. Desai, C.S. Chen, J. Johnston, R.L. Grant, G. Gao, and J.M. Wilson. 2006. Heparin binding directs activation of T cells against adeno-associated virus serotype 2 capsid. *Nature Medicine* 12:967-971.

Velu, V., K. Titanji, B. Zhu, S. Husain, A. Pladevega, L. Lai, T.H. Vanderford, L. Chennareddi, G. Silvestri, G.J. Freeman, R. Ahmed, and R.R. Amara. 2009. Enhancing SIV-specific immunity in vivo by PD-1 blockade. *Nature* 458:206-210.

Vetrini, F., and P. Ng. 2010. Gene therapy with helper-dependent adenoviral vectors: current advances and future perspectives. *Viruses* 2:1886-1917.

Victora, G.D., D. Dominguez-Sola, A.B. Holmes, S. Deroubaix, R. Dalla-Favera, and M.C. Nussenzweig. 2012. Identification of human germinal center light and dark zone cells and their relationship to human B-cell lymphomas. *Blood* 120:2240-2248.

Vieira, P., and K. Rajewsky. 1988. The half-lives of serum immunoglobulins in adult mice. *European Journal of Immunology* 18:313-316.

Vittecoq, D., B. Mattlinger, F. Barre-Sinoussi, A.M. Courouce, C. Rouzioux, C. Doinel, M. Bary, J.P. Viard, J.F. Bach, P. Rouger, and J.J. Lefrere. 1992. Passive Immunotherapy in AIDS: A Randomized Trial of Serial Human Immunodeficiency Virus-Positive Transfusions of Plasma Rich in p24 Antibodies versus Transfusions of Seronegative Plasma. *The Journal of Infectious Diseases* 165:364-368.

Walker, L.M., S.K. Phogat, P.-Y. Chan-Hui, D. Wagner, P. Phung, J.L. Goss, T. Wrin, M.D. Simek, S. Fling, J.L. Mitcham, J.K. Lehrman, F.H. Priddy, O.A. Olsen, S.M. Frey, P.W. Hammond, S. Kaminsky, T. Zamb, M. Moyle, W.C. Koff, P. Poignard, and D.R. Burton. 2009. Broad and Potent Neutralizing Antibodies from an African Donor Reveal a New HIV-1 Vaccine Target. *Science* 326:285-289.

Wardemann, H., S. Yurasov, A. Schaefer, J.W. Young, E. Meffre, and M.C. Nussenzweig. 2003. Predominant Autoantibody Production by Early Human B Cell Precursors. *Science* 301:1374-1377.

Weisel, Florian J., Griselda V. Zuccarino-Catania, M. Chikina, and Mark J. Shlomchik. 2016. A Temporal Switch in the Germinal Center Determines Differential Output of Memory B and Plasma Cells. *Immunity* 44:116-130.

Weiss, G.E., P.D. Crompton, S. Li, L.A. Walsh, S. Moir, B. Traore, K. Kayentao, A. Ongoiba, O.K. Doumbo, and S.K. Pierce. 2009. Atypical memory B cells are greatly expanded in individuals living in a malaria-endemic area. *J Immunol* 183:2176-2182.

Wesolowski, R., J. Markowitz, and W.E. Carson, 3rd. 2013. Myeloid derived suppressor cells - a new therapeutic target in the treatment of cancer. *J Immunother Cancer* 1:10.

Wheatley, A.K., A.B. Kristensen, W.N. Lay, and S.J. Kent. 2016. HIV-dependent depletion of influenza-specific memory B cells impacts B cell responsiveness to seasonal influenza immunisation. *Sci Rep* 6:26478.

Wherry, E.J., J.N. Blattman, K. Murali-Krishna, R. van der Most, and R. Ahmed. 2003. Viral Persistence Alters CD8 T-Cell Immunodominance and Tissue Distribution and Results in Distinct Stages of Functional Impairment. *Journal of Virology* 77:4911-4927.

Wherry, E.J., S.-J. Ha, S.M. Kaech, W.N. Haining, S. Sarkar, V. Kalia, S. Subramaniam, J.N. Blattman, D.L. Barber, and R. Ahmed. 2007. Molecular Signature of CD8+ T Cell Exhaustion during Chronic Viral Infection. *Immunity* 27:670-684.

Wieland, A., R. Shashidharamurthy, A.O. Kamphorst, J.-H. Han, R.D. Aubert, B.P. Choudhury, S.R. Stowell, J. Lee, G.A. Punkosdy, M.J. Shlomchik, P. Selvaraj, and R. Ahmed. 2015. Antibody Effector Functions Mediated by Fcγ-Receptors Are Compromised during Persistent Viral Infection. *Immunity* 42:367-378.

Williams, N., N. Kraft, and K. Shortman. 1972. The separation of different cell classes from lymphoid organs. VI. The effect of osmolarity of gradient media on the density distribution of cells. *Immunology* 22:885-899.

Wilson, E.B., D.H. Yamada, H. Elsaesser, J. Herskovitz, J. Deng, G. Cheng, B.J. Aronow, C.L. Karp, and D.G. Brooks. 2013. Blockade of chronic type I interferon signaling to control persistent LCMV infection. *Science* 340:202-207.

Wrammert, J., K. Smith, J. Miller, W.A. Langley, K. Kokko, C. Larsen, N.-Y. Zheng, I. Mays, L. Garman, C. Helms, J. James, G.M. Air, J.D. Capra, R. Ahmed, and P.C. Wilson. 2008. Rapid cloning of high-affinity human monoclonal antibodies against influenza virus. *Nature* 453:667.

Wu, X., Z.-Y. Yang, Y. Li, C.-M. Hogerkorp, W.R. Schief, M.S. Seaman, T. Zhou, S.D. Schmidt, L. Wu, L. Xu, N.S. Longo, K. McKee, S. O'Dell, M.K. Louder, D.L. Wycuff, Y. Feng, M. Nason, N. Doria-Rose, M. Connors, P.D. Kwong, M. Roederer, R.T. Wyatt, G.J. Nabel, and J.R. Mascola. 2010. Rational Design of Envelope Identifies Broadly Neutralizing Human Monoclonal Antibodies to HIV-1. *Science* 329:856-861.

Xiao, P.-J., and R.J. Samulski. 2012. Cytoplasmic Trafficking, Endosomal Escape, and Perinuclear Accumulation of Adeno-Associated Virus Type 2 Particles Are Facilitated by Microtubule Network. *Journal of Virology* 86:10462-10473.

Xiao, X., J. Li, and R.J. Samulski. 1998. Production of High-Titer Recombinant Adeno-Associated Virus Vectors in the Absence of Helper Adenovirus. *Journal of Virology* 72:2224-2232.

Xin, G., R. Zander, D.M. Schauder, Y. Chen, J.S. Weinstein, W.R. Drobyski, V. Tarakanova, J. Craft, and W. Cui. 2018. Single-cell RNA sequencing unveils an IL-10-producing helper subset that sustains humoral immunity during persistent infection. *Nature Communications* 9:5037.

Xu, H.C., M. Grusdat, A.A. Pandyra, R. Polz, J. Huang, P. Sharma, R. Deenen, K. Kohrer, R. Rahbar, A. Diefenbach, K. Gibbert, M. Lohning, L. Hocker, Z. Waibler, D. Haussinger, T.W. Mak, P.S. Ohashi, K.S. Lang, and P.A. Lang. 2014. Type I interferon protects antiviral CD8+ T cells from NK cell cytotoxicity. *Immunity* 40:949-960.

Yamada, D.H., H. Elsaesser, A. Lux, J.M. Timmerman, S.L. Morrison, J.C. de la Torre, F. Nimmerjahn, and D.G. Brooks. 2015. Suppression of Fcγ-Receptor-Mediated Antibody Effector Function during Persistent Viral Infection. *Immunity* 42:379-390.

Yi, J.S., M.A. Cox, and A.J. Zajac. 2010. T-cell exhaustion: characteristics, causes and conversion. *Immunology* 129:474-481.

Zajac, A.J., J.N. Blattman, K. Murali-Krishna, D.J. Sourdive, M. Suresh, J.D. Altman, and R. Ahmed. 1998. Viral immune evasion due to persistence of activated T cells without effector function. *The Journal of experimental medicine* 188:2205-2213.

Zaretsky, I., O. Atrakchi, R.D. Mazor, L. Stoler-Barak, A. Biram, S.W. Feigelson, A.D. Gitlin, B. Engelhardt, and Z. Shulman. 2017. ICAMs support B cell interactions with T follicular helper cells and promote clonal selection. *The Journal of Experimental Medicine* 214:3435-3448.

Zellweger, R.M., L. Hangartner, J. Weber, R.M. Zinkernagel, and H. Hengartner. 2006. Parameters governing exhaustion of rare T cell-independent neutralizing IgM-producing B cells after LCMV infection. *Eur J Immunol* 36:3175-3185.

Zhang, W.-W., L. Li, D. Li, J. Liu, X. Li, W. Li, X. Xu, M.J. Zhang, L.A. Chandler, H. Lin, A. Hu, W. Xu, and D.M.-K. Lam. 2018. The First Approved Gene Therapy Product for Cancer Ad-p53 (Gendicine): 12 Years in the Clinic. *Human Gene Therapy* 29:160-179.

Zhong, L., X. Zhou, Y. Li, K. Qing, X. Xiao, R.J. Samulski, and A. Srivastava. 2008. Single-polarity Recombinant Adeno-associated Virus 2 Vector-mediated Transgene Expression In Vitro and In Vivo: Mechanism of Transduction. *Molecular Therapy* 16:290-295.

Zinkernagel, R.M., C.J. Pfau, H. Hengartner, and A. Althage. 1985. Susceptibility to murine lymphocytic choriomeningitis maps to class I MHC genes—a model for MHC/disease associations. *Nature* 316:814-817.

Acknowledgements

Foremost, I would like to thank you, Daniel, for being a great mentor and motivating and supporting me for the last 5 years. It has been a long journey with a lot of ups and downs, but a very fruitful one! I am truly thankful for all the support and motivation you gave, whenever we were stumbled in the project, without your positiveness and vision, this process would have been much trickier to handle. I will always appreciate your generous and humble behavior to whenever I needed something, you always provided with utmost motivation and without hesitation for my scientific development and for the project. I am very grateful for your contribution to direct me to tackle problems and for helping me to learn how to become a didactic and independent scientist.

I would also like to thank to my faculty representative, Christoph Hess. Thank you, Christoph, for kindly accepting to be my faculty representative and helping for the smoothness of the organizations both during the admission and the graduation processes. Furthermore, thank you for all your scientific insights and mentoring support for a poor PhD student! I would like to sincerely thank my other committee member, Hanspeter Pircher. I am very grateful for all of our discussions and for your efforts to commute all the way from Freiburg to Basel for all the committee meetings! You have given precious insights into the project and supported the progress of the project with the invaluable protocols you have provided! I will always remember our nice walk to Biocenter and pondering about NP-staining protocol.

Very importantly and warmly, I would like to thank all the past and the present members of Pinschewer lab. When I first joined the lab, two other lovely members of our lab also joined more or less at similar times, namely Kerstin and Karen. It was such a nice pleasure to be newbies all together and even work in the same team to tackle the problems all together! And

of course, thank you Ben (!) for showing us all the techniques that you were using in the lab, padavan is finally finishing too! It was always so much fun to work with the precious B cell team!! I would like to thank AMY (Anna and Min) for being so positive all the time, it was, most of the time (☺) so much fun to sit side by side with you, Anna and talk about so many different things and support each other for all the hard times in a PhD's life. And as every PhD student knows there are quite a lot of them. Thank you, Min for being so loving and caring, you will always be my lab mom! It was so great to work with you. Also, very importantly, Weldy, thank you very much for basically knowing every valuable information about the lab! Without you I don't know how I could find that precious information no one else in the lab knows! And also I will always remember our precious conversations about life, and our mouse house chats.

I would like to thank all the other lab members of the Pinschewer lab, Peterchen, Katrin, Sandra, Lena, Mehmet, Marianna, Mirela, Melissa. Very importantly, thank you Karsten and Patricia, for taking care of our precious mice excellently! And for all the support whenever we needed without exception. I would also like to thank Cornelia for all the support she gave, when I first started in the lab, without her positivity and sarcastic comments (which I love), the lab wouldn't have been the same.

I would also like to thank Tobias Straub for helping me sort out one of the key tools in my project, NP production. It was always fun to pay you a visit in Freiburg, and sincerely thank you for helping without hesitation whenever I approached you to ask for your opinion. I would also like to thank Danny, and Lorenzo for their invaluable support for the sorting facility, those sorting hours wouldn't have been bearable without their excellent professional support and fun conversations.

Next, I would like to thank two very special friends Basel gave me. Berna and Loulieta. Loulieta, thank you so very much for choosing this lab to do your rotation! It was truly

unexpected to get to know an amazing friend, what we call a “dost” in Turkish. I cannot express how much valuable it was for me the conversations we had at the times I needed the most, and I think you are one of the most positive people I got to know and thank you for that! And Bernie, I am so glad you chose to start your PhD here in Basel, without you being here, my initial distance to Basel would definitely not turn into the homie feeling I have right now, thank you for supporting me in whatever way without condition like a sister! I will always appreciate that. And occasional spontaneous Berlin trips helped me tremendously for the depressive side of the PhD life ☺.

Before my “blood” family, I would like to thank my “chosen” family. I am so grateful for all the support from you Sila and happy that we have visited Switzerland together for the first time for professional reasons. For all my happy and stressful times, you were always there, you always came up with solutions and opportunities for both my professional life and personal life. I am so glad to have you right next to me, despite of the oceans we have at the moment between us. My PhD life would definitely not be as nice as it was without your contribution and your occasional visit to beautiful Basel!

Finally, I would like to thank my family, annem Emine, babam Mehmet, abim Kursat and the newest member of our family, my beloved nephew Kilicarslan. I want to thank them for providing me with all the emotional support for me to become who I am today. I am very grateful how much my parents supported me to achieve the best in my life and to become the happiest version of myself. Without their vision and kindness, my life wouldn’t have been the same. And throughout my PhD years, they were always the audience to hear all my success and failure stories and they were, without exception, supportive endlesly. Thank you so much my beloved family!

CURRICULUM VITAE

Yusuf Ismail ERTUNA, M.Sc.
yusufismail.ertuna@unibas.ch

Work
Experimental Virology Lab
Department of Biomedicine
University of Basel
Petersplatz 10, CH-4009
Basel, Switzerland
+41612673268

Home
Karl-Jaspersallee-40, CH-4052
Basel, Switzerland
+41768045844

CURRENT POSITION

University of Basel — Basel, Switzerland
PhD Candidate — 2014 – Present

EDUCATION

Department of Biomedicine, University of Basel — Basel, Switzerland
PhD, Microbiology — 2014 – Present (Expected graduation date 28.11.19)

Department of Molecular Biology and Genetics, Bilkent University — Ankara, Turkey
M.Sc., Molecular Biology and Genetics (CGPA: 3.90/4.00) — 2012 – 2014

Department of Molecular Biology and Genetics, Bilkent University — Ankara, Turkey
B.Sc., Molecular Biology and Genetics (CGPA: 3.64/4.00) — 2007 – 2012

RESEARCH EXPERIENCE

Department of Biomedicine, University of Basel — Basel, Switzerland
Graduate Researcher; Advisor: Prof. Daniel P. Pinschewer, MD — 2014 – Present
Faculty representative: Prof. Christoph Hess, MD, PhD

PhD Thesis Research

- Impact of AAV-vectored antibody delivery on chronic viral infection

Additional projects

- Dynamics of memory B cell subsets in the course of rechallenge with chronic infection

Department of Molecular Biology and Genetics, Bilkent University
Ankara,Turkey
M.Sc. Thesis; Advisors: Prof. Mehmet Öztürk, PhD & Prof. Ihsan Gürsel, PhD 2012 - 2014

M.Sc. Thesis Research

- Contribution of notch signaling on HCC stem cell status and utilizing TLR agonists and notch inhibition to improve HCC therapy

Harvard-MIT Health Sciences and Technology Boston, MA, USA
Research Intern; Advisor: Prof. Utkan Demirci, PhD July – October 2011

- Exploring methods for cryopreservation of sperms, oocytes and stem cells by using vitrification techniques.

UNAM (Institute of Materials Science and Nanotechnology) Ankara, Turkey
Research Intern; Advisor: Prof. Ayşe Begüm Tekinay, PhD 2009 – 2010

- Understanding he autophagy pathway in the green algae *C. reinhardtii*.

Department of Medical Genetics, Cukurova University Adana, Turkey
Research Intern July – August 2009

- Exploring the pathogenesis of Tuberculosis

AWARDS and HONORS

Travel grant awarded by European Federation of Immunological Societies (EFIS) and European Journal of Immunology (EJI) 2017

National Scholarship program for M.Sc. students funded by The Scientific and Technological Research Council of Turkey (TUBITAK) 2012 – 2014

Full Scholarship funded by Bilkent University (Top 1500th out of 1.8 million attendees in National University Entrance Exam) 2007 – 2012

Scholarship funded by The Scientific and Technological Research Council of Turkey (TUBITAK) (Top 1500th out of 1.8 million attendees in National University Entrance Exam) 2007 – 2012

Full scholarship founded by Ali and Rukiye Ozgoren Science High School (Depending on the degree in Turkey National High School Entrance Exam) 2004 – 2007

TEACHING EXPERIENCE

Teaching Assistant, Bilkent University

Genetics Lab-MBG210	Fall 2013 – 2014
Introduction to Modern Biology-MBG110	Fall and Spring 2012 – 2013
Biochemistry II – MBG312	Spring 2013 – 2014

PRESENTATIONS IN CONGRESSES

Yusuf Ertuna, Benedict Fallet, Kerstin Narr, Daniel Pinschewer. Complementarity and redundancy of memory B cell subset responses to viral challenge. 19th Germinal Center Conference, 14-17/9, 2017, Venice, ITALY. (Poster Presentation)

Y.I. Ertuna, M.D. Abusselamoglu, I. Gursel, M. Ozturk. Characterization of hepatocellular cancer stem cells: Notch pathway ligand Jagged-1 enhance CD133+ stem cell population in Huh7 cell line. 13th National Medical Biology and Genetics Congress, 27-31/10, Kusadasi, AYDIN, TURKEY. (Oral Short Communication)

M.D. Abusselamoglu, **Y. I. Ertuna**, I. Gursel, M. Ozturk. Characterization of hepatocellular cancer stem cells: inhibitory effects of Wnt and TGF-beta signaling on CD133+ stem cells. 13th National Medical Biology and Genetics Congress, 27-31/10, Kusadasi, AYDIN, TURKEY. (Poster Presentation)

PUBLICATIONS

B. Fallet, K. Narr, **Y. I. Ertuna**, M. Remy, R. Sommerstein, K. Cornille, M. Kreutzfeldt, N. Page, G. Zimmer, F. Geier, T. Straub, H. Pircher, K. Larimore, P. D. Greenberg, D. Merkler, D. D. Pinschewer, Interferon-driven deletion of antiviral B cells at the onset of chronic infection. Sci. Immunol. 1, eaah6817 (2016).

LANGUAGES

Turkish (Native), English (Advanced), German (Intermediate, B1)

COMPUTER SKILLS

- Microsoft Office and Applications, Prism8, FlowJo, FACSDiva, Adobe Illustrator.